

**UCSF**

**UC San Francisco Electronic Theses and Dissertations**

**Title**

Mitotic microtubule depolymerization and XMAP215

**Permalink**

<https://escholarship.org/uc/item/0vg7w9r6>

**Author**

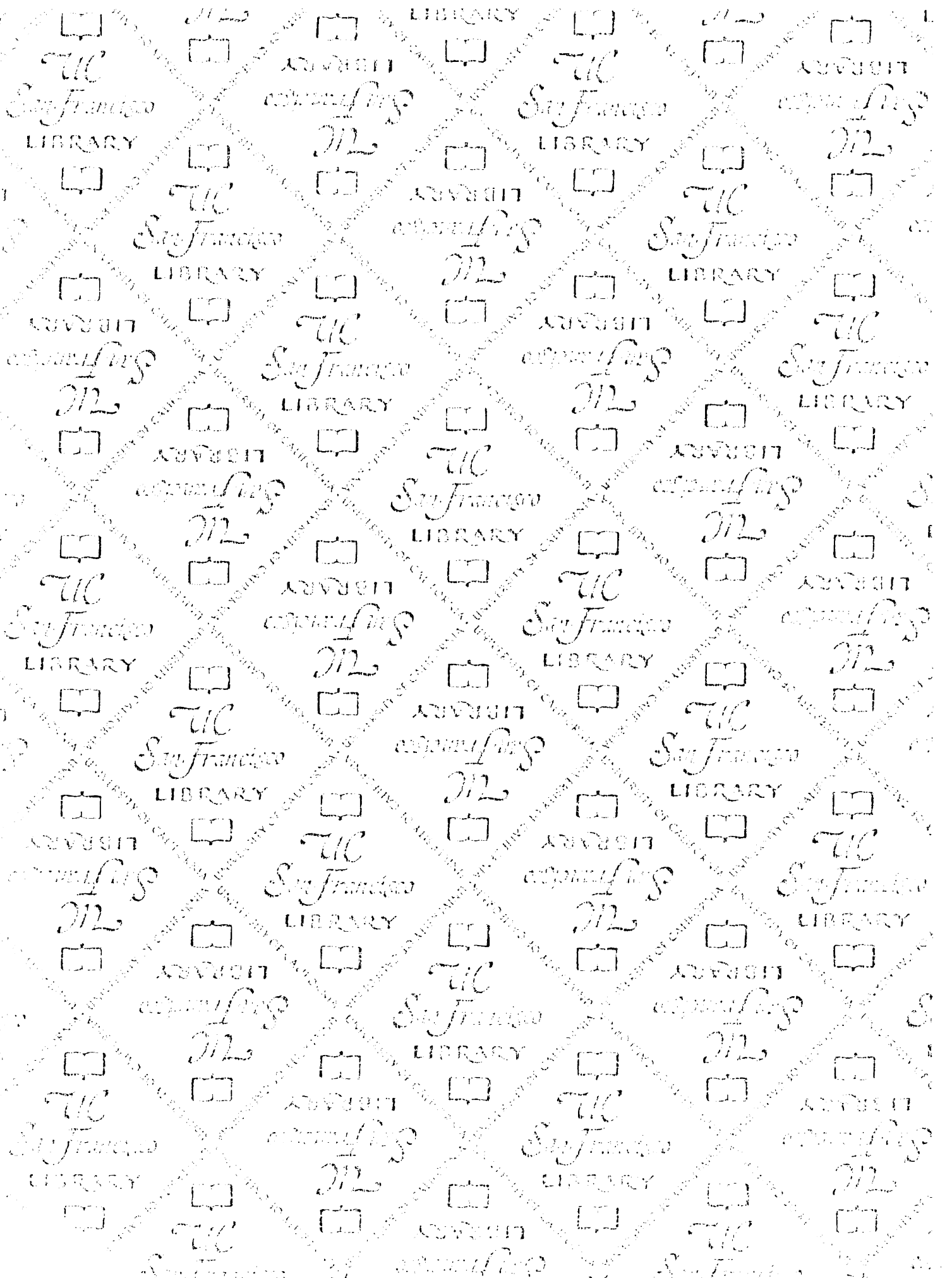
Shirasu-Hiza, Michele,

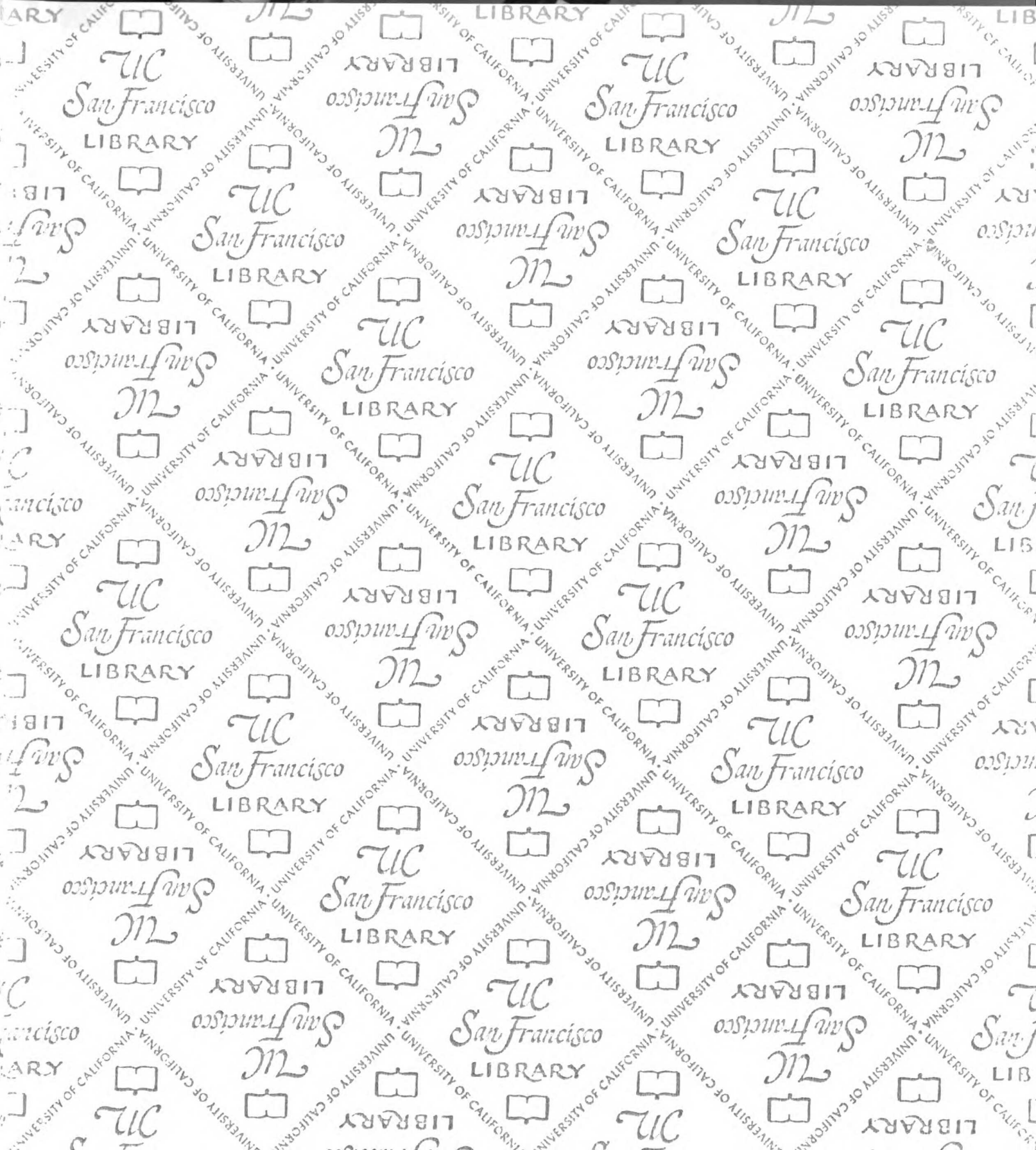
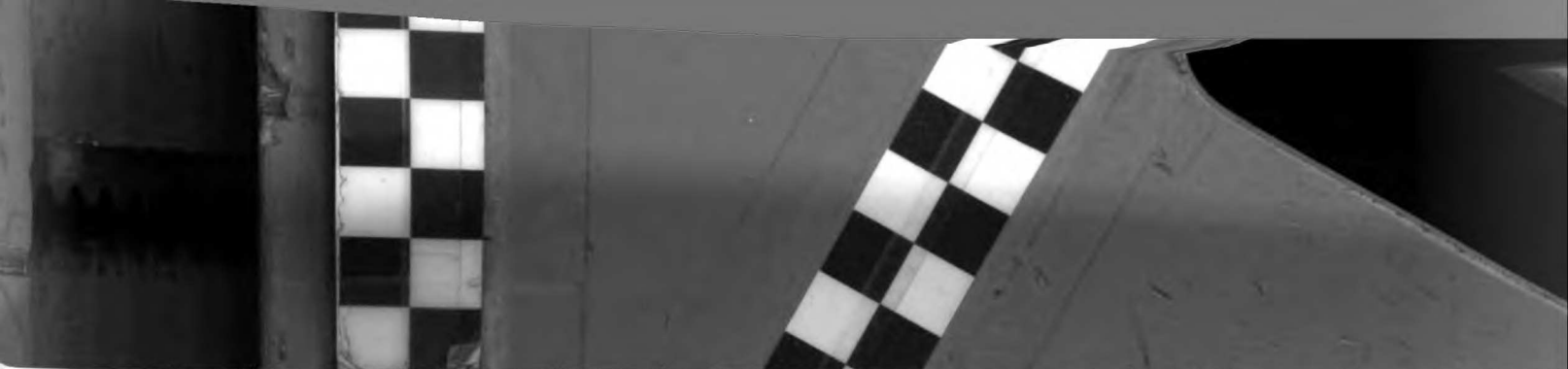
**Publication Date**

2004

Peer reviewed|Thesis/dissertation







Mitotic Microtubule Depolymerization and XMAP215

by

Michele Shirasu-Hiza

**DISSERTATION**

**Submitted in partial satisfaction of the requirements for the degree of**

**DOCTOR OF PHILOSOPHY**

in

Biochemistry/Cell Biology

in the

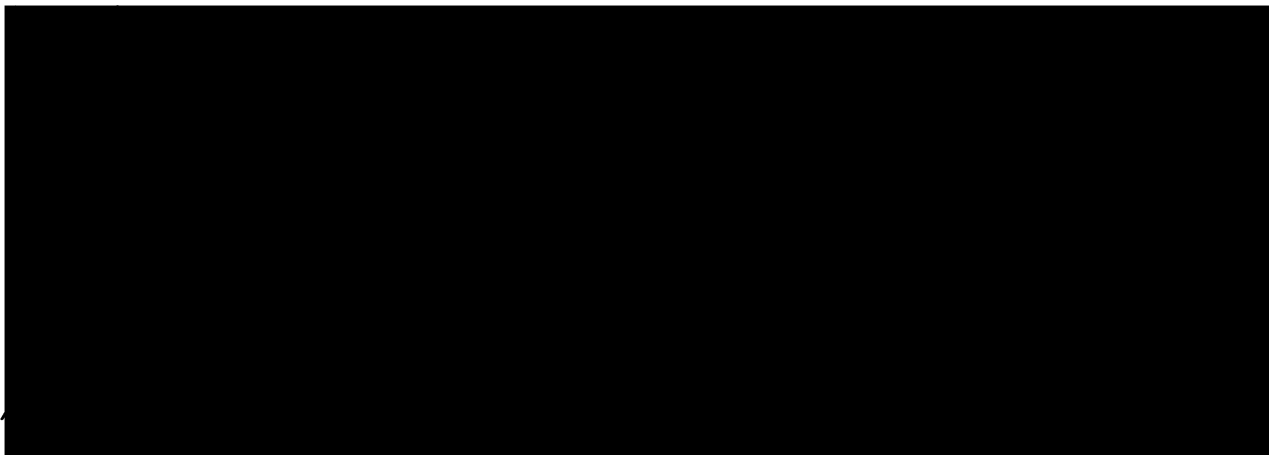
**GRADUATE DIVISIONS**

of the

**UNIVERSITY OF CALIFORNIA SAN FRANCISCO**

and

**UNIVERSITY OF CALIFORNIA BERKELEY**



Date

University Librarian

Degree Conferred: .....

# **Mitotic Microtubule Depolymerization and XMAP215**

copyright (2003)

by

**Michele Shirasu-Hiza**

# Acknowledgements

In scientific publications, it is common and even obligatory to acknowledge people who gave you reagents, who made an intellectual observation or performed an experiment, who gave you specific feedback on the manuscript, or otherwise made direct contributions to the experiments described. In the thesis dissertation, one gets the opportunity to thank the people who made intangible, indirect, but even more valuable contributions—those who helped to create an environment both stimulating and supportive of intellectual creativity, those who were scientific mentors and examples, those who provided friendship and support during dark cold room years. I've been in the lab a long time; if this list seems long, remember that this is my one opportunity to print sincere, unabashed thanks to these people.

First, thank you to all the San Francisco members of the Mitchison lab with whom I had the opportunity to interact. Special thanks to Tatsuya Hirano for introducing me to the extract system and being my first mentor; to Ken Sawin, my first bay mate, for late night conversations, for his love of wordplay, and for his gracious company in England at the University of Wye (and why not?); to Lisa Belmont, who first taught me to keep a freezer inventory and whose remarkable tenacity with biochemical purification served as a shining example in my later years; to Matt Welch for his calm methodical approach to biochemistry and for looking so damn good in a cheerleader's dress; to Louise Kramer, whose relentless energy and scientific rigor are balanced by unbelievable kindness; to Heather Deacon, my comrade in arms; to Claire Walczak for mentoring me and Ann



through our first review and for her wisdom over the years; and to Julie Theriot, for turning me on to cellular microbiology during dinner at ASCB.

I also have to thank the old sushi-loving 10<sup>th</sup> floor late-night crew, especially Paul Peluso, whose agility in climbing the arboretum gate in Golden Gate Park with cigars and whiskey in hand was matched only by his ability to elude Park security; Wallace Marshall, who taught me to microinject and is responsible for the tortured deaths of many innocent *Drosophila* embryos; Mike Pollard, who could say “I am here and I have brought the big fish” in at least ten different languages, including Icelandic; and Tom Wang, who introduced me to “Lion in Winter” and whose gentle nature and keen intellect have remained constant over the years.

I thank my fellow classmates for their love and support, especially Dara Friedman, Amy Kistler, Sheila Jaswal, Katherine Lemon, and Becca Smith. Most of all, I thank Marc Lenburg, for his artistic talents, wild creativity, and loving, generous temperament, for leading our expeditions to make soap and olives, and for being a friend in times of need.

I also want to thank Cori Bargmann, for long conversations and martinis at that bar on Haight where you get kicked out if you order anything but a martini; Carol Gross and her mother, both of whom teach a love of life by example; Sue Adams for her wisdom and experience; and Ron Vale and Dave Morgan, who are on my thesis committee, for their patience and support over the years.

In Boston, I again have to thank every Mitchison lab member with whom I've had a chance to interact. I owe a huge debt to so many of you. I am especially grateful to Jason Swedlow, for his help in the coldroom and his irreverent enthusiasm for drilling holes in the walls of Harvard; to Aneil Mallavarapu, whose sparkling wit, sharp intellect, and exacting aesthetic never kept him from indulging in a day off to make me leftover Indian food and watch *The Spy Who Shagged Me*; to Peg Coughlin for her EM expertise and an incredible mac and cheese; to Tarun Kapoor for his critical comments, warm support, and a small carved good luck frog from India; to Puck Ohi, for his infectious enthusiasm for science, sincere generosity with reagents, and many thoughtful discussions; to David Miyamoto, with whom it was a joy to write a review; to Laura Romberg for late-night skinny dipping at Walden Pond and for pushing me to make antibodies against XMAP215; to Steve Miller for his fierce support and daily lunch companionship; to Aaron Groen for his unbelievable energy and positive attitude and for persuading me to visit Woods Hole this summer; to Aaron Straight, for help in the coldroom, for his unquestioning straight-up critical honesty, and for installing a radio in the coldroom and bringing music to the B-team; and to Thomas Mayer, for always believing in me and persuading me to make lemons into lemonade.

Thank you to the Salmonites, who made every visit to Woods Hole a joyous experiment in combining ctenophores, whiskey, herbs, ocean skinny-dipping, long late night conversations, and 16 hours of microscopy at 18°C: Julie Canman, Amy Maddox, Paul Maddox, Ted and Nancy Salmon, and Lisa Cameron, to whom I will here concede that maybe the ocean is an organism.

I owe many thanks to Becky Ward, for her insightful comments, for assembling the Trashy Movie Club, for bringing pizza to the peons unpacking boxes late at the lab, for her loyalty and optimism in dark hours, and for being the person who finally persuaded me to cut that damn band out and get it sequenced.

Thank you to Chris Field, who keeps the lab functioning in so many unquestionable ways, for being my membrane biochemistry buddy and for long talks about life and science in the People's Office.

I sincerely thank all those who helped me with biochemistry, whose scientific rigor and extensive knowledge have been both inspirational and incredibly useful. The following people have been invaluable as mentors and friends: Karen Oegema, who taught me how to calculate spin times and change rotors at two in the morning; Jack Taunton, whose keen intellect, passion for science, and unparalleled taste in music kept me fueled long into the wee hours of the morning; and Bill Brieher, whose cynical hard-nosed stance conceals a gentle and thoughtful soul, who never failed to answer a question, never failed to be endearingly shocked by my vulgarities, and never failed to hold himself or me to the highest scientific standard.

I am also grateful to Arshad Desai, who was probably one of the most influential mentors I've ever had. From my first C2CF labeling to my first CPP MT assay to my first flow-

cell assay, I can trace the steps of the experiments in this thesis back to Arshad, whose intellectual and philosophical perspectives profoundly affected the way that I think today.

Thank you to Ann Yonetani for her love and friendship, for afternoon breaks in the stairwell, for almost getting her homeless boyfriend to build me a loft in the lab, for being the one person I could talk to that one terrible afternoon, and for inspiring me with her endurance and grace.

Thank you to my baymates: to Jennie Timnauer, for her keen insight, for long conversations about things microtubular, for guiding me through every paper-writing passage like a beacon of good judgment and shining logic; and to Zach Perlman, for his constant intellectualism and kindness, for letting me play Britney Spears over and over for days on end, and for helping me to overcome my hatred and fear of computers.

Thank you to the Wells family, for their continual love and support over the years, for welcoming me into their home and their lives, for sledding in the wintertime, and for giving me Quin, if only for a short time.

Thank you to Justin, without whom I might never have graduated. Truly. I owe him more than one human should owe another, especially one decked out with a floppy straw hat and ink-stained jeans. At least he gave up the duct-taped, plastic bagged shoes. Not only did our weekly SubSubGroup meetings flog me onward, but his stubborn loyalty and uncanny ability to make me laugh kept me afloat, even when activity crashed on the

column at the last step at three in the morning. Thanks for believing in me. Thanks for helping me to maintain precious perspective. And thanks for not running when I threw a brick at that security guard by accident.

Thanks to my writing group (Stephanie Neely-Aude, Liana Tuller, Audrey Kalmus, Nagi Ayad, Helen Bronk, and Andy Calafut) for keeping me sane.

Thank you to Tim, of course, whose brilliance and creativity are matched only by his intense passion for science and who has probably shaped my thinking more than any other. There is no question that the decision to move to Boston was an incredibly positive turning point in my life. Thank you for being patient; for taking me seriously; for giving me the freedom to make mistakes and learn hard lessons; for standing by me when it really counted; for sending Don a scathing letter of rebuttal when I was prepared to grovel; and for teaching me to think deeply and critically about every problem, whether it's about  $K^+$  versus  $Na^+$  salt, the fundamental mechanisms underlying mitotic spindle assembly, or the actual best song from Madonna's early years.

Thank you to my family, whose unquestioning love and support have sustained me for so long: my mom and dad, my sister Leslie, brother-in-law Ryan, and brother Stewart. I appreciate you with all my heart.

And most of all, thank you to my husband and best friend, Joel Shirasu-Hiza.

**The Rockefeller  
University Press**

1114 First Avenue, 4th Floor  
New York, New York 10021  
(212) 327-8025  
Fax (212) 327-8589

August 18, 2003

**Michele Mie Shirasu-Hiza  
39 Braddock Park # 3  
Boston, MA 02126**

**Dear Ms. Shirasu-Hiza:**

We will grant you permission for the print reproduction of JCB – vol:161(2), pgs. 349-358, 2003 - article as referred to in your letter dated August 14, 2003.

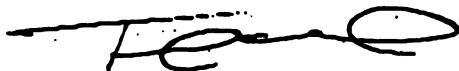
Permission is granted for one time use only. Please write to us each time for permission concerning future editions and translations, as we do not grant blanket permissions.

Since you are the author, a credit line is our only requirement.

We request that you please give suitable acknowledgment to the source in the following manner: Reproduced from **The Journal of Cell Biology**, year, vol., pp. by copyright permission of The Rockefeller University Press.

Sincerely yours,

**THE JOURNAL OF  
CELL BIOLOGY**



**Tracee Scott  
Permissions Coordinator**

Date: Thu, 21 Aug 2003 11:18:34 -0400  
From: "meijerl@mail.rockefeller.edu" <meijerl@mail.rockefeller.edu>  
To: "Shirasu-Hiza, Michele Mie" <michele\_shirasu@hms.harvard.edu>  
Subject: Re: reprint request  
X-OriginalArrivalTime: 21 Aug 2003 15:22:24.0505 (UTC)  
FILETIME=[05E68690:01C367F8]

Dear Ms. Shirasu-Hiza,

We grant you permission for the print reproduction of Chapter 35 from Progress in Cell Cycle Research, Vol. 5, 349-360, (2003), "Dynamics of the mitotic spindle - potential therapeutic targets".

Sincerely,  
Dr. Laurent Meijer  
<meijer@sb-roscoff.fr>



PERMISSIONS DEPARTMENT  
111 River Street  
Hoboken, NJ 07030

TEL 201.748.6000  
FAX 201.748.6008

August 25, 2003

Mimi Shirasu-Hiza  
39 Braddock Park #3  
Boston, MA 02126  
VIA FACSIMILE: 617 432 3702

Dear Ms. Shirasu-Hiza:

**RE:** Your August 14, 2003 request for permission to republish pages 435-445 from *Microscopy Research and Technique* (1999) Vol. 44. This material will appear in your forthcoming dissertation, to be published by University of California/San Francisco in 2003.

1. Permission is granted for this use, except that if the material appears in our work with credit to another source, you must also obtain permission from the original source cited in our work.
2. Permitted use is limited to your edition described above, and does not include the right to grant others permission to photocopy or otherwise reproduce this material except for versions made for use by visually or physically handicapped persons. Up to five copies of the published thesis may be photocopied by a microfilm company.
3. Appropriate credit to our publication must appear on every copy of your thesis, either on the first page of the quoted text, in a separate acknowledgment page, or figure legend. The following components must be included: Title, author(s) and /or editor(s), journal title (if applicable), Copyright © 1999 Wiley-Liss, Inc., a subsidiary of John Wiley & Sons, Inc.. Reprinted by permission of John Wiley & Sons, Inc.
4. This license is non-transferable. This license is for non-exclusive English language print rights and microfilm storage rights by University of California/San Francisco only, throughout the world. *For translation rights, please reapply for a license when you have plans to translate your work into a specific language.*

Sincerely,

  
Paulette Goldweber  
Senior Permissions Asst.



# **Mitotic Microtubule Depolymerization and XMAP215**

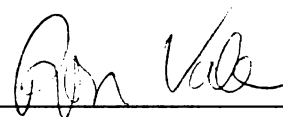
by Michele Shirasu-Hiza

## **Abstract**

The work in this thesis was directed toward understanding the regulation of microtubule dynamics in the mitotic spindle, specifically focusing on microtubule depolymerization and the microtubule dynamics regulator XMAP215. Chapter 1 examines the role of microtubule depolymerization in a complex spindle microtubule behavior called poleward microtubule flux, defined as the poleward translocation of spindle microtubules coupled to net polymerization at microtubule plus ends and net depolymerization at minus ends. We present evidence here that net minus end depolymerization can be uncoupled from poleward microtubule translocation, using a combination of reagents that caused spindles made in *Xenopus* egg extract to elongate at the rate of microtubule translocation. Though the energy released from microtubule depolymerization can be converted to mechanical force, this result suggests that minus end depolymerization does not provide the driving force for poleward flux.

During the course of experiments described above, it became clear that *Xenopus* egg extract contained microtubule destabilizing activity independent of the known destabilizing factors. As detailed in Chapter 2, we purified the factor responsible for this novel depolymerizing activity using biochemical fractionation and a functional assay and

identified it as XMAP215, previously identified as a prominent microtubule growth promoting protein in *Xenopus* extracts. The apparently contradictory behavior of XMAP215, able to increase both polymerization and depolymerization rates, led us to propose that XMAP215 might act as an anti-pause factor, destabilizing a semi-stable third state predicted to exist between growth and shrinkage. In Chapter 3, we describe our progress in exploring the molecular mechanism of XMAP215 and present evidence that XMAP215 stimulates nucleotide exchange in tubulin subunits of the microtubule lattice.



---

**Ron Vale, PhD**

**(Committee Chairman)**

**David Morgan, PhD**

**(Committee Member)**

**Timothy Mitchison, PhD**

**(Thesis Advisor)**

# Table of Contents

		page
Introduction		1
Chapter One	Minus-end Microtubule Depolymerization during Poleward Microtubule Flux	15
Chapter Two	Biochemical Purification of a Microtubule Destabilizing Factor from Xenopus Egg Extract	54
Chapter Three	Molecular Mechanism of XMAP215	102
Appendix I	Microtubule Dynamics in Xenopus Egg Extract	121
Appendix II	Dynamics of the Mitotic Spindle – Potential Therapeutic Targets	133

# List of Figures and Tables

		page
Figure 1-1	<i>Addition of both p50 and Xk1p2 tail results in lengthwise spindle elongation</i>	48
Figure 1-2	<i>Models for spindle elongation induced by p50+Xk1p2 tail</i>	49
Figure 1-3	<i>The rate of spindle elongation in p50/Xk1p2 tail spindles correlates with their flux rate</i>	50
Figure 1-4	<i>p50 and Xk1p2 tail additions have similar phenotypes in DNA bead spindles</i>	51-52
Figure 1-5	<i>p50/XK1p2 tail-induced spindle elongation is inhibited by AMPPNP</i>	53
Table 2-1	<i>Purification table</i>	93
Figure 2-1	<i>There is a GMPCPP microtubule depolymerizing activity in Xenopus egg extract independent of XKCM1.</i>	94
Figure 2-2	<i>Proteins of 130 and 160 kD were enriched during the purification and consistently co-peaked with activity.</i>	95
Figure 2-3	<i>XMAP215 contributes to GMPCPP microtubule depolymerizing activity in CSF extract.</i>	96
Figure 2-4	<i>Pure recombinant XMAP215 depolymerizes GMPCPP microtubules in vitro.</i>	97
Figure 2-5	<i>XMAP215 promotes GMPCPP microtubule depolymerization at microtubule plus ends.</i>	98

	page	
Figure 2-6	<i>Mechanism of GMPCPP microtubule depolymerization by XMAP215</i>	99
Figure 2-7	<i>Model for the potential mechanism of XMAP215 as an anti-pause factor.</i>	100
Figure S-1	<i>Depletion of XMAP215 inhibited centrosome-nucleated MT polymerization.</i>	101
Figure S-2	<i>Gel of recombinant proteins used for in vitro GMPCPP microtubule depolymerization assays.</i>	101
Figure 3-1	<i>XMAP215 depolymerization of CPP MTs in vitro is inhibited by exogenous GMPCPP</i>	119
Figure 3-2	<i>XMAP215 stimulates nucleotide exchange in CPP MTs</i>	120
Figure AI-1	<i>Microtubule morphology changes dramatically during the cell cycle</i>	123
Figure AI-2	<i>Dynamic behavior of microtubule polymers</i>	124
Figure AI-3	<i>Poleward microtubule flux (a) versus microtubule treadmilling</i>	128
Figure AI-4	<i>Overview of several molecular mechanisms involved in changing microtubule morphology/dynamics from interphase to mitosis</i>	129

Figure AII-1	<i>A. Four parameters are conventionally measured to describe microtubule dynamics.</i>	135
	<i>B. Tubulin inhibitors and microtubule-associated proteins affect the dynamics of microtubules</i>	
Figure AII-2	<i>Many distinct activities are required between chromosome condensation and sister chromatid separation</i>	135
Table AII-1	<i>Some potential drug targets in the spindle</i>	137
Figure AII-3	<i>Several assays that measure the activity of microtubule regulators can be adapted to high throughput format in multi-well plates.</i>	138
Figure AII-4	<i>Small molecule inhibitors of Eg5 result in monoastrial mitotic figures and mitotic arrest</i>	141

# **Introduction**

## Overview

Since the late 19<sup>th</sup> century, cell biologists have been fascinated by the question of how cells organize and faithfully transfer essential contents during the process of cell division. Early drawings by Walther Fleming and others (reviewed in (Wilson, 1928)) revealed a dramatic fusiform structure (now known as the mitotic spindle) composed of long fibers (microtubules) attached to paired threads (chromosomes). Later, observations of the active oscillatory motion of chromosomes in live cells indicated that the mitotic spindle is not a static scaffold (for review, see (Rieder and Khodjakov, 2003)). We now understand that the mitotic spindle is a complex and dynamic structure whose behavior reflects a number of distinct, spatially organized mechanical processes. Today, study of the mitotic spindle focuses on dissecting these mechanical processes into individual component forces, identifying the specific molecular factors involved in generating these forces, and understanding the mechanisms by which these molecular factors convert chemical energy into mechanical force.

The core structure of the mitotic spindle is made up of dynamic polymers called microtubules. Microtubules are hollow tubes, 25 nm in diameter, composed of 9 to 18 (but usually 13-14) laterally associated protofilaments (Chretien et al., 1992); each protofilament is made up of a linear, noncovalent head-to-tail arrangement of  $\alpha/\beta$  tubulin heterodimers. A microtubule thus has intrinsic polarity— $\beta$ -tubulin subunits are exposed at one end (the plus end), and  $\alpha$ -tubulin subunits are exposed at the other (the minus end) (Nogales et al., 1999). Each tubulin monomer binds a guanine nucleotide:  $\alpha$  tubulin binds GTP at a non-exchangeable, non-hydrolytic site (the N-site);  $\beta$  tubulin binds nucleotide at an exchangeable, hydrolyzing site (the E site) (Weisenberg et al., 1968).



GTP is required at the E-site for microtubule assembly (O'Brien and Erickson, 1989; Weisenberg et al., 1976) and is hydrolyzed concomitant with or soon after tubulin dimer associates with the end of a microtubule (David-Pfeuty et al., 1977; MacNeal and Purich, 1978; O'Brien et al., 1987; Vandecandelaere et al., 1999). Thus the microtubule lattice contains mainly tubulin with GDP in their E sites (we refer to these subunits as "GDP-tubulin")(Kobayashi, 1975), except for the E sites of very recently added tubulin subunits, which contain either GTP or GDP and Pi (GTP/GDP-Pi tubulin) (Panda et al., 2002; Voter et al., 1991).

This ability to hydrolyze GTP appears to underlie the unusual polymer dynamics of microtubules (for review, see(Desai and Mitchison, 1997)). Microtubules exhibit a non-equilibrium behavior termed dynamic instability, which is characterized by the coexistence of growing and shrinking microtubules in the same solution, with individual microtubules switching stochastically between the two (Kristofferson et al., 1986; Mitchison and Kirschner, 1984). The transition between growth and shrinkage is called catastrophe; the transition between shrinkage and growth is called rescue. The current model for dynamic instability postulates that the polymerization behavior of an individual microtubule is determined by the nucleotide content of tubulin subunits at its microtubule ends. During polymerization, microtubule ends are stabilized by newly-added GTP/GDP-Pi tubulin subunits, which quickly hydrolyze to GDP-tubulin. If GDP-tubulin subunits become exposed at the microtubule end, catastrophe is triggered and the microtubule depolymerizes. Depolymerizing ends can be rescued by the association of GTP-tubulin.

Structurally, it is thought that nucleotide content determines the preferred curvature of tubulin protofilaments: GTP-tubulin protofilaments are “straight”, while GDP-tubulin protofilaments are “curved” (Howard and Timasheff, 1986; Hyman et al., 1995; Nicholson et al., 1999). The curvature of protofilaments at the microtubule end is correlated with its polymerization behavior: by cryo-electron microscopy, growing microtubule ends have straight sheet-like structures and shrinking ends have curved “rams’ horns” of protofilaments (Arnal et al., 2000; Chretien et al., 1995; Mandelkow et al., 1986). The overall structure of a microtubule is straight, despite the fact that it is thought to consist primarily of GDP-tubulin” (Kobayashi, 1975). GDP-tubulin subunits in the microtubule lattice are presumably constrained to the straight conformation by interprotofilament bonds. This allows the chemical energy of hydrolysis to be “stored” in the microtubule lattice as mechanical strain (Caplow et al., 1994). When this free energy is released during depolymerization, it can be converted to mechanical force (Coue et al., 1991; Koshland et al., 1988; Lombillo et al., 1995), which is thought to drive some of the physical movements of chromosomes in the mitotic spindle.

Though dynamic instability is an intrinsic behavior of pure microtubules, multiple molecular factors are known to modulate microtubule dynamics spatially and temporally *in vivo*. The work presented here investigates microtubule dynamics in the mitotic spindle, specifically focusing on cellular regulation of microtubule depolymerization. In this introduction, I will first discuss the spatial organization of microtubule dynamics in the mitotic spindle and present our investigation of minus end microtubule depolymerization. Next I will describe the biochemical purification of a major microtubule depolymerizer from *Xenopus* egg extract; and finally, we outline our

progress in exploring the molecular mechanism of this depolymerizing factor, focusing on the possibility that it stimulates nucleotide exchange in tubulin subunits of the microtubule lattice.

### **Organization of microtubule dynamics**

To understand microtubule dynamics in the mitotic spindle one must first define the spatial organization of those dynamics. In the mitotic spindle of higher eukaryotes, microtubules are arranged in two antiparallel populations, each population organized with plus ends extending toward the chromosomes in the middle of the spindle and minus ends pointed toward the spindle poles (Euteneuer and McIntosh, 1981; Mastronarde et al., 1993; McIntosh and Euteneuer, 1984). As shown by photobleaching studies, the majority of microtubules in the spindle turn over rapidly, on the time scale of seconds (Salmon et al., 1984; Saxton et al., 1984). Microinjection of biotin-labeled tubulin demonstrated that tubulin incorporated preferentially into microtubule plus ends (Mitchison et al., 1986). Direct observation of microtubules confirm that, though both plus and minus ends exhibit dynamic instability *in vitro*, only the plus end appears to undergo dynamic instability *in vivo* (Belmont et al., 1990; Rusan et al., 2001; Tirnauer et al., 2002).

Minus ends instead appear to undergo slow and constant depolymerization, in a complex process called poleward microtubule flux. The first definitive evidence for this minus end depolymerization was obtained from photoactivation studies of mammalian tissue culture cells (Mitchison, 1989). Fluorescent marks made on spindle microtubules moved poleward over time. This overall microtubule translocation appears to result from a highly coordinated combination of net polymerization at microtubule plus ends and

equal net depolymerization at minus ends. One can think of poleward flux as microtubule treadmilling combined with translocation. It was originally called “flux” rather than treadmilling in order to avoid the implication that this was an *in vitro* equilibrium behavior arising from differential affinities at each end of the polymer (Margolis and Wilson, 1981; Mitchison, 1989).

The discovery of poleward flux, which could generate a “pulling” force on chromosomes, stimulated interest in older hypotheses postulating that depolymerizing microtubules could generate enough force to move chromosomes apart during segregation. The mechanical force generated by poleward flux might be exploited by a number of processes, including chromosome oscillation, a tension-sensing mitotic checkpoint, or chromosome segregation. Poleward flux does appear to contribute to chromosome segregation in meiotic *Xenopus* egg extract spindles (Desai et al., 1998), but none of the molecular factors required for poleward flux have been identified and its function in mitotic cells remains elusive.

Chapter one describes our investigation of flux-associated minus end microtubule depolymerization. Using a combination of reagents that cause spindle elongation in *Xenopus* egg extract, we show that minus end depolymerization can be uncoupled from poleward microtubule translocation. This result suggested that minus end depolymerization does not provide the driving force for poleward flux, leaving open the question of how poleward flux is generated and what its cellular function might be.

### **Control of microtubule depolymerization**

To explain some of our observations in the work described in Chapter 1, we hypothesized that there was an unidentified factor responsible for a large amount of microtubule depolymerization during mitosis. We set out to biochemically purify this unidentified depolymerizing factor(s) from *Xenopus* egg extract using conventional chromatography and a functional assay. Chapter Two describes the surprising identification of a protein called XMAP215 as a major microtubule destabilizing factor in *Xenopus* egg extract. XMAP215 had previously been identified as a major microtubule stabilizing factor from *Xenopus* egg extract, using biochemical fractionation and a visual assay for microtubule polymerization (Gard and Kirschner, 1987).

The apparently contradictory behavior of XMAP215, able to increase both polymerization and depolymerization rates, led us to a structurally-based model for its mechanism. In our biochemical purification, we used GMPCPP-stabilized microtubules (CPP MTs) as the substrate for our depolymerization assay. By electron microscopy, these microtubules have blunt ends (Desai et al., 1999; Shirasu-Hiza et al., 2003) and do not resemble growing microtubule ends (open sheets) or shrinking ends (rams' horns) (Arnal et al., 2000; Chretien et al., 1995; Mandelkow et al., 1986). We propose that blunt-ended CPP MTs instead present a model for the microtubule pause state, a semi-stable intermediate predicted to exist between growth and shrinkage (Tran et al., 1997). Thus XMAP215 might act as an anti-pause factor, destabilizing this intermediate state to push microtubules into either growth or shrinkage depending on environmental cues such as buffer, temperature, tubulin concentration, and other proteins. Our model of XMAP215 as an anti-pause factor potentially provides a unifying hypothesis to explain the behavior of XMAP215 in different contexts.

## **Molecular mechanism of XMAP215**

One mechanism by which XMAP215 might destabilize a microtubule end is to affect its nucleotide content. GTPases often have accessory proteins that affect their nucleotide content: GAPs (or GTP activating proteins) stimulate GTPases to hydrolyze their bound nucleotide; and GEFs (or GTP exchange factors) catalyze GTPases to release their bound nucleotide. Currently, tubulin (and its prokaryotic homologue, FtsZ) has no identified GEF. Tubulin dimer in solution has a low level of GTPase activity which is stimulated by the dimer sequestration and catastrophe factor, op18 (Amayed et al., 2000; Larsson et al., 1999). Structural data also offer tantalizing hints that tubulin may act as its own GAP in a microtubule. Residues from the  $\alpha$ -tubulin of one subunit appear to interact with the E-site of  $\beta$ -tubulin in the adjacent subunit (Nogales et al., 1999). In Chapter 2, we showed that XMAP215 does not act as a GAP for tubulin subunits in the microtubule lattice. We therefore explored the possibility that XMAP215 might instead stimulate nucleotide exchange. Although pure tubulin dimer in solution rapidly exchanges nucleotide with a half-life of 5 seconds (Brylawski and Caplow, 1983), tubulin subunits within the microtubule lattice are not thought to exchange their bound nucleotide except for  $\beta$ -tubulin subunits with exposed E-sites at the very tip of the microtubule plus end ((Caplow et al., 1984; Carlier and Pantaloni, 1981; Weisenberg et al., 1976), personal communication, T. Mitchison). In Chapter 3, we present evidence suggesting that XMAP215 increases both the rate and amount of nucleotide exchange in the microtubule lattice. We are currently trying to determine the exact proportion and sites of exchange. This model for the mechanism of XMAP215 as a nucleotide exchange factor for tubulin

subunits in the microtubule lattice extends our previous model and may provide insight into the molecular mechanism of dynamic instability.

Many of the important factors that regulate microtubule dynamics already seem to have been identified, either by their *in vitro* activity, through sequence gazing, or by their subcellular localization. However, it is clear that basic questions still remain. Further exploration of how microtubule regulating factors interact with each other *in vivo* and how they affect microtubule dynamics on structural and chemical level should help us to understand the complex mechanical forces underlying mitotic spindle assembly and chromosome segregation.

## References

- Amayed, P., M.F. Carrier, and D. Pantaloni. 2000. Stathmin slows down guanosine diphosphate dissociation from tubulin in a phosphorylation-controlled fashion. *Biochemistry*. 39:12295-302.
- Arnal, I., E. Karsenti, and A.A. Hyman. 2000. Structural transitions at microtubule ends correlate with their dynamic properties in *Xenopus* egg extracts. *J Cell Biol*. 149:767-74.
- Belmont, L.D., A.A. Hyman, K.E. Sawin, and T.J. Mitchison. 1990. Real-time visualization of cell cycle-dependent changes in microtubule dynamics in cytoplasmic extracts. *Cell*. 62:579-89.
- Brylawski, B.P., and M. Caplow. 1983. Rate for nucleotide release from tubulin. *J Biol Chem*. 258:760-3.

- Caplow, M., B.P. Brylawski, and R. Reid. 1984. Mechanism for nucleotide incorporation into steady-state microtubules. *Biochemistry*. 23:6745-52.
- Caplow, M., R.L. Ruhlen, and J. Shanks. 1994. The free energy for hydrolysis of a microtubule-bound nucleotide triphosphate is near zero: all of the free energy for hydrolysis is stored in the microtubule lattice. *J Cell Biol*. 127:779-88.
- Carrier, M.F., and D. Pantaloni. 1981. Kinetic analysis of guanosine 5'-triphosphate hydrolysis associated with tubulin polymerization. *Biochemistry*. 20:1918-24.
- Chretien, D., S.D. Fuller, and E. Karsenti. 1995. Structure of growing microtubule ends: two-dimensional sheets close into tubes at variable rates. *J Cell Biol*. 129:1311-28.
- Chretien, D., F. Metoz, F. Verde, E. Karsenti, and R.H. Wade. 1992. Lattice defects in microtubules: protofilament numbers vary within individual microtubules. *J Cell Biol*. 117:1031-40.
- Coue, M., V.A. Lombillo, and J.R. McIntosh. 1991. Microtubule depolymerization promotes particle and chromosome movement in vitro. *J Cell Biol*. 112:1165-75.
- David-Pfeuty, T., H.P. Erickson, and D. Pantaloni. 1977. Guanosinetriphosphatase activity of tubulin associated with microtubule assembly. *Proc Natl Acad Sci U S A*. 74:5372-6.
- Desai, A., P.S. Maddox, T.J. Mitchison, and E.D. Salmon. 1998. Anaphase A chromosome movement and poleward spindle microtubule flux occur at similar rates in *Xenopus* extract spindles. *J Cell Biol*. 141:703-13.
- Desai, A., and T.J. Mitchison. 1997. Microtubule polymerization dynamics. *Annu Rev Cell Dev Biol*. 13:83-117.



- Desai, A., S. Verma, T.J. Mitchison, and C.E. Walczak. 1999. Kin I kinesins are microtubule-destabilizing enzymes. *Cell*. 96:69-78.
- Euteneuer, U., and J.R. McIntosh. 1981. Structural polarity of kinetochore microtubules in PtK1 cells. *J Cell Biol*. 89:338-45.
- Gard, D.L., and M.W. Kirschner. 1987. A microtubule-associated protein from *Xenopus* eggs that specifically promotes assembly at the plus-end. *J Cell Biol*. 105:2203-15.
- Howard, W.D., and S.N. Timasheff. 1986. GDP state of tubulin: stabilization of double rings. *Biochemistry*. 25:8292-300.
- Hyman, A.A., D. Chretien, I. Arnal, and R.H. Wade. 1995. Structural changes accompanying GTP hydrolysis in microtubules: information from a slowly hydrolyzable analogue guanylyl-(alpha,beta)-methylene-diphosphonate. *J Cell Biol*. 128:117-25.
- Kobayashi, T. 1975. Dephosphorylation of tubulin-bound guanosine triphosphate during microtubule assembly. *J Biochem (Tokyo)*. 77:1193-7.
- Koshland, D.E., T.J. Mitchison, and M.W. Kirschner. 1988. Polewards chromosome movement driven by microtubule depolymerization in vitro. *Nature*. 331:499-504.
- Kristofferson, D., T. Mitchison, and M. Kirschner. 1986. Direct observation of steady-state microtubule dynamics. *J Cell Biol*. 102:1007-19.
- Larsson, N., B. Segerman, B. Howell, K. Fridell, L. Cassimeris, and M. Gullberg. 1999. Op18/stathmin mediates multiple region-specific tubulin and microtubule-regulating activities. *J Cell Biol*. 146:1289-302.

- Lombillo, V.A., C. Nislow, T.J. Yen, V.I. Gelfand, and J.R. McIntosh. 1995. Antibodies to the kinesin motor domain and CENP-E inhibit microtubule depolymerization-dependent motion of chromosomes in vitro. *J Cell Biol.* 128:107-15.
- MacNeal, R.K., and D.L. Purich. 1978. Stoichiometry and role of GTP hydrolysis in bovine neurotubule assembly. *J Biol Chem.* 253:4683-7.
- Mandelkow, E.M., R. Rapp, and E. Mandelkow. 1986. Microtubule structure studied by quick freezing: cryo-electron microscopy and freeze fracture. *J Microsc.* 141 ( Pt 3):361-73.
- Margolis, R.L., and L. Wilson. 1981. Microtubule treadmills--possible molecular machinery. *Nature.* 293:705-11.
- Mastrorade, D.N., K.L. McDonald, R. Ding, and J.R. McIntosh. 1993. Interpolar spindle microtubules in PTK cells. *J Cell Biol.* 123:1475-89.
- McIntosh, J.R., and U. Euteneuer. 1984. Tubulin hooks as probes for microtubule polarity: an analysis of the method and an evaluation of data on microtubule polarity in the mitotic spindle. *J Cell Biol.* 98:525-33.
- Mitchison, T., L. Evans, E. Schulze, and M. Kirschner. 1986. Sites of microtubule assembly and disassembly in the mitotic spindle. *Cell.* 45:515-27.
- Mitchison, T., and M. Kirschner. 1984. Dynamic instability of microtubule growth. *Nature.* 312:237-42.
- Mitchison, T.J. 1989. Polewards microtubule flux in the mitotic spindle: evidence from photoactivation of fluorescence. *J Cell Biol.* 109:637-52.
- Nicholson, W.V., M. Lee, K.H. Downing, and E. Nogales. 1999. Cryo-electron microscopy of GDP-tubulin rings. *Cell Biochem Biophys.* 31:175-83.

- Nogales, E., M. Whittaker, R.A. Milligan, and K.H. Downing. 1999. High-resolution model of the microtubule. *Cell*. 96:79-88.
- O'Brien, E.T., and H.P. Erickson. 1989. Assembly of pure tubulin in the absence of free GTP: effect of magnesium, glycerol, ATP, and the nonhydrolyzable GTP analogues. *Biochemistry*. 28:1413-22.
- O'Brien, E.T., W.A. Voter, and H.P. Erickson. 1987. GTP hydrolysis during microtubule assembly. *Biochemistry*. 26:4148-56.
- Panda, D., H.P. Miller, and L. Wilson. 2002. Determination of the size and chemical nature of the stabilizing "cap" at microtubule ends using modulators of polymerization dynamics. *Biochemistry*. 41:1609-17.
- Rieder, C.L., and A. Khodjakov. 2003. Mitosis through the microscope: advances in seeing inside live dividing cells. *Science*. 300:91-6.
- Rusan, N.M., C.J. Fagerstrom, A.M. Yvon, and P. Wadsworth. 2001. Cell cycle-dependent changes in microtubule dynamics in living cells expressing green fluorescent protein-alpha tubulin. *Mol Biol Cell*. 12:971-80.
- Salmon, E.D., R.J. Leslie, W.M. Saxton, M.L. Karow, and J.R. McIntosh. 1984. Spindle microtubule dynamics in sea urchin embryos: analysis using a fluorescein-labeled tubulin and measurements of fluorescence redistribution after laser photobleaching. *J Cell Biol*. 99:2165-74.
- Saxton, W.M., D.L. Stemple, R.J. Leslie, E.D. Salmon, M. Zavortink, and J.R. McIntosh. 1984. Tubulin dynamics in cultured mammalian cells. *J Cell Biol*. 99:2175-86.

- Shirasu-Hiza, M., P. Coughlin, and T. Mitchison. 2003. Identification of XMAP215 as a microtubule-destabilizing factor in *Xenopus* egg extract by biochemical purification. *J Cell Biol.* 161:349-58.
- Tirnauer, J.S., J.C. Canman, E.D. Salmon, and T.J. Mitchison. 2002. EB1 targets to kinetochores with attached, polymerizing microtubules. *Mol Biol Cell.* 13:4308-16.
- Tran, P.T., R.A. Walker, and E.D. Salmon. 1997. A metastable intermediate state of microtubule dynamic instability that differs significantly between plus and minus ends. *J Cell Biol.* 138:105-17.
- Vandecandelaere, A., M. Brune, M.R. Webb, S.R. Martin, and P.M. Bayley. 1999. Phosphate release during microtubule assembly: what stabilizes growing microtubules? *Biochemistry.* 38:8179-88.
- Voter, W.A., E.T. O'Brien, and H.P. Erickson. 1991. Dilution-induced disassembly of microtubules: relation to dynamic instability and the GTP cap. *Cell Motil Cytoskeleton.* 18:55-62.
- Weisenberg, R.C., G.G. Borisy, and E.W. Taylor. 1968. The colchicine-binding protein of mammalian brain and its relation to microtubules. *Biochemistry.* 7:4466-79.
- Weisenberg, R.C., W.J. Deery, and P.J. Dickinson. 1976. Tubulin-nucleotide interactions during the polymerization and depolymerization of microtubules. *Biochemistry.* 15:4248-54.
- Wilson, E.B. 1928. *The Cell in Development and Heredity.* MacMillan, New York.

## **Chapter 1**

# **Minus-end Microtubule Depolymerization during Poleward Microtubule Flux**

I performed all the experiments described in this chapter. This work was done in collaboration with Dr. Torsten Wittman, currently at UC San Diego, CA, who originally brought the phenotype of p50/Xklp2 tail addition to my attention and with whom I performed the DNA bead spindle experiments.

**p50 and Xklp2 Tail Domain Together Inhibit Minus End Microtubule  
Depolymerization in Xenopus Extract Spindles**

Mimi Shirasu-Hiza\*, Torsten Wittman#, and Timothy J. Mitchison<sup>§</sup>

\*Department of Biochemistry, University of California, San Francisco

#Department of Cell Biology, Scripps Research Institute, La Jolla

<sup>§</sup>Department of Cell Biology, Harvard Medical School, Boston

## **Abstract**

Poleward microtubule flux in the mitotic spindle involves at least three mechanistic components: growth at microtubule plus ends, shrinkage at minus ends, and translocation of the microtubule lattice toward spindle poles. These components are closely coupled, resulting in a spindle that does not change in length over time. However, simultaneous addition of two proteins, p50/dynamitin (a component of the dynactin complex) and a truncated version of the kinesin-related motor protein Xklp2 (Xklp2 tail), to spindles made in meiotic *Xenopus* egg extracts resulted in lengthwise spindle elongation. We show that this elongation occurred at a rate similar to poleward microtubule flux and propose that elongation is due to specific inhibition of minus end microtubule depolymerization with continued plus end growth and poleward translocation.

## **Introduction**

A major focus in the study of cell division of higher eukaryotes is the complex regulation of dynamic components in the mitotic spindle, a microtubule-based structure that ensures correct segregation of duplicated chromosomes. Until chromosome segregation, the mitotic spindle appears to be a static structure of stable average length. However, individual component microtubules have variable lengths (Mastronarde et al., 1993) and change in length rapidly and often (Tirnauer et al., 2002). This dynamic behavior is intimately linked to spindle assembly and function. Direct perturbations of microtubule dynamics arrest cells in mitosis and correlate with overall changes in average spindle length—for example, addition of drugs like paclitaxel at levels that inhibit dynamic behavior result in small spindles (Jordan et al., 1993; Waters et al., 1996), whereas

addition of growth-promoting reagents like DMSO or D<sub>2</sub>O (deuterium oxide) can make spindles both longer and wider (Krendel and Inoue, 1995; Sawin and Mitchison, 1994). Perturbations of microtubule-regulating proteins (ie, XMAP215) can also affect average spindle length (Tournebize et al., 2000) and disrupt proper segregation of chromosomes (Cullen et al., 1999). Spindle length therefore provides a useful (though crude) read-out for microtubule dynamics in the spindle, and agents which perturb spindle length provide important tools for further understanding of these dynamics.

An important issue in studying the regulation of microtubule dynamics in the spindle is defining the nature and spatial organization of those dynamics. Microtubules are polymers of intrinsic polarity, with a slow-growing minus end and a fast-growing plus end (Allen and Borisy, 1974); in the mitotic spindle, microtubules are arranged with their minus ends at the poles and plus ends extending toward the center of the spindle (Euteneuer and McIntosh, 1981; Mastronarde et al., 1993; McIntosh and Euteneuer, 1984). Microinjection of biotin-labeled tubulin into mitotic cells followed by rapid fixation revealed that tubulin preferentially incorporates into microtubule plus ends on the time-scale of seconds (Mitchison et al., 1986). Microtubule plus ends undergo a non-equilibrium behavior called dynamic instability, stochastically interconverting between phases of rapid growth and shrinkage. Microtubule minus ends do not exhibit dynamic instability but appear to undergo slow and constant depolymerization as part of a complex process called poleward microtubule flux.

We define poleward flux as the translocation of microtubules in both halves of the mitotic spindle to their associated pole, with no change in average spindle length.

Poleward microtubule flux is perhaps best illustrated by the following photoactivation



experiment (Mitchison, 1989). Tubulin labeled with a caged carboxyfluorescein derivative was allowed to incorporate into spindle microtubules and then activated with a bar of UV light, perpendicular to the pole-to-pole spindle axis. This created a bar of fluorescent tubulin in the middle of the spindle. Over time, this bar split in two and each bar “migrated” to the nearest pole at constant rate. Because tubulin subunits are incorporated into microtubules, this demonstrated that the microtubules themselves are translocating toward the poles. Poleward flux has also been observed by fluorescent speckle microscopy (FSM), in which a small amount of fluorescently labeled tubulin is incorporated into spindle microtubules to create “speckles” or fiduciary marks which can then be used to track microtubule movement (Waterman-Storer et al., 1999). Though microtubules translocate toward the poles, average spindle length does not change, implying that this translocation is coupled to net subunit loss at spindle poles (microtubule minus ends) and an equal net subunit gain in the middle of the spindle (at microtubule plus ends). One can think of poleward flux as a combination of microtubule treadmilling and translocation; it was called “flux” rather than treadmilling in order to avoid confusion with *in vitro* equilibrium dynamics arising from differential affinities at each end of the polymer (Margolis and Wilson, 1981; Mitchison, 1989).

Though many cellular factors are known to regulate plus end dynamic instability, none of the factors involved in poleward flux have been identified. Flux has been observed in several different cell types (Maddox et al., 2002; Mitchison, 1989; Mitchison and Salmon, 1992; Wilson et al., 1994) as well as in spindles made in *Xenopus* egg extract (Sawin and Mitchison, 1991). It has been demonstrated *in vitro* that the energy released during microtubule depolymerization can be converted to mechanical force

(Coue et al., 1991; Koshland et al., 1988; Lombillo et al., 1995). The discovery of poleward flux, which could generate a “pulling” force on chromosomes, stimulated interest in hypotheses postulating that depolymerizing microtubules could generate enough force to move chromosomes apart during segregation. The mechanical force generated by poleward flux might be exploited by a number of processes, including chromosome oscillation, a tension-sensing spindle assembly checkpoint, or chromosome segregation. Poleward flux does appear to contribute significantly to chromosome segregation in meiotic *Xenopus* egg extract spindles (Desai et al., 1998); however, flux contributes less significantly to anaphase A in mitotic cells (Mitchison and Salmon, 1992; Zhai et al., 1995). Thus the major function of poleward flux in mitotic cells remains elusive.

In this work, we examine whether minus end depolymerization produces the force that translocates microtubules poleward during poleward flux. Though we can dissect poleward flux into three mechanistic components (poleward microtubule translocation, plus end polymerization, and minus end depolymerization), it is not clear if these components are mechanistically or molecularly separable. Is one factor responsible for all three components or are there three separate factors, one at microtubule plus ends, another translocating microtubules, and a third at spindle poles? Which of these components provides the driving force for flux? In other words, is the rate of poleward movement determined by the rate of translocation factors, by the rate of plus end polymerization, or by the rate of minus end depolymerization? An important step toward answering these questions is defining which mechanistic components, if any, are

independent of the others. We set out to find conditions that would specifically inhibit minus end depolymerization.

Currently there are only two known inhibitors of flux: AMPPNP, a non-hydrolyzable ATP analogue that inhibits a range of ATPases; and paclitaxel, a potent microtubule stabilizing drug. Addition of AMPPNP to *Xenopus* spindles *in vitro* inhibited poleward microtubule translocation and caused no change in spindle length (Sawin and Mitchison, 1991). This result implies that microtubule translocation, plus end polymerization, and minus end depolymerization were all inhibited. Addition of paclitaxel to mitotic PtK cells (Waters et al., 1996) or *Xenopus* egg extract spindles (Desai et al., 1998), on the other hand, inhibited microtubule translocation and caused spindle contraction. This result implies that paclitaxel inhibited plus end polymerization and microtubule translocation but not minus end depolymerization, which continued to chew up the microtubules. Both of these experiments are consistent with the model that flux-associated plus end polymerization and microtubule translocation are mechanistically linked but that flux-associated minus end depolymerization is an independent component.

We were interested in the inverse of the paclitaxel experiment. If inhibition of polymerization and translocation caused spindles to shrink at the rate of flux, will inhibition of minus end depolymerization cause spindles to elongate at the rate of flux? Reagents like DMSO or D<sub>2</sub>O cause an increase in both spindle length and width but spindles quickly achieve a stable average size that does not change over time (unpublished results, Shirasu-Hiza). In the course of experiments investigating the effects of combining reagents that affect spindle assembly in *Xenopus* egg extract

(Walczak et al., 1998), one combination was found to result in elongated spindles with no increase in width (personal communication, R. Heald and C. Walczak). Intrigued by this phenotype, we set out to explore the possibility that this phenotype results from inhibition of minus end depolymerization.

The two proteins that, when added together to *Xenopus* egg extract, cause elongated spindles are p50/dynamitin and a truncated form of Xklp2. p50/dynamitin is a 50 kD protein component of the dynactin complex, which binds to cytoplasmic dynein and anchors it to cargo like organelles (Dell, 2003); recently the dynactin complex was also shown to interact with kinesin II for organelle transport during interphase (Deacon et al., 2003). When added in excess, p50/dynamitin has been shown to disrupt the dynactin complex and cause unfocused spindle poles (Echeverri et al., 1996; Wittmann and Hyman, 1999), possibly by preventing poleward transport and localization of two spindle pole scaffold proteins, NuMA and TPX2 (Merdes et al., 2000; Wittmann et al., 2000). Xklp2 is a plus-end directed, KinN (NH<sub>2</sub>-terminal motor domain) member of the kinesin-related protein family thought to be involved in spindle pole separation and spindle assembly (Boleti et al., 1996). Xklp2 is localized to spindle poles by the dynactin complex and also binds TPX2 (Wittmann et al., 1998). Like conventional kinesin, Xklp2 appears to have a conserved NH<sub>2</sub>-terminal motor domain, a COOH-terminal tail domain (in kinesin, responsible for cargo binding), and a stalk domain linking the two. A truncated Xklp2 protein containing only the tail domain (Xklp2 tail) can bind TPX2 and localize to spindle poles in *Xenopus* egg extract (Wittmann et al., 2000). TPX2 (Targeting Protein for Xklp2) was in fact first purified by its ability to mediate association of the COOH-terminal domain of Xklp2 with microtubules.

We confirmed that treatment of *Xenopus* egg extract with these two reagents together produced elongated spindles and subsequently found that, rather than achieving a stable average length, these spindles elongated continuously at a rate similar to the rate of flux in normal spindles. When we measured the rate of poleward microtubule translocation in these p50/Xklp2 tail-treated spindles, we found that this rate was similar to that of untreated spindles and had strong linear correlation with the rate of spindle elongation in individual spindles. This was tested both on spindles assembled with demembrated sperm nuclei and on spindles assembled with DNA-coated beads. These results are consistent with the hypothesis that p50/Xklp2 tail-induced spindle elongation is caused by inhibition of minus end depolymerization with continued microtubule translocation and plus end polymerization and suggest that minus end depolymerization does not drive microtubule translocation during poleward microtubule flux.

## **Results**

*Addition of p50 and XKlp2 tail together to Xenopus egg extract spindles induces continuous lengthwise spindle elongation*

During a series of experiments investigating the effects of combining two or more spindle-perturbing reagents, it was found that the COOH-terminal domain of Xklp2 (Xklp2 tail) and p50 added together caused long spindles in *Xenopus* egg extract (personal communication, R. Heald and C. Walczak). We wanted to determine if the effect of these proteins was different from that of growth-promoting reagents like DMSO, which cause rapid spindle expansion both lengthwise and widthwise to a stable average size. Initially, we took fixed time-points of extract containing rhodamine-labeled tubulin

to examine spindles treated with buffer, p50/dynamitin (henceforth referred to as p50), GST-Xklp2 tail (henceforth Xklp2 tail), or both p50 and Xklp2 tail (p50+Xklp2 tail). We show here polarized light microscopy images of examples for each treatment (fig. 1A). Addition of recombinant p50 to *Xenopus* egg extract before spindle assembly resulted in unfocused spindle poles (fig. 1A, bottom left), as seen previously (Heald et al., 1997; Wittmann and Hyman, 1999). Purified recombinant GST-XKlp tail has previously been shown to induce spindle collapse and produce monopolar structures (Boleti et al., 1996). In our hands, Xklp2 tail addition before spindle assembly did result in monopolar structures; however, addition after spindle assembly did not cause spindle collapse. Xklp2-tail treated spindles remained bipolar, had enlarged spindle poles (“barrel spindles”) and did not change in average length (fig. 1A, top right). In contrast, addition of Xklp2 tail to p50-treated spindles resulted in highly elongated spindles (fig. 1A, bottom right). Buffer addition had no effect on spindle length (fig. 1A, top left). Visual inspection of p50+Xklp2 tail treated spindles showed that these spindles were longer but not wider than control spindles.

We next tested whether these spindles continued to elongate at a constant rate, using time-lapse polarized light microscopy. Several frames from two sample movies, one treated with buffer and the other with p50+Xklp2 tail, are shown here (fig. 1B). p50+Xklp2 tail spindles elongated continuously at an average rate of  $1.0 \pm 0.3 \mu\text{m}/\text{min}$  and continued for over 20 min (data not shown), while spindles treated either with buffer, p50 alone, or Xklp2 tail alone expanded minimally ( $-0.07 \pm 0.2$ ,  $0.1 \pm 0.05$ ,  $0.0 \pm 0.2 \mu\text{m}/\text{min}$ , respectively) over this time course (fig. 1C). Together, the results that spindles increased in length but not width and elongated continuously over time indicated that

p50+Xklp2 tail treatment did not cause longer spindles by the same mechanism as growth-promoting reagents like DMSO.

*The rate of spindle elongation in p50/Xklp2 tail spindles correlates with the rate of poleward microtubule translocation*

Hypothetically, p50+Xklp2 tail might cause spindle elongation in one of four ways, schematically illustrated in figure 2. A control spindle is depicted in figure 2A: plus ends undergo net polymerization (red segment represents new polymer); minus ends undergo net depolymerization (green segment represents old polymer); and microtubules translocate toward their minus ends (direction of translocation is indicated by arrows; rate is indicated by the angle of red dashed line). Control spindles do not elongate over time (black dashed lines indicate spindle edges). In the first model for spindle elongation, we show the hypothetical effects of specifically inhibiting poleward microtubule translocation. If microtubules extend the full length of the spindle, inhibition of poleward translocation and continued plus end polymerization and minus end depolymerization would cause apparent spindle elongation as new polymer gets added to microtubule plus ends (fig. 2B-1). In this case, we predict that the rate of microtubule translocation will be less than that of control spindles and less than the rate of spindle elongation. On the other hand, an increase in microtubule translocation with no coordinated increase in minus end depolymerization could also cause spindle elongation (fig. 2B-2). In this second case, the rate of translocation will be greater than in control spindles and greater than the rate of spindle elongation. In the third model, spindle elongation could be caused by specific inhibition of microtubule minus end (fig. 2B-3). The rate of translocation should be

equal to that of control spindles and also equal to the rate of spindle elongation. Finally, spindle elongation might not be the result of any effect on microtubule translocation or minus end depolymerization but due to increased plus end polymerization (fig. 2B-4). In this case, the rate of microtubule translocation should also be equal to that of control spindles and could be greater than, less than, or equal to the rate of spindle elongation.

To distinguish between these four models, we set out to measure the rates of poleward microtubule translocation and spindle elongation in treated spindles using fluorescent speckle microscopy (FSM). Sample kymographs are shown for one control spindle (buffer) and one spindle treated with p50+Xklp2 tail in figure 3A. The angles of the diagonal streaks in these kymographs are similar, though the p50+Xklp2 tail spindle was clearly expanding, indicating that speckles were translocating poleward at similar rates. As seen in fig. 3B, the average rate of flux was similar for all four types of spindles ( $2.5 \pm 0.2$ ,  $2.9 \pm 0.4$ ,  $2.5 \pm 0.26$ ,  $1.8 \pm 0.7$   $\mu\text{m}/\text{min}$ , respectively). Elongation rates were more difficult to quantitate by FSM than by polarized light microscopy, due to the low levels of rhodamine tubulin. We measured the average rate of elongation in spindles treated with p50+Xklp2 tail to be  $1.4 \pm 0.5$   $\mu\text{m}/\text{min}$  (fig. 3B), slightly less than their average rate of flux. As seen previously, spindles treated with buffer, p50 alone, or Xklp2 tail alone underwent minimal elongation (fig. 3B).

Using these data, we can consider the four models in fig. 2B. The rate of poleward microtubule translocation was not significantly higher in p50+Xklp2 tail spindles, ruling out model 2B-2 (increased microtubule translocation). The rate of microtubule translocation was slightly lower than control spindles, as is predicted in model 2B-1; however, we do not favor this model, as the rate of translocation is not



significantly inhibited. This model also predicts that microtubule translocation will be slower than spindle elongation but in these spindles, the rate of translocation is consistently higher than the rate of elongation. We are not able to distinguish between models 3 and 4 using solely the rate of translocation, since both predict approximately normal rates.

However, these last two models (inhibition of minus end depolymerization vs. increased plus end polymerization) offer significantly different predictions as to microtubule orientation at elongating spindle edges. In model 3, as the spindle elongates, its edges become enriched in microtubule minus ends; in model 4, these spindle edges are enriched in plus ends. In kymographs, diagonal streaks representing moving speckles give us valuable information about the orientation of microtubules in the spindle. Assuming that microtubules still translocate toward their minus ends (poleward), each diagonal points down toward the microtubule minus end. Therefore, if spindle edges are enriched in plus ends (model 4), we predict that diagonals originating near the spindle edge will point inward toward their minus ends at the center of the spindle. If spindle edges are enriched in minus ends (model 3), we predict that diagonals will point outward, toward minus ends at the edges of the spindle. Visual inspection of p50+Xklp2 tail spindle kymographs reveal that the majority of diagonals at elongating spindle edges point outward, not inward, supporting model 3 and a mechanism of spindle elongation by inhibition of minus end depolymerization.

The rate of elongation was not exactly equal to the rate of microtubule translocation. This could be due to incomplete inhibition of minus end depolymerization. We predicted that if microtubule translocation causes spindle elongation, changes in the

rate of translocation should correlate with changes in the rate of elongation. There was a large range of spindle elongation and flux rates, possibly due to the fact that a significant fraction of p50/Xklp2 tail spindles were prepared as thin samples. In very thin preparations of extract, both flux rate and elongation rate appeared to be slower than usual for spindles treated with p50 and Xklp2 tail. The mechanism of this partial inhibition is not known but may be due to effects of the glass coverslip (“pinning” spindles down) (Kapoor and Mitchison, 2001). In any case, plotting flux rates against elongation rates for individual spindles revealed a strong linear correlation (figure 2C). These data suggest that spindle elongation induced by the addition of p50+Xklp2 tail is caused by poleward microtubule translocation and inhibition of net minus end depolymerization.

*p50 and Xklp2 tail additions have similar phenotypes in DNA bead spindles*

p50 and Xklp2 tail each have disruptive effects on spindle poles which, in spindles assembled in *Xenopus* egg extract with demembrated sperm nuclei, contain both centrosomes (brought in by the sperm nuclei) and spindle pole proteins (extract proteins that bind and accumulate at spindle poles). We were curious to see if p50 and Xklp2 tail have similar effects on so-called “centrosome-less” DNA bead spindles: bipolar spindle-like structures assembled around DNA-coated beads (Heald et al., 1996). These structures have many of the same spindle pole proteins as sperm spindles, including NuMA and  $\gamma$ -tubulin, but lack sperm centrosomes (and sperm-specific proteins) and kinetochores (specific attachment sites between chromatin and microtubules that mediate chromosome segregation) (Heald et al., 1997).

Similar to sperm spindles, p50 addition to DNA bead spindle assembly reactions resulted in spindles with unfocused poles as has been previously reported (Heald et al., 1996); Xklp2 tail addition after spindle assembly resulted in barrel-shaped DNA bead spindles; and addition of p50+Xklp2 tail together resulted in elongated DNA bead spindles (data not shown). These results suggest that p50 and Xklp2 tail do not affect spindle morphology through proteins specific to sperm spindles.

We next tested the rate of poleward microtubule translocation for each type of structure using photoactivation techniques. To our knowledge, no one has yet published whether DNA bead spindles exhibit poleward flux and if so, at what rate. In fig. 4A, we show average flux rates for DNA bead spindles treated with buffer ( $2.0 \pm 0.4 \mu\text{m}/\text{min}$ ), p50 alone ( $3.0 \pm 0.9 \mu\text{m}/\text{min}$ ), Xklp2 tail alone ( $2.9 \pm 0.8 \mu\text{m}/\text{min}$ ), or both p50+Xklp2 tail together ( $2.8 \pm 0.8 \mu\text{m}/\text{min}$ ). Thus, rates of flux for each type of structure were similar to the rates of flux seen with sperm spindles.

To determine the rate of elongation of DNA bead spindles, we added standard imaging levels (5-10  $\mu\text{g}/\text{ml}$ ) of rhodamine-labeled tubulin to the extract. As was seen with sperm spindles, DNA bead spindles did not expand when treated with buffer or p50 alone (data not shown). In fig. 4C, we show a plot comparing the rates of poleward microtubule translocation and spindle elongation for DNA bead spindles treated with p50+Xklp2 tail or Xklp2 tail alone. While their rate of poleward microtubule translocation (measured by photoactivation) was similar ( $2.3 \pm .7 \mu\text{m}/\text{min}$  for Xklp2 tail alone,  $2.2 \pm 0.6 \mu\text{m}/\text{min}$  for p50+Xklp2 tail), the rate of spindle elongation was significantly higher for p50+Xklp2 tail spindles ( $1.5 \pm 0.7 \mu\text{m}/\text{min}$ ) than for Xklp2 tail alone ( $0.01 \pm 0.7 \mu\text{m}/\text{min}$ ). Plots showing the relative positions of bead, UV mark, and

pole allow us to visualize which components are moving relative to each other. We present plots for one spindle treated with Xklp2 tail alone and one spindle treated with both p50 and Xklp2 tail together (fig. 4B). It is clear in this example that the fluorescent mark moves away from the beads and toward the pole at a similar rate in both structures. However, while the pole remains stationary relative to the beads in the control spindle, the pole moves away from the beads at a rate similar to the rate of movement of the mark in the p50+Xklp2 tail spindle. In this spindle, spindle elongation occurs at the same rate as poleward microtubule translocation.

To test if there was a linear correlation between the rates of microtubule translocation and spindle elongation, these rates were plotted against each other for individual DNA bead spindles (fig. 4D). Most of the p50/Xklp2 tail spindles elongated at approximately the rate of microtubule translocation, while most of the Xklp2 tail spindles appeared to shrink slightly over the course of observation. Note that there are several exceptions, where Xklp2 tail spindles elongated. These spindles also had very high rates of microtubule translocation, indicating that elongation in these spindles may be due to increased microtubule translocation rather than inhibition of minus end depolymerization (see models, fig. 2B).

From these experiments, we concluded that p50+Xklp2 tail treatment had the same effect on DNA bead spindles as they did on sperm spindles, suggesting that this effect does not require the presence of sperm centrosomes, kinetochores, or kinetochore microtubules.. These data are also consistent with the hypothesis that p50+Xklp2 tail-induced spindle elongation is caused by inhibition of flux-associated minus end depolymerization.

### *AMPPNP inhibits both flux and spindle elongation in p50/XKlp2 tail spindles*

Though the linear correlation between the rates of microtubule translocation and spindle elongation in p50+Xklp2 tail spindles suggests a causal relationship, we wanted to test a known inhibitor of flux to see if it would also inhibit elongation in these spindles.

AMPPNP, a non-hydrolyzable ATP analogue and general ATPase inhibitor, is one of only two known inhibitors of flux (Sawin and Mitchison, 1991). We added 1 mM AMPPNP to sperm-nucleated p50/Xklp2 tail spindles in *Xenopus* egg extracts and observed the effects on both flux rate and spindle elongation rate by FSM. As can be seen by the sample kymograph (fig. 5A), both were completely inhibited by the presence of AMPPNP. The average rate of poleward translocation was  $0.02 \pm 0.02$   $\mu\text{m}/\text{min}$  and the average rate of spindle elongation was  $0.02 \pm 0.03$   $\mu\text{m}/\text{min}$  (fig. 5B). Rates of translocation and elongation for p50+Xklp2 tail spindles in the absence of AMPPNP are included for comparison. Thus, inhibiting the rate of microtubule translocation blocks the rate of spindle elongation in these spindles, consistent with the hypothesis that spindle elongation is caused by microtubule translocation in the absence of minus end depolymerization.

### **Discussion**

The results of this work support a model of poleward microtubule flux in which microtubule translocation is driven by either plus end polymerization or microtubule translocation factors but not by force generated by minus end depolymerization. Minus end depolymerization appears to be an independent mechanistic component of flux.

We found that treatment of *Xenopus* egg extract spindles with a combination of p50 and Xklp2 tail together induce continuous spindle elongation, at a rate that closely correlates with the rate of microtubule translocation. Microtubule translocation rate in these spindles was the same or slightly less than control spindles, ruling out the possibility that spindle elongation was due to increased microtubule translocation (model 2B-2). Microtubule translocation rate was also greater than the rate of spindle elongation, ruling out the model of spindle elongation due to decreased microtubule translocation (model 2B-1). Kymographs of expanding spindles did not support a model of increased plus end microtubule polymerization (model 2B-4). Instead, we favor a model of inhibition of minus end depolymerization (model 2B-3). This is the first evidence that any one component of flux is molecularly separable from the others and can be specifically inhibited. These results also demonstrate that minus end depolymerization does not cause microtubule translocation, though the fact that this translocation rate is consistently slightly slower than in control spindles might reflect its relative contribution.

Before discussing how these reagents might be used to identify a molecular factor involved in flux, we should examine several assumptions underlying our analysis of these data. First, we assumed that p50+Xklp2 tail treatment does not induce dramatic structural changes in the microtubule lattice. By polarized light microscopy, microtubules appear to maintain parallel arrangement along the pole-to-pole axis and to elongate along that axis. However, our methods are relatively insensitive to microtubule polarity. Our models assume that (a) microtubules exist in two anti-parallel populations; and (b) microtubules translocating within the spindle are moving toward their minus ends. The former seems to be a reasonable assumption; we are confident that we have

looked at early time-points after addition of Xklp2 tail and would have detected a massive re-orientation of microtubules to form a completely parallel lattice. Though it is difficult to rule out the possibility that microtubules might be translocating toward their plus ends, we consider this to be highly unlikely. Second, we assume that the observed changes in spindle length are due to changes in microtubule length. It is possible that we are observing instead more complex behavior like increased microtubule nucleation or aggregation. Finally, we assume that microtubule movement in these spindles is due to the same molecular mechanisms as that of poleward flux in control spindles. We have not ruled out the possibility that we are watching an entirely novel type of microtubule transport (ie, stimulation of a different kinesin or slow dynein/dynactin transport).

We now consider the molecular implications of this work. If treatment of p50+Xklp2 tail together specifically inhibits minus-end depolymerization, can we use this information to identify molecular components involved in flux? First, one might use p50+Xklp2 tail spindles as substrates for a complementation assay, trying to add back proteins to restore minus end depolymerization. We consider this option somewhat impractical. Both p50 and Xklp2 tail are dominant negative reagents added in excess and still present in the extract; any protein addback would have to overcome their effects. Second, one might characterize the effects of these two proteins on candidate protein localization or activity and test those candidates directly for a role in poleward flux. There are several proteins already known to be affected by p50 and Xklp2 tail—p50 blocks the localization of at least two spindle pole proteins (NuMA and TPX2 (Merdes et al., 2000; Wittmann et al., 2000)) and Xklp2 tail binds TPX2 (Wittmann et al., 2000). Dynein is not thought to be involved in poleward flux, since addition of an inhibitor

(vanadate) did not affect the rate of poleward translocation or spindle length (Sawin and Mitchison, 1991). There are also several other candidate proteins that may play a role in minus end depolymerization (XKCM1, Xkif2, katanin, XMAP215); it will be interesting to see if their activity or localization is affected by p50+Xklp2 tail treatment.

Xklp2 itself should be further examined for a role in poleward microtubule flux. Inhibition of XKlp2 by immunodepletion does not produce barrel-spindles like those seen with Xklp2 tail addition after spindle assembly (unpublished data, T. Wittman). There are at least two possible explanations for this. Xklp2 tail added after spindle assembly has been shown to bind spindle poles and was previously thought to compete with endogenous full-length Xklp2 (Boleti et al., 1996). However, it is possible that Xlp2 tail has an additional dominant negative effect, such as causing excess accumulation of another binding partner. Alternatively, Xklp2 may have two temporally separable roles, one in spindle assembly and the other in spindle maintenance. Immunodepletion of Xklp2 from extracts might uncover the first role; depletion of Xklp2 from spindle poles after spindle assembly using Xklp2 tail might uncover the second.

Though this work does not directly identify a molecular component involved in poleward MT flux, the combination of p50 and Xklp2 tail provides a novel system for studying poleward microtubule flux. Neither of the other two known inhibitors of flux, AMPPNP and taxol, has led to a molecular handle on the problem. Moreover, these drugs are not ideal for probing the cellular function of flux, the former being too general an inhibitor of cellular processes and the latter having general effects on microtubule dynamics not specific to poleward flux. It will be interesting to see if p50+Xklp2 tail treatment will inhibit minus end depolymerization in mitotic cells and whether this



affects any aspect of microtubule function, whether microtubule-chromatin interaction, chromosome oscillation, spindle assembly checkpoint, or chromosome segregation.

## **Materials and Methods**

### *Spindle assembly in Xenopus egg extract*

All experiments were performed using fresh cytostatic factor (CSF) arrested *Xenopus* egg extracts prepared according to (Murray, 1991). Cycled spindle assembly reactions were performed as previously described (Desai et al., 1999). Briefly, addition of 0.4 mM CaCl<sub>2</sub> (from a 10x (4 mM) stock in sperm dilution buffer (SD: 10 mM K-HEPES, pH 7.7, 100 mM KCl, 1 mM MgCl<sub>2</sub>, 150 mM sucrose)) was added to 25 µl of extract containing demembrated sperm nuclei (~200-400/ µl) to drive the extract into interphase and incubated at room temperature for 60-90 min, after which 25 µl of fresh CSF extract (without chromatin) was added to drive the reaction into metaphase and induce bipolar spindle assembly.

DNA bead spindles were assembled in CSF-arrested extract as previously described (Heald et al., 1996). DNA beads (lambda DNA fragments covalently bound to small magnetic beads) were a generous gift from R. Heald (UC Berkeley, CA). Briefly, 5 µl of DNA beads were washed in 50 µl of extract and isolated with a magnetic holder before being incubated for 2 h at room temperature in 150 µl of interphase *Xenopus* egg extract with continuous rotation. One volume of fresh CSF extract was added to the DNA bead reaction to induce mitotic condensation and incubated for 30 min at room temperature with continuous rotation. DNA beads were re-isolated with magnetic tube holder and resuspended in 250 µl of fresh CSF extract for DNA bead spindle assembly.

*Reagents added to spindle assembly reactions*

Tubulin was labeled with tetramethyl- or X-rhodamine (Molecular Probes) or a caged, photoactivatable carboxyfluorescein derivative, C2CF (Mitchison, 1989), as previously described (Hyman et al., 1991). Stoichiometry of dye:tubulin was approximately 0.8-1.0 for each label. Rhodamine-labeled tubulin was added at 0.5  $\mu$ M for visual analysis of microtubule structures and 10-50 nM for speckle microscopy. C2CF tubulin was added at 2  $\mu$ M and the extract was exposed to minimal light before photoactivation.

Purified recombinant p50/dynamitin was a generous gift from either E. Karsenti (Heidelberg, Germany) or E. Salmon (UNC Chapel Hill, N. Carolina) and was added to a final concentration of  $\sim$ 1 mg/ml either at the beginning of the interphase incubation at room temperature or simultaneous with the addition of CSF-arrested extract, before spindle assembly.

A plasmid construct of glutathione-S-transferase fusion protein containing the COOH-terminal domain of Xklp2 (GST-Xklp2 tail) was a generous gift from C. Walczak (Indiana University, IN). Recombinant GST-Xklp2 tail was overexpressed in *E. coli* and purified by glutathione affinity chromatography using standard protocols. Briefly, protein was induced overnight by IPTG (Sigma); 2 L of cells were spun down and frozen in liquid nitrogen; cell pellets were lysed with lysozyme and sonication before being clarified by centrifugation; supernatant was poured over 2 ml of GST-agarose beads at  $\sim$ 1 ml/min; beads were washed with ten vol of buffer and eluted with 10 mM glutathione. Protein ( $\sim$ 50 mg) was subsequently dialyzed against CSF-XB (10 mM K-Hepes, pH 7.7, 50 mM sucrose, 100 mM KCl, 2 mM MgCl<sub>2</sub>, 0.1 mM CaCl<sub>2</sub>, and 5 mM

EGTA), aliquoted and frozen in liquid nitrogen before storage at  $-80^{\circ}\text{C}$ . Purified recombinant GST-XKlp2 tail was added to *Xenopus* egg extract at a final concentration of 0.125 mg/ml after at least 60 min of incubation with added CSF-arrested extract, or post-spindle assembly.

AMPPNP was purchased from Sigma and used at a final concentration of 1 mM. For all additions, total dilution of the extract did not exceed 10% total volume.

*Assays for spindle elongation and poleward microtubule flux*

Polarized light microscopy was performed on an inverted Nikon TE300 microscope with 20X objective and no binning. Samples were prepared in the following way:  $\sim 5\ \mu\text{l}$  of extract was thinly spread with a pipette tip on a large (22x22 mm) coverslip affixed to an aluminum holder and covered with  $\sim 250\ \mu\text{l}$  of mineral oil, which protected the sample from evaporation but allowed free gas transfer, while sample was observed from below with 20X objective. Spindles prepared in this way were observed to last at least an hour with no change in normal morphology. Images were acquired using a CCD detector (Orca ER camera, Hamamatsu Photonics) and Metamorph software (Universal Imaging, Westchester, PA). For time-lapse movies, we used exposures of 750 ms, with no binning, at 20 sec intervals.

Fluorescent speckle microscopy (FSM) experiments were performed on an upright Nikon E-600 or E-800 conventional wide-field fluorescence light microscope with 60X or 100X Planapo objectives or on a TE300 Nikon inverted microscope outfitted with a Yokogawa spinning disk confocal unit with 60X or 100X Planapo objectives. Samples were prepared in conventional squashes between an 18x18 mm glass coverslip

and glass slide, sealed with melted VALAP (1:1:1 ratio of vaseline, lanolin, and paraffin). Typically, samples consisted of no less than 6-8 ml of extract, to avoid spindle contact with glass surfaces. Because rhodamine-tubulin levels were so low, 1  $\mu\text{g/ml}$  Hoechst dye was added to extracts so that spindles could be located by the UV fluorescence of their chromatin. All microscopes were equipped with cooled charge-coupled device cameras (widefield: Princeton Instruments, Trenton, NJ; confocal: Hamamatsu Photonics) controlled by MetaMorph software (Universal Imaging, Westchester, PA). For time-lapse movies, we used exposures of 200-500 ms (bin = 2), with time intervals of 5-10 sec.

All polarized light and FSM movies were analyzed using the Kymograph function in Metamorph. If necessary, spindles were first aligned (to compensate for spindle movement in the field) using a MatLab program created by Z. Perlman. For each kymograph, we drew a line of 5-10 pixels wide along the pole-to-pole spindle axis and created a kymograph using the maximum fluorescence in the region; we then drew lines following the movement of speckles or spindle edges on each kymograph. The angles of these lines were logged and analyzed in Microsoft Excel 2000 to extract rate information. Each angle was converted to radians and the inverse tangent of this value was multiplied by conversion factors for pixels per min (total time elapsed divided by number of frames) and mm per pixel (empirically obtained for each microscope and objective) to get rates of movement in mm per minute. The rate of flux can be highly variable even within the same spindle and the angle of the original kymograph line can make a large difference in final rates. Therefore, for flux analysis, we made 1-3 kymographs per sample and averaged the slopes of ~10-40 lines per kymograph.

Photoactivation experiments were performed in the dark on an upright Zeiss Photoscope III with a rotating stage and 60X, 1.4 NA Planapo objective. Samples were prepared as described above for FSM samples. Spindles were located at low magnification and aligned with respect to the photoactivation beam using phase contrast microscopy. Modifications of the microscope for photoactivation have been described (Mitchison et al., 1998; Sawin and Mitchison, 1991; Sawin and Mitchison, 1994). 100W mercury arc lamps were used for both illumination and photoactivation. Photoactivation was done with 2-4 second exposure through an adjustable slit (Ealing Optical, S. Natick, MA) placed so that its image was in the same focal plane as the specimen. A SIT video camera (Dage-MTI, Wabash, WI) was used to acquire images, controlled by Princeton Instrument's WinView software with additional software written by A. Mallavarapu (Mallavarapu and Mitchison, 1999). Images at each wavelength were acquired 5 seconds apart and sequential images at a specific wavelength were acquired 20-30 seconds apart. Images were stored on optical disks using a Panasonic TQ 3038F optical memory disc recorder and each movie was analyzed manually on large screen video monitor.

### **Acknowledgments**

We are grateful to Rebecca Heald, Claire Walczak, Eric Karsenti, and Ted Salmon for their gifts of reagents. We also thank Lisa Cameron, Aaron Groen, Ted Salmon, and Christine Field for their help and comraderie at Woods Hole and Zach Perlman, Ann Yonetani, and Becky Ward for their advice on this manuscript. We are especially grateful Jennifer Timauer for her insightful comments and guidance, and Justin Yarrow for always being right.

This project was supported by a fellowship from the National Science Foundation to M.S.H. and NIH grant (GM39565) to T.J.M.

## References

- Allen, C., and G.G. Borisy. 1974. Structural polarity and directional growth of microtubules of *Chlamydomonas* flagella. *J Mol Biol.* 90:381-402.
- Boleti, H., E. Karsenti, and I. Vernos. 1996. Xklp2, a novel *Xenopus* centrosomal kinesin-like protein required for centrosome separation during mitosis. *Cell.* 84:49-59.
- Coue, M., V.A. Lombillo, and J.R. McIntosh. 1991. Microtubule depolymerization promotes particle and chromosome movement in vitro. *J Cell Biol.* 112:1165-75.
- Cullen, C.F., P. Deak, D.M. Glover, and H. Ohkura. 1999. mini spindles: A gene encoding a conserved microtubule-associated protein required for the integrity of the mitotic spindle in *Drosophila*. *J Cell Biol.* 146:1005-18.
- Deacon, S.W., A.S. Serpinskaya, P.S. Vaughan, M. Lopez Fanarraga, I. Vernos, K.T. Vaughan, and V.I. Gelfand. 2003. Dynactin is required for bidirectional organelle transport. *J Cell Biol.* 160:297-301.
- Dell, K.R. 2003. Dynactin polices two-way organelle traffic. *J Cell Biol.* 160:291-3.
- Desai, A., P.S. Maddox, T.J. Mitchison, and E.D. Salmon. 1998. Anaphase A chromosome movement and poleward spindle microtubule flux occur at similar rates in *Xenopus* extract spindles. *J Cell Biol.* 141:703-13.

- Desai, A., A. Murray, T.J. Mitchison, and C.E. Walczak. 1999. The use of *Xenopus* egg extracts to study mitotic spindle assembly and function in vitro. *Methods Cell Biol.* 61:385-412.
- Echeverri, C.J., B.M. Paschal, K.T. Vaughan, and R.B. Vallee. 1996. Molecular characterization of the 50-kD subunit of dynactin reveals function for the complex in chromosome alignment and spindle organization during mitosis. *J Cell Biol.* 132:617-33.
- Euteneuer, U., and J.R. McIntosh. 1981. Structural polarity of kinetochore microtubules in PtK1 cells. *J Cell Biol.* 89:338-45.
- Heald, R., R. Tournebize, T. Blank, R. Sandaltzopoulos, P. Becker, A. Hyman, and E. Karsenti. 1996. Self-organization of microtubules into bipolar spindles around artificial chromosomes in *Xenopus* egg extracts. *Nature.* 382:420-5.
- Heald, R., R. Tournebize, A. Habermann, E. Karsenti, and A. Hyman. 1997. Spindle assembly in *Xenopus* egg extracts: respective roles of centrosomes and microtubule self-organization. *J Cell Biol.* 138:615-28.
- Hyman, A., D. Drechsel, D. Kellogg, S. Salser, K. Sawin, P. Steffen, L. Wordeman, and T. Mitchison. 1991. Preparation of modified tubulins. *Methods Enzymol.* 196:478-85.
- Jordan, M.A., R.J. Toso, D. Thrower, and L. Wilson. 1993. Mechanism of mitotic block and inhibition of cell proliferation by taxol at low concentrations. *Proc Natl Acad Sci U S A.* 90:9552-6.
- Kapoor, T.M., and T.J. Mitchison. 2001. Eg5 is static in bipolar spindles relative to tubulin: evidence for a static spindle matrix. *J Cell Biol.* 154:1125-33.

- Koshland, D.E., T.J. Mitchison, and M.W. Kirschner. 1988. Polewards chromosome movement driven by microtubule depolymerization in vitro. *Nature*. 331:499-504.
- Krendel, M., and S. Inoue. 1995. Anaphase spindle dynamics under D2O-enhanced microtubule polymerization. *Biol Bull*. 189:204-5.
- Lombillo, V.A., C. Nislow, T.J. Yen, V.I. Gelfand, and J.R. McIntosh. 1995. Antibodies to the kinesin motor domain and CENP-E inhibit microtubule depolymerization-dependent motion of chromosomes in vitro. *J Cell Biol*. 128:107-15.
- Maddox, P., A. Desai, K. Oegema, T.J. Mitchison, and E.D. Salmon. 2002. Poleward microtubule flux is a major component of spindle dynamics and anaphase a in mitotic *Drosophila* embryos. *Curr Biol*. 12:1670-4.
- Mallavarapu, A., and T. Mitchison. 1999. Regulated actin cytoskeleton assembly at filopodium tips controls their extension and retraction. *J Cell Biol*. 146:1097-106.
- Margolis, R.L., and L. Wilson. 1981. Microtubule treadmills--possible molecular machinery. *Nature*. 293:705-11.
- Mastrorarde, D.N., K.L. McDonald, R. Ding, and J.R. McIntosh. 1993. Interpolar spindle microtubules in PTK cells. *J Cell Biol*. 123:1475-89.
- McIntosh, J.R., and U. Euteneuer. 1984. Tubulin hooks as probes for microtubule polarity: an analysis of the method and an evaluation of data on microtubule polarity in the mitotic spindle. *J Cell Biol*. 98:525-33.
- Merdes, A., R. Heald, K. Samejima, W.C. Earnshaw, and D.W. Cleveland. 2000. Formation of spindle poles by dynein/dynactin-dependent transport of NuMA. *J Cell Biol*. 149:851-62.



- Mitchison, T., L. Evans, E. Schulze, and M. Kirschner. 1986. Sites of microtubule assembly and disassembly in the mitotic spindle. *Cell*. 45:515-27.
- Mitchison, T.J. 1989. Polewards microtubule flux in the mitotic spindle: evidence from photoactivation of fluorescence. *J Cell Biol*. 109:637-52.
- Mitchison, T.J., and E.D. Salmon. 1992. Poleward kinetochore fiber movement occurs during both metaphase and anaphase-A in newt lung cell mitosis. *J Cell Biol*. 119:569-82.
- Mitchison, T.J., K.E. Sawin, J.A. Theriot, K. Gee, and A. Mallavarapu. 1998. Caged fluorescent probes. *Methods Enzymol*. 291:63-78.
- Murray, A.W. 1991. Cell cycle extracts. *Methods Cell Biol*. 36:581-605.
- Sawin, K.E., and T.J. Mitchison. 1991. Poleward microtubule flux mitotic spindles assembled in vitro. *J Cell Biol*. 112:941-54.
- Sawin, K.E., and T.J. Mitchison. 1994. Microtubule flux in mitosis is independent of chromosomes, centrosomes, and antiparallel microtubules. *Mol Biol Cell*. 5:217-26.
- Tirnauer, J.S., J.C. Canman, E.D. Salmon, and T.J. Mitchison. 2002. EB1 targets to kinetochores with attached, polymerizing microtubules. *Mol Biol Cell*. 13:4308-16.
- Tournebize, R., A. Popov, K. Kinoshita, A.J. Ashford, S. Rybina, A. Pozniakovsky, T.U. Mayer, C.E. Walczak, E. Karsenti, and A.A. Hyman. 2000. Control of microtubule dynamics by the antagonistic activities of XMAP215 and XKCM1 in *Xenopus* egg extracts. *Nat Cell Biol*. 2:13-9.

- Walczak, C.E., I. Vernos, T.J. Mitchison, E. Karsenti, and R. Heald. 1998. A model for the proposed roles of different microtubule-based motor proteins in establishing spindle bipolarity. *Curr Biol.* 8:903-13.
- Waterman-Storer, C., A. Desai, and E.D. Salmon. 1999. Fluorescent speckle microscopy of spindle microtubule assembly and motility in living cells. *Methods Cell Biol.* 61:155-73.
- Waters, J.C., T.J. Mitchison, C.L. Rieder, and E.D. Salmon. 1996. The kinetochore microtubule minus-end disassembly associated with poleward flux produces a force that can do work. *Mol Biol Cell.* 7:1547-58.
- Wilson, P.J., A. Forer, and C. Leggiadro. 1994. Evidence that kinetochore microtubules in crane-fly spermatocytes disassemble during anaphase primarily at the poleward end. *J Cell Sci.* 107 ( Pt 11):3015-27.
- Wittmann, T., H. Boleti, C. Antony, E. Karsenti, and I. Vernos. 1998. Localization of the kinesin-like protein Xklp2 to spindle poles requires a leucine zipper, a microtubule-associated protein, and dynein. *J Cell Biol.* 143:673-85.
- Wittmann, T., and T. Hyman. 1999. Recombinant p50/dynamitin as a tool to examine the role of dynactin in intracellular processes. *Methods Cell Biol.* 61:137-43.
- Wittmann, T., M. Wilm, E. Karsenti, and I. Vernos. 2000. TPX2, A novel xenopus MAP involved in spindle pole organization. *J Cell Biol.* 149:1405-18.
- Zhai, Y., P.J. Kronebusch, and G.G. Borisy. 1995. Kinetochore microtubule dynamics and the metaphase-anaphase transition. *J Cell Biol.* 131:721-34.

## Figure legends

*Figure 1: Addition of both p50 and XKlp2 tail results in lengthwise spindle elongation.*

Meiotic spindles were assembled by addition of demembrated sperm nuclei to *Xenopus* egg extract and visualized using polarized light microscopy. (A) Examples of spindle morphology are shown here for addition of buffer (top left), p50 (top right), Xklp2 tail (bottom left), and p50+Xklp2 tail together (bottom right). Blue dashed line indicates location of DNA at spindle midzone. (B) Frames from a time-lapse movie of a spindle treated with p50+Xklp2 tail shows continuous elongation over time. (C) Average rates of elongation were quantitated for each type of spindle structure.

*Figure 2: Models for spindle elongation induced by p50+Xklp2 tail*

Four models for spindle elongation induced are schematized here as the hypothetical results of an experiment in which spindles are assembled with green and then red tubulin. In these diagrams of bipolar spindles, antiparallel microtubules are represented by two green bars. Red regions indicate newly-incorporated tubulin. Tubulin dimer is represented by small colored boxes. Arrows on the green bars indicate the direction of microtubule translocation; slope of red dashed line indicates rate of translocation. For simplicity, red dashed line is shown only for the top bar. (A) Control spindle. Spindle length does not change (black dashed lines). Microtubule plus ends undergo net polymerization (red segment), minus ends undergo net depolymerization (green segment), and microtubules translocate toward their minus ends (arrows, red dashed line). (B) Four models for spindle elongation are shown here. (1) Inhibition of poleward microtubule translocation. Plus end polymerization and minus end depolymerization

rates are similar to those of the control spindle but the rate of microtubule translocation is inhibited (note steeper slope of red dashed line). (2) Increased microtubule translocation. Plus end polymerization and minus end depolymerization are similar to control spindle but microtubule translocation is faster (note shallower slope of red dashed line). (3) Inhibition of minus end depolymerization. The rates of microtubule translocation and plus end polymerization are similar to those of the control spindle, but minus end depolymerization is inhibited (note that green segment does not shorten). (4) Increase in plus end polymerization. The rates of microtubule translocation and minus end depolymerization are similar to those of control spindle but plus end polymerization is faster than control spindle (note increase in length of red segment).

*Figure 3: The rate of spindle elongation in p50/Xklp2 tail spindles correlates with their flux rate*

Flux rate was monitored in meiotic spindles treated with buffer, p50, Xklp2 tail, or p50+Xklp2 tail using fluorescent speckle microscopy (FSM). (A) Sample kymographs are shown here for one spindle treated with buffer (top) and one spindle treated with p50+Xklp2 tail (bottom). (B) Graph of average rates of flux and elongation shows that each type of spindle had normal rates of poleward microtubule translocation but only p50+Xklp2 tail structures elongated significantly. (C) Plot of translocation rate versus elongation rate for individual p50+Xklp2 tail spindles reveals a strong linear correlation.

*Figure 4: p50 and Xklp2 tail additions have similar phenotypes in DNA bead spindles*

Flux rates and spindle elongation rates were measured using photoactivation and fluorescent microscopy in DNA bead spindles treated with buffer, p50, Xklp2 tail, or both p50 and Xklp2 tail. (A) Graph of average flux rates for each type of structure, similar to rates seen for spindles assembled from sperm nuclei. (B) Plots for relative positions of spindle pole (pink), photoactivated mark (blue), and DNA beads (yellow) illustrate the movement of fluorescent marks and spindle poles over time for two sample spindles, one treated with Xklp2 tail alone and the other with p50+Xklp2 tail. (C) Graph of average rates of flux and elongation shows that elongation rate was significantly higher for p50+Xklp2 tail spindles than for control spindles and this elongation rate was similar to the rate of flux. (D) Plot of flux rate vs. elongation rate for individual spindles treated with Xklp2 tail alone (black) or p50+Xklp2 tail (red) shows a weak correlation.

*Figure 5: p50/Xklp2 tail-induced spindle elongation is inhibited by AMPPNP*

Sperm spindles were treated with p50+Xklp2 tail to induce elongation and then treated with 1 mM AMPPNP. (A) A sample kymograph of an AMPPNP-treated spindle is shown here. (B) AMPPNP reduced both the rate of microtubule translocation and the rate of elongation in these spindles to nearly zero; p50+Xklp2 tail spindle rates not treated with AMPPNP (fig. 1) are included here for comparison.

Figure 1-1:

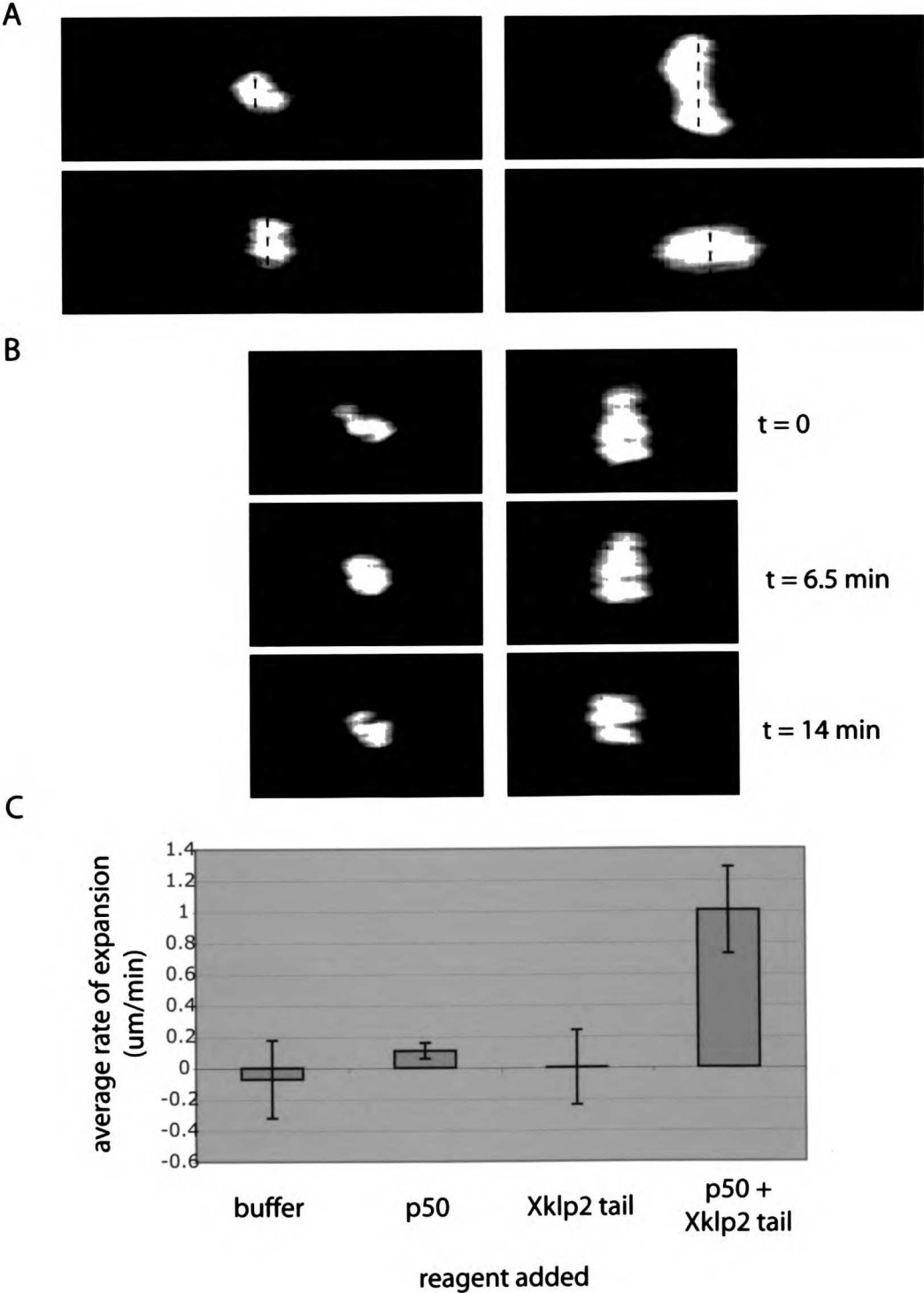


Fig. 1-2:

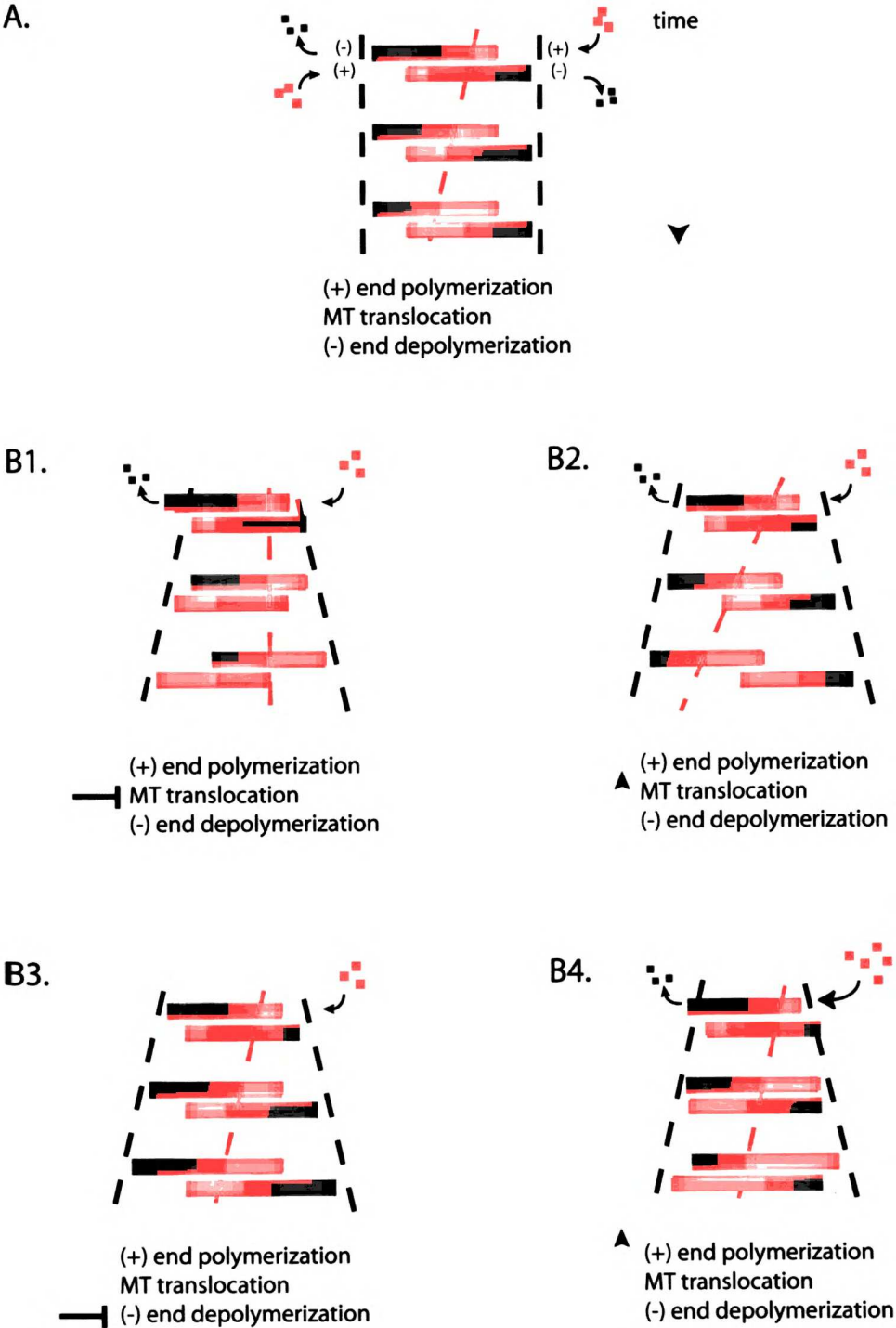


Figure 1-3:

**A**

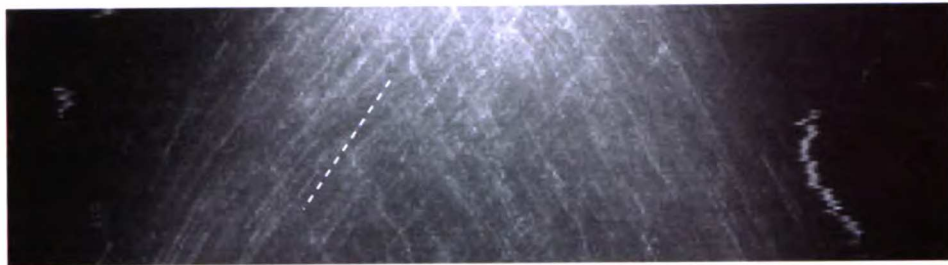
control



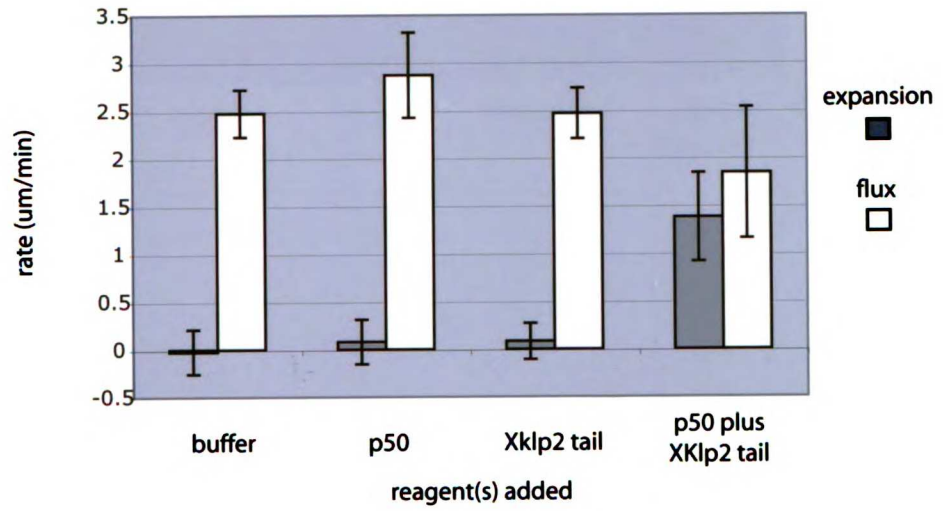
time



p50 plus  
Xklp2 tail



**B**



**C**

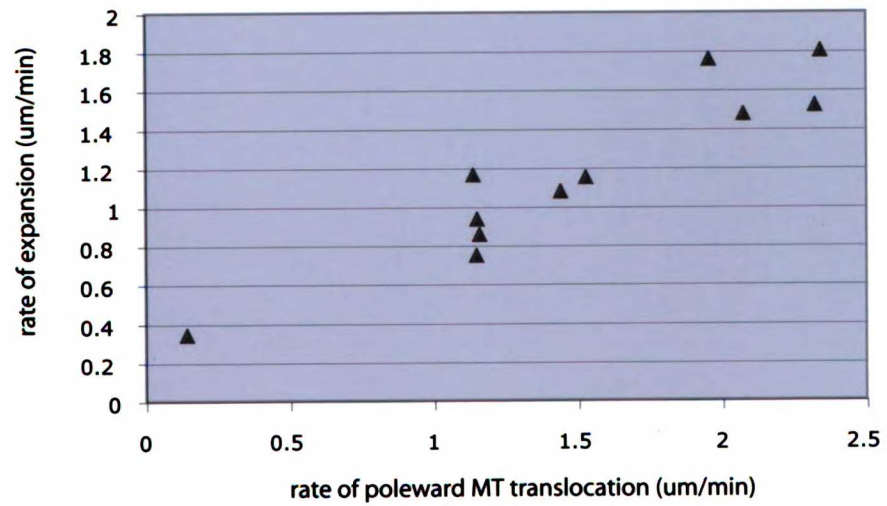




Figure 1-4:

A

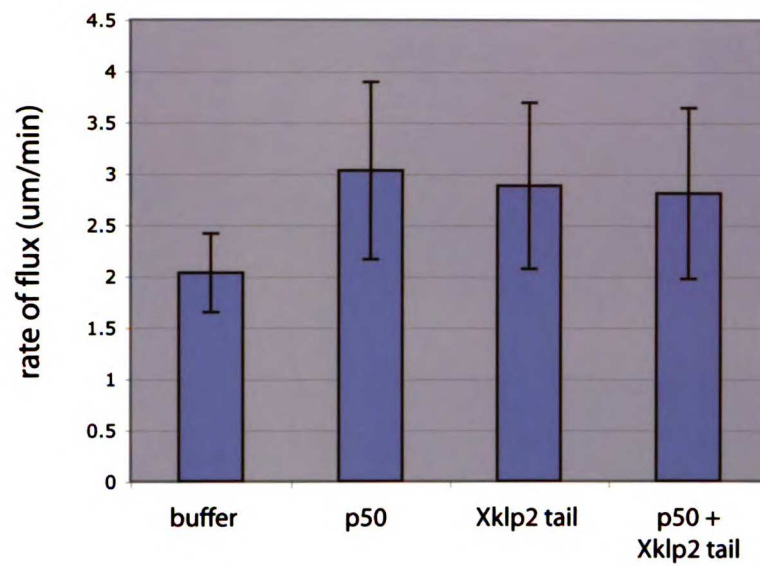
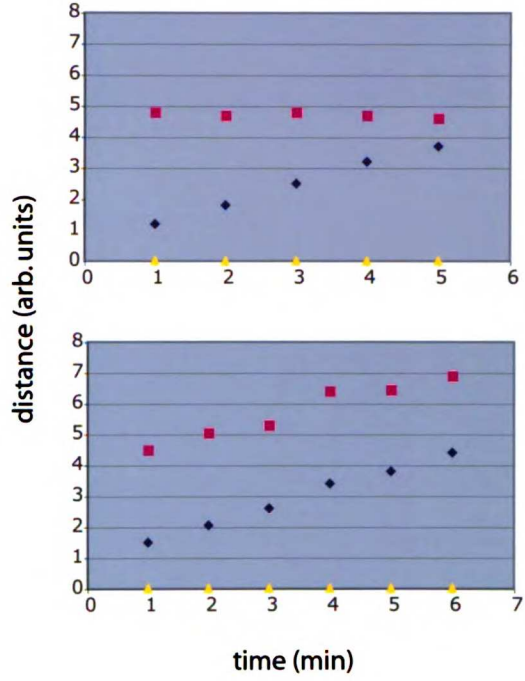
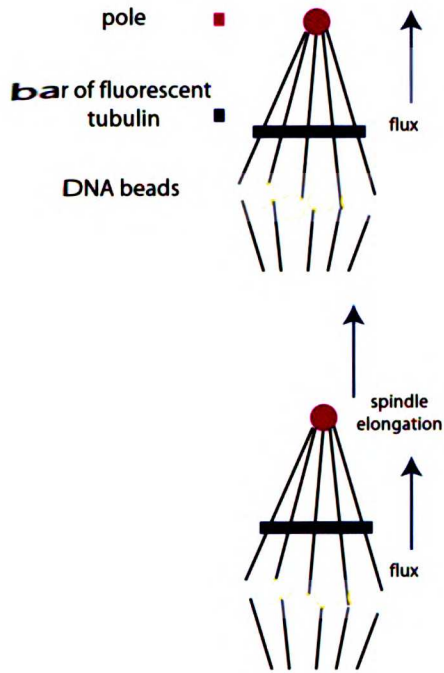
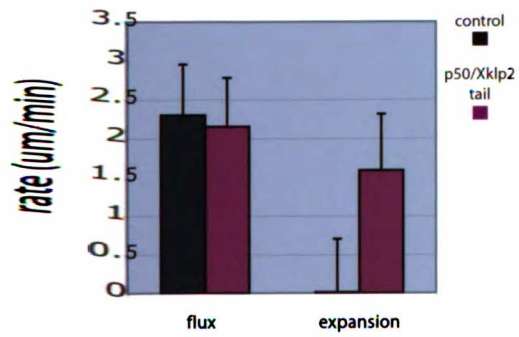


Figure 1-4: (cont.)

**B**



**C**



**D**

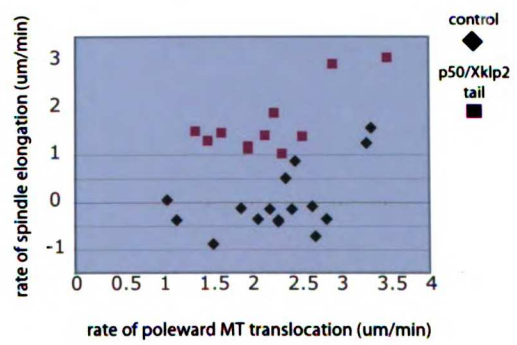
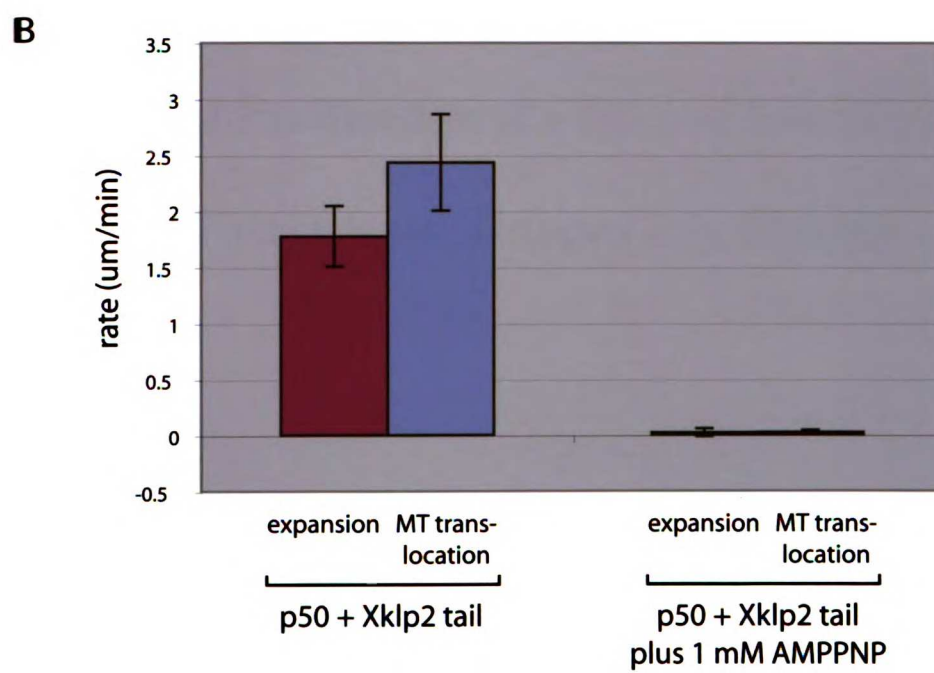


Figure 1-5:



## **Chapter 2**

# **Biochemical Purification of a Microtubule Destabilizing Factor from Xenopus Egg Extract**

**The text** of this chapter has been reproduced from the Journal of Cell Biology (2003),  
**Volume** 161, Number 2, pages 349-358. ©The Rockefeller University Press.  
**I performed** all the experiments described here except the negative-stain electron  
**microscopy**, which was done in collaboration with Peg Coughlin, a technician in the  
**Mitchison lab**.

# Identification of XMAP215 as a Microtubule Destabilizing Factor in Xenopus Egg

## Extract by Biochemical Purification

Mimi Shirasu-Hiza<sup>§</sup>, Peg Coughlin<sup>\*</sup>, and Tim Mitchison<sup>\*</sup>

<sup>§</sup>Department of Biochemistry  
U. of California, San Francisco  
San Francisco, CA 94114

<sup>\*</sup>Department of Cell Biology  
Harvard University Medical School  
Boston, MA 02115

Address correspondence to: Mimi Shirasu-Hiza, Dept. of Cell Biology, Harvard Medical School, 250 Longwood Ave, Boston MA 02115. Tel: 617 432-3805. Fax: 617 432-3702. E-mail: [mshirasu@hms.harvard.edu](mailto:mshirasu@hms.harvard.edu)

Running title: XMAP215 is a microtubule destabilizer

Key words: microtubule dynamics, microtubule-associated protein, XMAP215, GMPCPP

Number of characters: 50,310 (51,636 including supplemental materials)

JCB #200211095

Original submission date: Nov. 20, 2002; resubmitted March 3, 2003; final version March 17, 2003

## **Abstract**

Microtubules polymerized with GMPCPP, a slowly-hydrolyzable GTP analogue, are stable in buffer but are rapidly depolymerized in *Xenopus* egg extracts. This depolymerization is independent of three previously identified microtubule destabilizers (Op18, Katanin, and XKCM1/KinI). We purified the factor responsible for this novel depolymerizing activity using biochemical fractionation and a visual activity assay and identified it as XMAP215, previously identified as a prominent microtubule growth promoting protein in *Xenopus* extracts. Consistent with the purification results, we find that XMAP215 is necessary for GMPCPP-microtubule destabilization in extracts and that recombinant full-length XMAP215 as well as an N-terminal fragment have depolymerizing activity *in vitro*. Stimulation of depolymerization is specific for the microtubule plus end. These results provide evidence for a robust microtubule destabilizing activity intrinsic to this MAP and suggest destabilization may be part of its essential biochemical functions. We propose that the substrate in our assay, GMPCPP-stabilized microtubules, serves as a model for the pause state of microtubule ends and that the multiple activities of XMAP215 are unified by a mechanism of antagonizing microtubule pauses.

## **Introduction**

Microtubule (“MT”) polymerization dynamics have been implicated in many important cellular events, including cell polarization, motility, and division. They are regulated by cellular factors that both stabilize and destabilize the microtubule lattice. During mitosis, for example, increased microtubule dynamicity allows more efficient search and capture of kinetochores by microtubule ends (Holy and Leibler, 1994). This increased

dynamicity is driven by increases in catastrophe rate in some systems (Belmont et al., 1990) and/or decreases in rescue rate in others (Rusan et al., 2001) (Gliksman et al., 1992). A number of MT dynamics regulators have been identified and characterized in recent years, and investigators in the field are actively pursuing the assignment of specific regulators to specific cellular events.

Three important MT destabilizers have been characterized in meiotic *Xenopus* egg extract: Katanin (McNally and Vale, 1993), Op18/stathmin (Belmont and Mitchison, 1996), and XKCM1/MCAK (a member of the KinI family of kinesins) (Walczak et al., 1996). Of these three, the KinI family members appear to be the most important negative regulators of MT polymerization during mitosis (Belmont and Mitchison, 1996; Kline-Smith and Walczak, 2002; Maney et al., 2001). We set out to determine if there were any other MT destabilizers in *Xenopus* egg extract, using GMPCPP-stabilized microtubules (“CPP MTs”) as the substrate in our depolymerization assays. CPP MTs were used in part for practical reasons—they are stable to dilution in buffer—and in part because they provide a novel assay that might identify factors with new mechanisms of action.

CPP MTs are stable to dilution because the nucleotide is only slowly hydrolyzed, and thus mimics the GTP or GDP-Pi bound state (Hyman et al). However, we do not know precisely what state of physiological MTs they most closely resemble. They have been hypothesized to mimic the GTP cap, a hypothetical structure stabilizing the ends of actively growing microtubules (Caplow and Shanks, 1996; Drechsel and Kirschner, 1994). In this paper we suggest an alternative possibility, that CPP MTs most closely mimic a hypothetical “paused” state of the microtubule lattice, an intermediate between the growing and shrinking states (Tran et al., 1997).

## Results

### *Meiotic Xenopus egg extracts contain a novel microtubule depolymerizing factor*

To assay for microtubule depolymerizing factors, we added rhodamine-labeled CPP MTs to crude or clarified CSF-arrested *Xenopus* egg extract (“CSF extract”) and observed their disappearance over time. CPP MTs are stable to dilution in buffer but, when added to extract, depolymerize in five to ten minutes (M. Caplow and J. Shanks, ASCB 1996, #2326). To characterize this depolymerizing activity, we sedimented clarified CSF extract on a 5-20% sucrose gradient and assayed fractions for depolymerizing activity. A single ATP-independent peak of activity was observed at ~9.5S (fig. 1B). XKCM1 co-sedimented with this peak (fig. 1A) but Katanin and Op18 did not (data not shown). The activity appeared to be independent of XKCM1 since XKCM1 requires ATP for efficient MT depolymerization (Desai et al., 1999b). To confirm that XKCM1 was not responsible for the depolymerizing activity, we assayed those fractions in the absence of ATP and in the presence of inhibitory  $\alpha$ -XKCM1 antibody (Walczak et al., 1996) (fig. 1B). Depolymerizing activity was not blocked, suggesting that another factor was responsible.

### *Identification of the depolymerizing activity as a fragment of XMAP215*

We purified the unknown CPP MT depolymerizing factor using conventional chromatography. The assay consisted of adding rhodamine-labeled CPP MTs to each fraction and fixing at timepoints to observe the disappearance of these microtubules by fluorescence microscopy. Relative activity of each fraction was estimated by serial



dilution. The key strategic issue was separation of the novel CPP MT depolymerizing activity from other activities that either inhibited the assay (bundling factors) or scored in the assay (known destabilizers). To avoid confusion between the novel activity and XKCM1, we purified the novel activity from a 40% ammonium sulfate supernatant of clarified CSF extract, which contained only a fraction of total depolymerizing activity, but was free of the known depolymerizers, XKCM1, Katanin, and Op18, by western blot (data not shown).

The CPP MT depolymerizing factor was purified using seven steps: ammonium sulfate precipitation, phenyl sepharose, heparin, monoS, gel filtration, monoQ (pH 7.2), and a final monoS column. When fractions were separated by SDS-PAGE and silver-stained, a set of polypeptides of ~130 kD and a protein of ~160 kD consistently co-eluted with activity on the last two columns in the purification (arrows, fig. 2A; fig. 2B). We estimated that specific activity was enriched several thousand fold by the final monoS step (see Table I).

Attempts at further purification resulted in extensive loss of activity and protein. Instead, two independent purification steps (sucrose gradient and monoQ, pH 8.8) were performed in parallel with the above purification, starting with active fractions from the gel filtration step. In both of these steps, the same set of 130 kD and 160 kD proteins continued to peak in active fractions (data not shown).

The cluster of polypeptides at 130 kD were excised from an 8% polyacrylamide gel and identified by liquid chromatography tandem mass spectrometry. Twenty-one peptides from the tryptic digest matched the sequence of XMAP215, a previously identified 215 kD *Xenopus* microtubule-binding protein (Gard and Kirschner, 1987).

Each of these peptides mapped to the N-terminal half of the sequence, suggesting we had purified an N-terminal fragment of XMAP215 (data not shown). Western blots using antibodies specific to the N and C termini of XMAP215 (fig. 2C) confirmed that the set of p130 bands as well as the p160 band enriched in our purification were N-terminal fragments of XMAP215.

*XMAP215 is a major CPP MT depolymerizing factor in Xenopus egg extract*

We next investigated whether XMAP215 constituted a CPP MT depolymerizing factor in CSF extracts. Though we had purified a set of N-terminal XMAP215 fragments from crude extract, we could not detect those fragments by Western blot in crude or clarified extract. XMAP215 appeared to exist as a full-length 215 kD species. This full-length XMAP215 co-migrated with the 9.5S peak of depolymerizing activity we originally observed during sucrose gradient sedimentation of clarified extract (fig. 3A). It is not clear if we purified a rare, truncated species of XMAP215 that is highly active in our assay or if endogenous full-length protein was proteolyzed during the purification. The latter explanation seems likely since our depolymerizing factor decreased in sedimentation value from 9.5 to 6S (data not shown) during the purification and since XMAP215 is known to be labile to a variety of non-specific proteases *in vitro* (personal communication, D. Gard).

To test if removal of this full-length XMAP215 would decrease CPP MT destabilizing activity, crude extracts were immunodepleted of XMAP215 using a C-terminal antibody. Unfortunately, N-terminal antibodies were not able to deplete efficiently and N-terminal fragments, if they were present, remained in the extracts. We

also performed immunodepletion of XKCM1 and double depletion of both XMAP215 and XKCM1. Western blots of the depleted extracts demonstrated >95% depletion of each protein (fig. 3B). Levels of non-depleted protein (XKCM1 or XMAP215), as well as Katanin and Op18, were unchanged in depleted extracts relative to mock-depleted extracts (3B). Nocodazole, a small molecule that sequesters tubulin dimer, was added to each assay to prevent endogenous tubulin from polymerizing onto the ends of the CPP MTs, since MT elongation would complicate analysis of destabilization. Depleted extracts had spindle phenotypes similar to those previously published (Tournebize et al., 2000) (Walczak et al., 1996); see fig. S1 in Supplemental Materials.

When rhodamine-labeled CPP MTs were added to mock-depleted extracts, there was a large decrease in the total amount of polymer within five minutes (fig. 3C). In extract depleted of XMAP215, CPP MT depolymerization was partially inhibited. This inhibition was roughly similar to XKCM1 depletion and was partially restored by addition of recombinant full-length protein (data not shown). Furthermore, depletion of both XKCM1 and XMAP215 led to less total depolymerizing activity than did single depletion of either alone. In the experiment shown here, for example, at the five-minute timepoint  $\Delta$ XKCM1 extract had 21 times more polymer than mock-depleted extract,  $\Delta$ XMAP215 had 23 times more polymer, and double-depleted extract had 37-fold more MT polymer. Evidently both proteins contribute significantly to the total CPP MT depolymerizing activity of crude extract. MT polymer was determined by total fluorescent pixel area above background--a measurement that reflects both MT number and MT length.

### *XMAP215 depolymerizes CPP MTs in vitro*

We next assayed pure, baculovirus-expressed XMAP215 for CPP MT depolymerizing activity *in vitro*, using both full-length and truncated XMAP215 constructs previously characterized in (Popov et al., 2001); see fig. S2 in Supplemental Materials. Both full-length protein and an N-terminal fragment (aa 1-560) were able to depolymerize rhodamine-labeled CPP MTs *in vitro* (fig. 4A). In serial titrations, activity for both polypeptides was similar and measurable, beginning between 6.25 and 12.5 nM (fig. 4B). The full-length protein sample does contain a small amount of cleaved protein, so we cannot definitively rule out that this is not the active species in our assay; however, the majority of the protein is full-length. The N-terminal fragment does not appear to be significantly more potent than the full-length protein. A C-terminal fragment of XMAP215 (aa 1168-2065), on the other hand, was completely inactive in the depolymerization assay (fig. 4A,B). We measured depolymerizing activity in the visual assay by using fluorescent pixel area per visual field to quantitate MT polymer. Sedimentation assays and quantitation of tubulin in supes and pellets gave similar results (data not shown). Samples with high concentrations of full-length XMAP215 (stoichiometric with tubulin, about 200 nM) showed less depolymerization and highly bundled MTs (fig. 4A). This was also seen, to a lesser extent, in samples with very high concentrations of N-terminal fragment (data not shown). The C-terminal fragment did not cause bundling at any concentration.

It is not surprising that we do not normally see the polymerization-promoting activity of XMAP215 in our assay, even at concentrations similar to previously published reports. Our assay differs from dynamic MT assays in several ways that strongly select

for depolymerizing activity: the assay is performed at room temperature, uses CSF-XB instead of BRB80 buffer, and contains little or no soluble tubulin dimer for polymerization. The same full-length XMAP215 construct used in our depolymerization assays was shown to have polymerization-promoting activity in dynamic MT assays (Kinoshita et al., 2001).

*XMAP215-promoted depolymerization is specific to MT plus ends*

To test if XMAP215 promotes CPP MTs depolymerization by an end-dependent mechanism, we recorded depolymerization live in glass flow-cells using time-lapse fluorescence microscopy. Rhodamine-labeled CPP MTs were bound to glass using kinesin and then treated with buffer or buffer containing XMAP215. In buffer alone, MTs were relatively stable for half an hour; in the presence of 19 nM XMAP215, they depolymerized over several minutes in an endwise fashion (fig. 5A). There was a strong polarity bias to depolymerization. We used dim-bright CPP MTs and kinesin motility to determine that XMAP215 depolymerized the MT plus end at a rate 5-10x faster than buffer alone, while minus end depolymerization was not measurably affected (fig. 5B). In the presence of XMAP215, 92 out of 95 microtubules (96.8%) had faster rates of depolymerization on their lagging (plus) ends than on their leading (minus) ends. Thus, XMAP215 specifically promotes CPP MT depolymerization at plus ends (see also fig. S3, video in Supplemental Materials). Its polymerization-promoting activity is also plus-end specific (Gard and Kirschner, 1987; Vasquez et al., 1994).

*Mechanism of CPP MT depolymerization by XMAP215*

There are several mechanisms by which XMAP215 might accelerate CPP MT depolymerization. XMAP215 might sequester GMPCPP-tubulin dimers, increase the rate of GMPCPP hydrolysis, or increase the dissociation rate by disrupting the lattice. We ruled out the trivial possibility that our XMAP215 protein preparation contained proteolytic activity by performing SDS-PAGE of depolymerization products (data not shown).

To test if dimer sequestration accelerates apparent CPP MT depolymerization (by inhibiting readdition of subunits to microtubule ends), we added nocodazole to CPP MTs diluted in buffer alone (figure 6A). The same concentration of nocodazole added before CPP MT polymerization completely inhibited polymerization (data not shown).

However, this potent monomer-sequestering drug did not stimulate depolymerization of CPP MTs in our assay, presumably because the total tubulin concentration is too low to allow significant readdition of dimer to MT ends. To test if GMPCPP was hydrolyzed during XMAP215-promoted depolymerization, we used MTs polymerized with [ $\gamma$ - $^{32}$ P] GMPCPP and separated from unbound nucleotides by sedimentation through a sucrose cushion. No hydrolysis was observed in buffer or XMAP215, though Na-BRB80/60% glycerol (a positive control, (Caplow et al., 1994)) did stimulate hydrolysis (6B).

To test if XMAP215 disrupted protofilament interactions within the MT lattice, we imaged CPP MTs before and during treatment with either full-length or N-terminal XMAP215 by negative-stain electron microscopy. In buffer alone, CPP MT ends were blunt (figure 6C). In the presence of XMAP215 (full-length or N terminal fragment), we consistently observed bulbs of material at the ends of the depolymerizing MTs. In some images, these bulbs appeared to contain curled up protofilaments. We cannot state

definitively if these structures contain tubulin, XMAP215, or both—however, they are reminiscent of those resulting from treatment with KinI kinesins (Desai et al., 1999b). We favor a similar unpeeling mechanism for CPP MT depolymerization by XMAP215, though KinI and XMAP215 do differ mechanistically in two interesting ways. First, KinI requires ATP hydrolysis to depolymerize CPP MTs efficiently, and XMAP215 does not. Second, unlike KinI, XMAP215 did not depolymerize taxol-stabilized GDP MTs (data not shown).

## **Discussion**

### *XMAP215 is a major CPP MT depolymerizing factor in Xenopus egg extract*

Microtubule dynamics are subject to regulation by both stabilizing and destabilizing factors *in vivo*. Our overall goal in this project was to identify and characterize novel destabilizers. While three such factors were already known in *Xenopus* egg extracts (Op18/stathmin, XKCM/KinI and Katanin), our initial experiments with CPP MTs suggested that these factors could not account for all destabilizing activity. We set out to isolate the novel factor(s) using biochemical fractionation and purified a fragment of XMAP215. We subsequently showed that XMAP215 is a major CPP MT depolymerizing factor in *Xenopus* egg extract and that low concentrations of pure recombinant XMAP215 promote depolymerization of CPP MTs *in vitro*. XMAP215 had not previously been tested for its ability to depolymerize CPP MTs, an artificial microtubule substrate. We believe that this *in vitro* activity could have important mechanistic implications for both the molecular mechanism of XMAP215 and, more

broadly, the mechanism of dynamic instability. Before discussing those mechanistic implications, we will first briefly discuss the physiological significance of our results.

Finding that XMAP215 is a major MT destabilizing factor is at odds with the current view of this protein as an important MT growth-promoting factor. It was first discovered more than ten years ago by Gard and Kirschner, through biochemical fractionation and a visual assay for MT polymerization—almost the converse of our depolymerization assay. Homologues exist in almost every organism, including *S. cerevisiae* (*stu2*), *S. pombe* (*dis1*, *alp14*), *C. elegans* (*zyg-9*), *D. melanogaster* (*mmps*), *arabidopsis* (*mor1*), and humans (*ch-TOG*) (reviewed in (Ohkura et al., 2001)). The two most common phenotypes for decreased levels of this protein family are short microtubules and defects in spindle pole formation. *In vitro*, pure XMAP215 is known to promote polymerization specifically on the microtubule plus end (Gard and Kirschner, 1987) (Vasquez et al., 1994). And careful combination of brain tubulin, XKCM1, and XMAP215 can recapitulate nearly physiological levels of all four parameters of dynamic instability (Kinoshita et al., 2001). Together, these *in vivo* and *in vitro* data have led to the model that members of the Dis1/XMAP215 family are important factors regulating physiological MT dynamics in all cells by promoting polymerization.

In light of our results, it will be interesting to investigate more closely whether Dis1/XMAP215 family members might also play a role in MT depolymerization in the cell. Consistent with this, recent work by van Breugel et al (accompanying manuscript) demonstrates that the *S. cerevisiae* homologue (*Stu2*) does not promote MT growth *in vitro* but instead slows polymerization and promotes catastrophes. There are at least two places where Dis1/XMAP215 family members are candidates for site-specific



depolymerizing activity. First, in fission yeast, both homologues (Dis1 and Alp14) localize to kinetochores, which are sites for plus end depolymerization (as well as polymerization) during chromosome oscillation and segregation (Garcia et al., 2001; Nakaseko et al., 2001). Tantalizingly, recent evidence in that system points to a synergistic, not antagonistic, relationship between Dis1/Alp14 and the KinI-like kinesins klp5/6 at the kinetochore (Garcia, 2002). Second, in every system examined to date, Dis1/XMAP215 localizes tightly to centrosomes and mitotic spindle poles (Ohkura et al., 2001). A MT depolymerizing factor that localizes to spindle poles would be an attractive candidate for the minus-end depolymerizing activity associated with poleward microtubule flux. The tiny spindles that result from XMAP215 depletion in frog extract have not been tested for their flux rates. However, at least *in vitro*, XMAP215 depolymerization appears to be specific to MT plus ends. It is possible that XMAP215 acts as a MT polymerizer at centrosomes and a MT depolymerizer at kinetochores. Or it is possible that XMAP215 at centrosomes depolymerizes MTs that are misoriented with their minus ends out or, at spindle poles, depolymerizes spurious plus ends from the opposite pole. Interestingly, the major phenotype of decreasing ch-TOG levels in HeLa cells by RNAi is not MT destabilization (as would be expected for a MT stabilizer) but spindle MT disorganization (Gergely et al., 2003). Further investigation will be necessary to determine if XMAP215 ever functions *in vivo* as an overt depolymerizer.

#### *Mechanistic implications for XMAP215*

Although most of the literature focuses on the ability of XMAP215 to promote polymerization, our observation that XMAP215 can destabilize microtubules is not

without precedent. Vasquez et al had previously shown that purified XMAP215 increased MT depolymerization rate as well as polymerization rate, and that it inhibits rescue events (Vasquez et al., 1994). These data are consistent with lattice destabilizing activity, as is the data of Van Breugel et al for Stu2 (accompanying manuscript).

Because full-length XMAP215 had depolymerizing activity in our *in vitro* assay, proteolysis cannot account for conversion of a polymerizing factor into a depolymerizing factor. Both polymerizing activity (Popov et al., 2001) and depolymerizing activity map roughly to the N-terminal 1/4 of XMAP215. More precise mapping might separate these functions in the future. However, given that both activities act primarily on MT plus ends, our current working model is that XMAP215's polymerization promoting and CPP MT destabilizing activities are two aspects of a common biochemical mechanism.

What might this common mechanism be? Our preliminary studies suggest a model in which XMAP215 alters the conformation of the MT end to promote depolymerization, possibly by affecting interactions between protofilaments. The mechanism by which XMAP215 promotes polymerization specifically on the microtubule plus end is not known. Two hypotheses have been considered (Spittle et al., 2000): XMAP215 might oligomerize tubulin dimers in solution and thus catalyze addition of several dimers per association event; alternatively, it might alter the structure of the growing end, promoting a structure that either adds dimers more rapidly or is less likely to undergo brief pause events. The latter model, in which Dis1/XMAP215 modifies the end of the microtubule lattice so as to promote dynamicity, potentially allows a unified explanation for all four activities of the protein (promoting polymerization, promoting depolymerization, antagonizing/inhibiting rescue, depolymerizing CPP MTs). A key clue might come from

the specialized, non-physiological CPP MT substrate and in understanding what physiological state it mimics most closely.

The CPP lattice has most often been used as a model for the GTP cap (Caplow and Shanks, 1996; Drechsel and Kirschner, 1994). However, the blunt-ended, closed-tube structure of the CPP MT lattice is not similar to the sheet-like end of a growing MT—nor does it resemble the rams' horns of a shrinking microtubule (Chretien et al., 1995; Mandelkow et al., 1991; Simon and Salmon, 1990). We propose instead that CPP MTs are a model for the microtubule pause state. Tran and Salmon proposed a 3-state model for dynamic instability in which the pause state is an obligate intermediate between polymerization and depolymerization (Tran et al., 1997). Neither the structure nor the bound nucleotide of the hypothetical pause state is known. It seems reasonable to suggest that the pause state might have a blunt-ended, closed tube structure, intermediate between the sheetlike protofilament extensions and curled protofilaments characteristic of growth and shrinkage. Consistent with this idea, Chretien et al proposed that loss of sheet-like protofilament extensions correlated with slower growth (Chretien et al., 1995). A plus end that paused long enough would presumably exchange nucleotide at the exposed E-sites (Mitchison, 1993), resulting in GTP-bound tubulin subunits at the tip of a paused plus ends. The exposed end of a CPP MT, that is blunt and contains a GTP analogue, may mimic this hypothetical blunt, exchanged state of a MT in which all the internal subunits are GDP-bound.

This interpretation of what the CPP lattice mimics prompts us to propose that XMAP215 destabilizes the pause state, acting as an anti-pause factor (fig. 7). Microtubules frequently pause *in vivo*, spending prolonged time neither growing nor

shrinking at the resolution level of the light microscope (Rusan et al., 2001; Shelden and Wadsworth, 1993; Tirnauer et al., 1999). Microtubules also pause during phases of polymerization and depolymerization in *Xenopus* extracts (Tirnauer et al., 2002). Pauses are infrequent in reports of pure tubulin dynamics (Walker et al., 1988) but it is possible that pure MTs undergo micro-pauses too short to be detected by conventional imaging. In this pause state, microtubules can theoretically transition into either growth or shrinkage and a factor that destabilizes the pause state would increase microtubule dynamicity. Whether the microtubule transits to growth or shrinkage may depend on its environmental cues (tubulin concentration, other proteins, nucleotides, salt, or buffer)—this would explain the apparently contradictory behavior of XMAP215 in different contexts. An anti-pause factor would also increase both apparent polymerization and depolymerization rate if polymerization and depolymerization were rate-limited by micro-pauses. Higher resolution tracking of growing ends with pure tubulin could test this assumption. The anti-pause hypothesis could also account for the plus end specificity of XMAP215 if, for example, micro-pauses, corresponding to loss of protofilament extensions (Chretien et al., 1995), limit plus end growth and shrinkage more than minus end growth and shrinkage. Indeed the pause model was introduced to account for different stabilities of the plus and minus ends (Tran et al., 1997).

Microtubule depolymerization is necessary for every aspect of mitotic spindle function, from the breakdown of microtubules in prophase to the search-and-capture of kinetochores to kinetochore oscillations, flux, anaphase movement, and spindle disassembly after anaphase. The *in vivo* function of Dis1/XMAP215, currently thought of as a microtubule growth-promoting factor, should be re-examined to look for functions

that might depend on its microtubule destabilizing activity, an equally important aspect of its biochemistry. Interesting areas of future research include determining whether the two apparently opposed activities of XMAP215 are separable, either biochemically or by mutation, and asking if XMAP215 exhibits these two activities because it is, fundamentally, an anti-pause factor. Addressing these questions should inform us as to the molecular mechanisms underlying physiological microtubule dynamics.

## **Materials and Methods**

### *Xenopus Egg Extracts*

CSF-arrested extracts and *in vitro* spindle assembly reactions were prepared as previously described (Desai et al., 1999a). For large-scale purification, the following adjustments were made. Packing and crushing spins were performed in 50 ml (28.7 x 103.3 mm) tubes (Nalgene Nunc), with 25-30 mls of eggs per tube. The packing spin consisted of 1 min at 500 rpm and 30 sec at 1 krpm in a clinical centrifuge (Sorvall); the crushing spin was performed at 12.5 Krpm (~21K xg) for 15' at 16°C in a Surespin 630 rotor (Sorvall). Crude CSF extract was then clarified at 4°C either in a TH-641 rotor (Sorvall) for 4 hours at 41K rpm (~200K xg) or in two AH650 rotors (Sorvall) for 2 hours at 50K (~235K xg). Typically, 20-25 mls of clarified CSF extract (~40 mg/ml protein) were obtained from 1 L of eggs (pre-dejellinging volume). Clarified extract was supplemented with cyto D (Sigma, 10 µg/ml final), protease inhibitors (Sigma, 10 µg/ml final each: leupeptin, pepstatin A, chymostatin), and energy mix (7.5 mM creatine phosphate, 1 mM ATP, 1 MgCl<sub>2</sub> final) before being flash-frozen in liquid nitrogen in 1 ml aliquots.

### *In vitro assay for CPP MT depolymerization*

Tubulin was labeled with tetramethyl- or X-rhodamine (Molecular Probes) as previously described (Hyman, 1991) and was used to prepare GMPCPP-stabilized microtubules (CPP MTs) using standard procedures (Caplow et al., 1994; Hyman et al., 1992).

Concentration of tubulin (1:3, labeled:unlabeled) during polymerization was 0.4 mg/ml (4  $\mu$ M) and GMPCPP concentration was 200  $\mu$ M. After polymerization at 37°C for 30', MTs were removed from the water bath and placed to cool at room temperature for 5-15'. For each reaction, 0.5  $\mu$ l of polymerized CPP MTs were added to 10  $\mu$ l of buffer or buffer plus sample, for a final tubulin concentration of 200 nM. Reactions were staggered for fixed time-points. One  $\mu$ l of each reaction was fixed with 2  $\mu$ l of 80% glycerol/0.1% glutaraldehyde after 10 or 15 min incubation. During the purification, column fractions were assayed after >10-fold dilution in assay buffer (50 mM  $\beta$ -glycerol phosphate, pH 6.8, 50 mM sucrose, 5 mM EGTA, 1 mM DTT). When necessary, 100  $\mu$ l of each fraction was desalted using 1 ml disposable spin columns filled with equilibrated G-25 fine resin. Desalting of samples with low protein concentration led to high loss of activity unless detergent was added (0.5% CHAPS) or protein concentration supplemented to 0.5 mg/ml with purified ovalbumin (Sigma).

For quantitative measurement of activity with pure XMAP215 constructs, the following adjustments were made. Assays were performed in extract buffer ("CSF-XB", 100 mM KCl, 50 mM sucrose, 10 mM K-HEPES, pH 7.7, 5 mM EGTA, 2 mM MgCl<sub>2</sub>, 0.1 mM CaCl<sub>2</sub>). After 15', 3  $\mu$ l of each reaction was mixed thoroughly with 3  $\mu$ l of fix. Two  $\mu$ l of this mixture were squashed under a coverslip for a thin homogenous sample. Images (~50 random fields per sample) were acquired on an upright Nikon E-600 or E-

800 microscope equipped with a cooled charge-coupled device camera (Princeton Instruments, Trenton, NJ) using MetaMorph software (Universal Imaging, West Chester, PA). Images for each sample were made into a stack and thresholded using an average background value for that set (which was always much lower than the intensity of MT fluorescence). Integrated Morphometry Analysis was used to count the number of objects (microtubules) per field, the length of each object, and the fluorescent pixel area of each object. Results were logged and analysed in Microsoft Excel 2000. Average MT length can be skewed by a few long microtubules in the field (versus many microtubules of varied length) and average MT number per field by a large number of very small microtubules. We felt that fluorescent pixel area values best represent total MT polymer as these measurements incorporate both length and number. Other parameters (such as average length x number or the average sum of MT lengths per field) would take into account both length and number but assume that all microtubules are the same width; unfortunately, some fields (such as samples with high concentrations of full-length XMAP215) contained bundled microtubules that were considerably wider than the average microtubule. Also, fluorescent pixel area was an easier parameter to quantitate for multiple fields using automated IMA.

Recombinant full-length XMAP215 and truncated proteins tested in the *in vitro* CPP MT depolymerization assay were generous gifts from K. Kinoshita, D. Drechsel, and A. Hyman.

*Determination of sedimentation value*

50  $\mu$ l of clarified extract or 10-20  $\mu$ l of purified fraction (sup6 or monoS2) were sedimented through a 5 ml linear 5-20% sucrose gradient in assay buffer or CSF-XB (both buffers contains 50 mM sucrose on top of additional sucrose) for 5-14 hours at 50K in an SW50 (Beckman) or AH650 (Sorvall) rotor. 250  $\mu$ l fractions were collected from top to bottom. 20  $\mu$ l of protein standard solution were run on two parallel gradients. Protein standard solution consisted of ovalbumin (3.55S), bovine serum albumin (4.3S), aldolase (7.3S) and catalase (11.3S).

*Purification of XMAP215 as a CPP MT depolymerizing factor*

20 ml of *Xenopus* HSS was thawed, pooled, and split into 2x 15 ml snap-cap tubes. After addition of supplemental energy mix and creatine kinase (Sigma, 50  $\mu$ g/ml final), the extract was spun in a Sorvall SA-600 rotor for 15 min at 10K rpm, 4°C. The supernatant was recovered and 0.226 g of finely ground ammonium sulfate (AS) powder was added per ml, slowly and with continuous stirring, for a final concentration of 40% AS. Extract was rotated in the coldroom for 1 h and spun for 10 min at 10K in the SA-600 rotor, 4°C. Supernatant was collected and diluted 5-fold into PS buffer (40% AS, 50 mM  $\beta$ -glycerol phosphate, 50 mM sucrose, 5 mM EGTA, 1 mM DTT).  $\beta$ -glycerol phosphate served as both buffer and phosphatase inhibitor, being useful for maintaining proteins in mitotic state during purification from *Xenopus* egg extract (Takada et al., 2000). Diluted supernatant ("AS supe") was syringe-filtered through 0.45  $\mu$ m membrane and loaded slowly (1 ml/min) with a Gilson pump directly onto an ~30 ml XK 26/16 phenyl sepharose column (Pharmacia). A 300 ml reverse gradient of 40-0% AS was applied to



the column at 3 ml/min and 10 ml fractions were collected. Activity eluted between 24% and 17% AS.

After desalting over a 50 ml HiPrep 26/10 desalting column (Pharmacia) equilibrated in MS buffer (20 mM MOPS, pH 7.0, 50 mM  $\beta$ -glycerol phosphate, 50 mM sucrose, 5 mM EGTA, 1 mM DTT), protein ("PS pool") was loaded onto a 5 ml Hi-Trap heparin column (Pharmacia) and eluted with a linear 50 ml gradient up to 0.5 M KCl. Activity eluted at about 250 mM KCl. Active fractions were pooled ("hep pool"), supplemented with 0.5 mg/ml ovalbumin or human serum albumin final, concentrated via pre-blocked microcons, and re-diluted until conductivity assays showed that total salt had been reduced to 0.35 mS. Pooled fractions were loaded on a 1 ml MonoS column (Pharmacia) at 0.5 ml/min or, alternatively, on a 100  $\mu$ l SMART system MonoS column (Pharmacia) with repeated cycles of loading and elution. In both cases, >90% of the protein flowed through. Bound protein was eluted with a linear gradient of 0-500 mM KCl in MS buffer and activity eluted at 160 mM KCl.

These fractions were pooled ("monoS1"), concentrated via microcon to a final volume of 100  $\mu$ l, re-filtered through a 0.22  $\mu$ m spin-filter, and applied to a 1 ml SMART system Superose 6 column (Pharmacia) which had been previously equilibrated with assay buffer. Activity eluted at about 1.45 ml. Four or five fractions of 50  $\mu$ l each were pooled ("sup6"), diluted into MQ buffer (180 mM KCl, 20 mM Tris-HCl, pH 6.0, 50 mM sucrose, 5 mM EGTA, 5 mM  $MgCl_2$ ), and loaded on a 100  $\mu$ l SMART system MonoQ column (Pharmacia). Activity appeared in the flow-through ("Q FT"), which was supplemented with MOPS to pH 7.0 and diluted to a final KCl concentration of 50 mM. The Q FT was applied to a 100  $\mu$ l SMART system MonoS column (Pharmacia). During

a linear gradient of 0-500 mM KCl, a single peak of activity again eluted at 160 mM KCl. 50  $\mu$ l fractions ("monoS2") were collected and assayed. Fractions were pooled and sedimented on a 2 ml 5-20% sucrose gradient (TLS-55 rotor, 50K, 4 h, 4°C), or run on SDS-PAGE for silver-stain.

Purification was complicated by non-specific losses in activity when protein concentration was too low. For this reason, in the last two or three steps protein levels were supplemented to 0.5 mg/ml during column loading with purified ovalbumin, which binds monoQ and flows through monoS in our MQ and MS buffers, respectively. Since losses in activity were also incurred by freeze-thaw, the purification protocol was performed over several days at 4°C, without freezing any active fractions.

#### *Mass spectrometry*

MS final fractions were separated on an 8% polyacrylamide gel by SDS-PAGE. The gel was silver-stained with the following protocol: 10 min in 50% methanol; 10 min in 5% methanol; 10 min in 250 ml H<sub>2</sub>O containing 8  $\mu$ l of 1 M DTT; 10 min in "silver solution" (0.2% AgNO<sub>3</sub>); brief wash with milliQ water (3 x 10 sec); brief wash with a small amount of "developing solution" (7.5 g of Na<sub>2</sub>CO<sub>3</sub> in 250 ml water plus 125  $\mu$ l 37% formaldehyde); brief wash with a small amount of milliQ water; addition of the remaining developing solution until bands are of desired intensity; quench by pouring off developing solution and adding 5% AcOH; 3x15 min washes with water. After silver-stain, p130 bands were carefully excised and subjected to tryptic digest before liquid chromatography tandem mass spectrometry and database analysis; these procedures were performed at Taplin Biological Mass Spectrometry Facility at Harvard Medical School.

### *Immunoreagents*

Antibodies specific to the N-terminal 560 aa of ch-TOG and antibodies specific to the C-terminal 15 aa of ch-TOG were a generous gift from K. Kinoshita and A. Hyman. Anti-Katanin antibody was a generous gift from F. McNally. Inhibitory XKCM1 antibodies were kindly provided by both C. Walczak and R. Ohi; inhibitory activity was confirmed both in extract (fig. 3D) and in *in vitro* assays with recombinant XKCM1 (data not shown). Immunodepletion of *Xenopus* egg extracts was performed with Dynabeads as previously described (Tournebize et al., 2000). Efficient depletion of XMAP215 was achieved using a polyclonal rabbit antibody raised against the last 16 aa at the C-terminus after two rounds of depletion, using 12.5  $\mu\text{g}$  of antibody per 50  $\mu\text{l}$  of beads per round for 140  $\mu\text{l}$  of crude extract. Similar concentrations of rabbit IgG (Sigma) and anti-XKCM1 antibody were used for each round of mock- and XKCM1 depletions.

### *Time-lapse microscopy and flow-cell assay*

Flow-cells were constructed using GoldSeal glass slides, 18x18 mm square GoldSeal coverslips, and thin strips of double-sided Scotch tape. Each coverslip was rinsed in acetone for 10-15 minutes before being spun dry and then air-dried on whatman paper (15-30 min). Coverslips were inverted onto two pieces of double-sided tape stuck to a glass slide, creating chambers of  $\sim$ 10-15  $\mu\text{l}$ . Reagents were pipetted into one end and drawn out the other with triangles of whatman paper in this order: 1) 1 vol of 100  $\mu\text{g}/\text{ml}$  kinesin (generous gift from Z. Maliga) in 20 mM Tris-HCl, pH 7.0, 1 mM DTT, incubated 10 min; 2) 5-8 vol of 6.5 mg/ml casein, incubated 10 min; 3) 5-8 vol BRB80 +

1 mM DTT; 4) 3-5 vol of CPP MTs, usually diluted to 400 nM, incubated 10 min; 5) 5-8 vol BRB80 + 1x Oxygen Scavenging mix ("OS"= 4.5 mg/ml glucose, 0.035 mg/ml catalase, 0.2 mg/ml glucose oxidase, 0.5%  $\beta$ -mercaptoethanol in CSF-XB); 6) 5-8 vol CSF-XB + OS; 7) 3-5 vol CSF-XB + OS +/- 19 nM XMAP215 (full-length recombinant protein) +/- 10  $\mu$ M MgATP. Though kinesin motility was fast and reliable in BRB80, CPP MTs were often released by kinesin in CSF-XB + ATP, necessitating high concentrations of kinesin in step 1 and low ATP concentrations in step 7. Dim-bright CPP MTs were made as previously described (Hyman, 1991), polymerizing 0.4 mg/ml of 1:1 (labeled:unlabeled) tubulin plus 200  $\mu$ M CPP for bright seeds and using 36  $\mu$ g/ml of these seeds in ~0.2 mg/ml of 1:7 (labeled:unlabeled) tubulin for dim MT elongation. Time-lapse movies were made by taking 100 ms exposures (bin=2) every 5-15 seconds, using microscopy equipment as described above. Movies were analyzed using Metamorph as follows: movies were recorded as stacks; planes corresponding to two time-points were duplicated from the stack; using "color combine," the two planes were overlaid in two different colors; using the line region tool, MT lengths were measured on either side of a fiduciary mark; polarity could be assigned by comparing the location of the fiduciary mark in each plane. We only used MTs with clearly distinguishable ends in both planes and clear movement of the fiduciary mark. MT length measurements were logged to a spreadsheet in Microsoft Excel for further analysis.

#### *GMPCPP hydrolysis*

[ $\gamma$ -<sup>32</sup>P] GMPCPP was synthesized from GMPCP and [ $\gamma$ -<sup>32</sup>P] ATP. 2 u of nucleotide diphosphate kinase (Sigma), 15  $\mu$ l of 1 mM GMPCP in BRB80, 15  $\mu$ l of [ $\gamma$ -<sup>32</sup>P] ATP

were incubated at room temperature for 6 hours. The reaction was spun for 15 min in a microfuge and the supernatant was filtered through a 10K cut-off filter. 0.1  $\mu$ l of each reaction products was analyzed by thin-layer chromatography (TLC) using PEI-cellulose plates (Baker-Flex) run in 1.0 M LiCl and detected using a phosphorimager (Biorad Molecular Imager FX) and Quantity One v.4.1.1 software. Standards (1  $\mu$ l each of 10 mM GMPCPP, ATP stocks) were run in parallel and detected using a handheld UV lamp.

[ $\gamma$ -<sup>32</sup>P] GMPCPP was used to monitor phosphate hydrolysis in the depolymerization reaction. Depolymerization reactions were performed as described above, using 75 nM full-length, recombinant XMAP215 or N-terminal fragment, except that 15  $\mu$ l of [ $\gamma$ -<sup>32</sup>P] GMPCPP was added during CPP MT polymerization to incorporate it into the lattice. Reactions without [ $\gamma$ -<sup>32</sup>P] GMPCPP were performed in parallel, to monitor the extent of depolymerization by visual assay. Phosphate hydrolysis was monitored by taking 6.7  $\mu$ l of each reaction at 0 min, 10 min, and 20 min for assays in assay buffer and at 0 min, 30 min, and 60 min for assays performed in BRB80 or BRB80 + 5 mM EDTA. Results were equivalent for each buffer condition. Time-points were quenched by addition of an equal volume of denaturing buffer (8 M urea, 20 mM Tris-HCl, pH 7.0, 5 mM EDTA). As a positive control, depolymerization reactions were performed in 60% glycerol/Na-BRB80, which is known to induce hydrolysis of GMPCPP. Free <sup>32</sup>Pi was separated from [ $\gamma$ -<sup>32</sup>P] GMPCPP by TLC on PEI-cellulose using 0.75 M sodium phosphate, pH 4.2, after first pre-running (post-load) each TLC plate with ddH<sub>2</sub>O to get rid of excess salt, urea, and glycerol. Radioactive reaction products were detected using a Molecular Imager FX phosphorimager (Biorad) and Quantity One v.4.1.1 software.

### *Negative stain EM*

Negative stain electron microscopy was performed as previously described (Desai et al., 1999b). Standard depolymerization reactions were performed, using 38.5 nM XMAP215, except that each sample was spun for 15 min on high at 4°C in a microfuge before addition of rhodamine-labeled CPP MTs and reactions were performed in BRB80 buffer.

### **Supplementary Material**

*Fig. S-1: Depletion of XMAP215 inhibited centrosome-nucleated MT polymerization.*

Demembrated *Xenopus* sperm nuclei were added to extracts depleted as noted (see Results) to confirm previously published reports that depletion of XKCM1 inhibits MT depolymerization (Walczak et al., 1996) and depletion of XMAP215 inhibits MT polymerization (Tournebize et al., 2000); samples were fixed after 60 minutes. As reported,  $\Delta$ XMAP215 extract had very short MTs and  $\Delta$ XKCM1 extract had very long MTs. In extract depleted of both XMAP215 and XKCM1, microtubules appeared to be restored to approximately normal lengths (data not shown).

*Fig. S-2: Gel of recombinant proteins used for in vitro GMPCPP microtubule depolymerization assays.* Full-length XMAP215 (“F”, 1.7  $\mu$ g), N-terminal fragment (“N”, 3.6  $\mu$ g), and C-terminal fragment (“C”, 10.4  $\mu$ g) were separated by SDS-PAGE on a 10% gel and Coomassie-stained.

*Fig. S-3: Movie of real-time depolymerization assay (see Methods).* The sequence of events is as follows: Condition 1 (buffer plus 10  $\mu$ M ATP); Condition 1 (new field of view); Condition 2 (buffer plus 10  $\mu$ M ATP plus 19  $\mu$ M XMAP215. In the presence of XMAP215, microtubules depolymerize at their (lagging) plus ends. Two depolymerizing microtubule plus ends are highlighted with arrows. Note that almost every microtubule in the field undergoes similar depolymerization. Kinesin motility was used to determine microtubule polarity. Images were taken every 5 sec; movie is being played one frame per 1/10 second. For still images, see fig. 5A.

### **Acknowledgments**

We are grateful to Frank McNally, Puck Ohi, Claire Walczak, Zoltan Maliga, Kazu Kinoshita, David Drechsel, and Tony Hyman for their gifts of reagents. We also thank Chris Field, Thomas Mayer, David Miyamoto, Ann Yonetani, Zach Perlman, and other members of the Mitchison lab SubGroup for their help and insightful comments. We especially appreciate Karen Oegema, Arshad Desai, Jack Taunton, and Bill Brierer for their guidance in biochemical purification, Jennifer Tirnauer for multiple readings of this manuscript and insightful discussion, and Justin Yarrow for SubSub meetings and thoughtful analysis. M.S.H. writes this manuscript in remembrance of Quin Wells.

This project was supported by a fellowship from the National Science Foundation to M.S.H. and NIH grant (GM39565) to T.J.M.

## **Abbreviations list**

**CPP, GMPCPP:** guanylyl-(alpha, beta)-methylene-diphosphonate

**CSF extract:** cytostatic factor arrested *Xenopus* egg extract

**MAP:** microtubule-associated protein

**MT:** microtubule

**TLC:** thin-layer chromatography

## **References**

- Belmont, L.D., A.A. Hyman, K.E. Sawin, and T.J. Mitchison.** 1990. Real-time visualization of cell cycle-dependent changes in microtubule dynamics in cytoplasmic extracts. *Cell*. 62:579-89.
- Belmont, L.D., and T.J. Mitchison.** 1996. Identification of a protein that interacts with tubulin dimers and increases the catastrophe rate of microtubules. *Cell*. 84:623-31.
- Caplow, M., R.L. Ruhlen, and J. Shanks.** 1994. The free energy for hydrolysis of a microtubule-bound nucleotide triphosphate is near zero: all of the free energy for hydrolysis is stored in the microtubule lattice. *J Cell Biol*. 127:779-88.
- Caplow, M., and J. Shanks.** 1996. Evidence that a single monolayer tubulin-GTP cap is both necessary and sufficient to stabilize microtubules. *Mol Biol Cell*. 7:663-75.
- Cassimeris, L., D. Gard, P.T. Tran, and H.P. Erickson.** 2001. XMAP215 is a long thin molecule that does not increase microtubule stiffness. *J Cell Sci*. 114:3025-33.



- Chretien, D., S.D. Fuller, and E. Karsenti. 1995. Structure of growing microtubule ends: two-dimensional sheets close into tubes at variable rates. *J Cell Biol.* 129:1311-28.
- Desai, A., A. Murray, T.J. Mitchison, and C.E. Walczak. 1999a. The use of *Xenopus* egg extracts to study mitotic spindle assembly and function in vitro. *Methods Cell Biol.* 61:385-412.
- Desai, A., S. Verma, T.J. Mitchison, and C.E. Walczak. 1999b. Kin I kinesins are microtubule-destabilizing enzymes. *Cell.* 96:69-78.
- Drechsel, D.N., and M.W. Kirschner. 1994. The minimum GTP cap required to stabilize microtubules. *Curr Biol.* 4:1053-61.
- Garcia, M.A., L. Vardy, N. Koonruga, and T. Toda. 2001. Fission yeast ch-TOG/XMAP215 homologue Alp14 connects mitotic spindles with the kinetochore and is a component of the Mad2-dependent spindle checkpoint. *Embo J.* 20:3389-401.
- Gard, D.L., and M.W. Kirschner. 1987. A microtubule-associated protein from *Xenopus* eggs that specifically promotes assembly at the plus-end. *J Cell Biol.* 105:2203-15.
- Gergely, F., V.M. Draviam, and J.W. Raff. 2003. The ch-TOG/XMAP215 protein is essential for spindle pole organization in human somatic cells. *Genes Dev.* 17:336-41.
- Gliksman, N.R., S.F. Parsons, and E.D. Salmon. 1992. Okadaic acid induces interphase to mitotic-like microtubule dynamic instability by inactivating rescue. *J Cell Biol.* 119:1271-6.

- Holy, T.E., and S. Leibler. 1994. Dynamic instability of microtubules as an efficient way to search in space. *Proc Natl Acad Sci U S A*. 91:5682-5.
- Hyman, A.A. 1991. Preparation of marked microtubules for the assay of the polarity of microtubule-based motors by fluorescence. *J Cell Sci Suppl*. 14:125-7.
- Hyman, A.A., S. Salser, D.N. Drechsel, N. Unwin, and T.J. Mitchison. 1992. Role of GTP hydrolysis in microtubule dynamics: information from a slowly hydrolyzable analogue, GMPCPP. *Mol Biol Cell*. 3:1155-67.
- Kinoshita, K., I. Arnal, A. Desai, D.N. Drechsel, and A.A. Hyman. 2001. Reconstitution of physiological microtubule dynamics using purified components. *Science*. 294:1340-3.
- Kline-Smith, S.L., and C.E. Walczak. 2002. The Microtubule-destabilizing Kinesin XKCM1 Regulates Microtubule Dynamic Instability in Cells. *Mol Biol Cell*. 13:2718-31.
- Mandelkow, E.M., E. Mandelkow, and R.A. Milligan. 1991. Microtubule dynamics and microtubule caps: a time-resolved cryo-electron microscopy study. *J Cell Biol*. 114:977-91.
- Maney, T., M. Wagenbach, and L. Wordeman. 2001. Molecular dissection of the microtubule depolymerizing activity of mitotic centromere-associated kinesin. *J Biol Chem*. 276:34753-8.
- McNally, F.J., and R.D. Vale. 1993. Identification of katanin, an ATPase that severs and disassembles stable microtubules. *Cell*. 75:419-29.
- Mitchison, T.J. 1993. Localization of an exchangeable GTP binding site at the plus end of microtubules. *Science*. 261:1044-7.

- Miyamoto, D., Z. Perlman, T. Mitchison, and M. Shirasu-Hiza. 2002. Dynamics of the mitotic spindle - potential therapeutic targets. *In Progress in Cell Cycle Research*. Vol. 5. L. Meijer, A. Jezequel, and M. Roberge, editors. Plenum Press, New York.
- Nakaseko, Y., G. Goshima, J. Morishita, and M. Yanagida. 2001. M phase-specific kinetochore proteins in fission yeast: microtubule- associating Dis1 and Mtc1 display rapid separation and segregation during anaphase. *Curr Biol*. 11:537-49.
- Ohkura, H., M.A. Garcia, and T. Toda. 2001. Dis1/TOG universal microtubule adaptors - one MAP for all? *J Cell Sci*. 114:3805-12.
- Popov, A.V., A. Pozniakovsky, I. Arnal, C. Antony, A.J. Ashford, K. Kinoshita, R. Tournebize, A.A. Hyman, and E. Karsenti. 2001. XMAP215 regulates microtubule dynamics through two distinct domains. *Embo J*. 20:397-410.
- Rusan, N.M., C.J. Fagerstrom, A.M. Yvon, and P. Wadsworth. 2001. Cell cycle-dependent changes in microtubule dynamics in living cells expressing green fluorescent protein-alpha tubulin. *Mol Biol Cell*. 12:971-80.
- Shelden, E., and P. Wadsworth. 1993. Observation and quantification of individual microtubule behavior in vivo: microtubule dynamics are cell-type specific. *J Cell Biol*. 120:935-45.
- Simon, J.R., and E.D. Salmon. 1990. The structure of microtubule ends during the elongation and shortening phases of dynamic instability examined by negative-stain electron microscopy. *J Cell Sci*. 96 ( Pt 4):571-82.
- Spittle, C., S. Charrasse, C. Larroque, and L. Cassimeris. 2000. The interaction of TOGp with microtubules and tubulin. *J Biol Chem*. 275:20748-53.

- Takada, S., T. Shibata, Y. Hiraoka, and H. Masuda. 2000. Identification of ribonucleotide reductase protein R1 as an activator of microtubule nucleation in *Xenopus* egg mitotic extracts. *Mol Biol Cell*. 11:4173-87.
- Timnauer, J.S., S. Grego, E.D. Salmon, and T.J. Mitchison. 2002. EB1-Microtubule Interactions in *Xenopus* Egg Extracts: Role of EB1 in Microtubule Stabilization and Mechanisms of Targeting to Microtubules. *Mol Biol Cell*. 13:3614-26.
- Timnauer, J.S., E. O'Toole, L. Berrueta, B.E. Bierer, and D. Pellman. 1999. Yeast Bim1p promotes the G1-specific dynamics of microtubules. *J Cell Biol*. 145:993-1007.
- Tournebize, R., A. Popov, K. Kinoshita, A.J. Ashford, S. Rybina, A. Pozniakovsky, T.U. Mayer, C.E. Walczak, E. Karsenti, and A.A. Hyman. 2000. Control of microtubule dynamics by the antagonistic activities of XMAP215 and XKCM1 in *Xenopus* egg extracts. *Nat Cell Biol*. 2:13-9.
- Tran, P.T., R.A. Walker, and E.D. Salmon. 1997. A metastable intermediate state of microtubule dynamic instability that differs significantly between plus and minus ends. *J Cell Biol*. 138:105-17.
- Vasquez, R.J., D.L. Gard, and L. Cassimeris. 1994. XMAP from *Xenopus* eggs promotes rapid plus end assembly of microtubules and rapid microtubule polymer turnover. *J Cell Biol*. 127:985-93.
- Walczak, C.E., T.J. Mitchison, and A. Desai. 1996. XKCM1: a *Xenopus* kinesin-related protein that regulates microtubule dynamics during mitotic spindle assembly. *Cell*. 84:37-47.
- Walker, R.A., E.T. O'Brien, N.K. Pryer, M.F. Soboeiro, W.A. Voter, H.P. Erickson, and E.D. Salmon. 1988. Dynamic instability of individual microtubules analyzed by

video light microscopy: rate constants and transition frequencies. *J Cell Biol.*  
107:1437-48.

### Figure legends

Fig.1: There is a GMPCPP microtubule depolymerizing activity in *Xenopus* egg extract independent of XKCM1.

(A) *XKCM1* overlaps with the peak of depolymerizing activity on sucrose gradients. 50  $\mu$ l of clarified CSF extract was sedimented over a 5-20% sucrose gradient. Western blot of fractions showed that XKCM1 is present in fractions 10-18. CPP MT depolymerizing activity peaked in fractions 9-14 (see B). Arrows below the blot indicate sedimentation values for protein standards run on a parallel gradient. Active fractions are labeled with asterisks.

(B) *Inhibition of XKCM1 did not inhibit depolymerizing activity in sucrose gradient fractions.* Fractions from the sucrose gradient shown in (A) were assayed for depolymerizing activity, using rhodamine-labeled CPP MTs as described in Methods. Each fraction was assayed in the absence of ATP and in the presence of random IgG or inhibitory amounts of  $\alpha$ -XKCM1 antibody and fixed after ten minutes. XKCM1 depolymerizing activity is ATP-dependent. As shown, neither the absence of ATP nor the presence of  $\alpha$ XKCM1 antibody blocked the depolymerizing activity of active fractions. Active fractions are labeled with asterisks. Bar, 10  $\mu$ m.

Fig. 2: Proteins of 130 and 160 kD were enriched during the purification and consistently co-peaked with activity.

(A) *Specific activity increased with each step of the purification, as did the prominence of p160 and p130 bands (arrows).* Shown here is a silver-stained polyacrylamide gel containing fractions from the purification. Samples for the first seven lanes are listed as follows: mw = molecular weight markers; AS supe = 40% ammonium sulfate supernatant (5  $\mu$ g protein; 4 units of specific activity); PS pool = phenyl sepharose pool of active fractions (4  $\mu$ g, 10 units); hep pool = heparin pool (4.8  $\mu$ g, 300 units); monoS 1 = first monoS column (5  $\mu$ g, 600 units); sup6 = gel filtration/superose 6 (2.5  $\mu$ g, 600 units). The remaining lanes (“monoS2”) represent fractions from the second monoS column; depolymerizing activity peaked in fractions 16, 17, and 18 (see B). Lanes loaded with these fractions each contain  $\sim$ 1.3  $\mu$ g of total protein and 1260 units of specific activity. Arrows indicate p130 and p160 bands. Identity of the p130 bands (lower arrows) from these fractions was determined by mass spectrometry.

(B) *Activity profile for fractions for the monoS2 step.* Relative activity was estimated for fractions 8-24 by serial titration in the depolymerization assay and is presented in this graph as arbitrary units per  $\mu$ g protein.

(C) *p160 and p130 bands are N-terminal fragments of XMAP215.* Western blots of high-speed supernatant (“hss”) and monoS2 fractions were probed for XMAP215 with N-terminal or C-terminal specific antibodies.

Fig. 3: XMAP215 contributes to GMPCPP microtubule depolymerizing activity in CSF extract.

*(A) Full-length XMAP215 co-peaks with depolymerizing activity on a sucrose gradient.*

Sucrose gradient fractions were analyzed by Western blot with C-terminal specific  $\alpha$ -XMAP215 antibody. Active fractions are labeled with asterisks.

*(B) Crude extract was specifically depleted of full-length XMAP215, XKCM1, or both.*

Samples were depleted with random IgG, C-terminal  $\alpha$ -XMAP215 antibody

( $\Delta$ XMAP215),  $\alpha$ -XKCM1 antibody ( $\Delta$ XKCM1), or both  $\alpha$ -XMAP215 and  $\alpha$ -XKCM1 antibodies ( $\Delta$ both). Western blots for the four major depolymerizers (XMAP215,

XKCM1, Katanin, and Op18) are shown for each condition.

*(C) Depletion of XMAP215 and XKCM1 from crude extract inhibited GMPCPP*

*microtubule depolymerization.* Rhodamine-labeled CPP MTs were incubated in depleted extracts for 10 minutes. Representative fluorescence images of each sample are shown.

Buffer used for negative control was CSF-XB (extract buffer used, see Methods). Bar, 10  $\mu$ m.

Fig. 4: Pure recombinant XMAP215 depolymerizes GMPCPP microtubules *in vitro*.

*(A) Full-length XMAP215 and an N-terminal fragment of XMAP215 both depolymerize*

*GMPCPP microtubules but a C-terminal fragment does not.* Rhodamine-labeled CPP MTs were incubated for 15 minutes in buffer containing different concentrations of full-length XMAP215 (“F”), an N-terminal fragment (“N”), or a C-terminal fragment (“C”).

Shown here are representative fluorescence images for four concentrations of each protein. Bar, 10  $\mu$ m.

*(B) Full-length XMAP215 and the N-terminal fragment have depolymerizing activity*

*between 6.25 and 200 nM.* Microtubule polymer was quantitated for each sample by

calculating average fluorescent pixel area per field for each protein concentration of full-length (“F”), N-terminal (“N”), and C-terminal (“C”) XMAP215. Microtubule polymer is expressed as % median value of buffer control; error bars denote 10<sup>th</sup> and 90<sup>th</sup> percentile; the 75<sup>th</sup>, 50<sup>th</sup>, and 25<sup>th</sup> percentiles are represented by the top, middle and bottom of each box.

Fig. 5: XMAP215 promotes GMPCPP microtubule depolymerization at microtubule plus ends.

(A) *XMAP215 promotes end-dependent GMPCPP microtubule depolymerization.*

Shown here are images from a time-lapse series of dim-bright CPP MTs (see Methods) treated with buffer alone or buffer plus 19 nM XMAP215 (interval between still images is 40 seconds). In each sample, kinesin motility was used to determine microtubule polarity: translocation of the microtubule from left to right represents minus end leading and plus end lagging. In the XMAP215-treated sample, the plus end shortens while the minus end remains stable. (See also Fig. S-3 in Supplemental Materials for video.)

(B) *Depolymerization by XMAP215 is specific to microtubule plus ends.*

Depolymerization rates were quantitated for each microtubule end from experiments as in (A). Error bars denote 10<sup>th</sup> and 90<sup>th</sup> percentile; 75<sup>th</sup>, 50<sup>th</sup>, and 25<sup>th</sup> percentiles are represented by the top, middle and bottom of each box.

Fig. 6: Mechanism of GMPCPP microtubule depolymerization by XMAP215.



(A) *Nocodazole does not depolymerize GMPCPP microtubules in our assay.* Dimer sequestration was tested by incubating rhodamine-labeled CPP MTs with buffer plus DMSO or 20  $\mu$ M nocodazole.

(B) *XMAP215 does not accelerate hydrolysis of GMPCPP.* Thin-layer chromatography was used to detect the hydrolysis of  $\gamma$ -<sup>32</sup>P labeled GMPCPP in CPP MTs treated with buffer alone; full-length XMAP215; N-terminal fragment of XMAP215; or Na-BRB80/60% glycerol (positive control). Timepoints were taken from each reaction at 0, 30, and 60 min.  $\gamma$ -<sup>32</sup>P-GMPCPP (“CPP”),  $\gamma$ -<sup>32</sup>P-ATP (“ATP”), and <sup>32</sup>Pi (“Pi”) are loaded as markers. Release of Pi is seen by the appearance of a second spot in Na-BRB80/60% glycerol, but not in XMAP215 or N-terminal XMAP215 samples. Microscopy assays run in parallel demonstrated that treatment with XMAP215 and the N-terminal construct depolymerized CPP MTs by the final time point (data not shown).

(C) *XMAP215 causes protofilament curling on microtubule ends.* CPP MTs were incubated in buffer alone or buffer plus 38.5 nM full-length XMAP215 for two min and imaged by negative stain EM. Left bar, 200 nm. Right bar, 50 nm.

Fig. 7: Model for the potential mechanism of XMAP215 as an anti-pause factor.

Depicted here are the growing MT end (top) as a sheetlike structure of protofilament extensions and the shrinking MT end (bottom) with curled protofilaments (adapted from (Miyamoto et al., 2002)). The hypothetical paused MT end structure (middle) is positioned as an obligate intermediate between the two, drawn here with a blunt-ended, closed tube structure. We propose that XMAP215 destabilizes this pause state by weakening interprotofilament bonds and/or preventing tube closure, increasing transition

to either the growing or shrinking state (arrows). Based on work by Cassimeris et al, we depict XMAP215 here as a long curved molecule that can bind protofilaments along their long axis (Cassimeris et al., 2001).

Table 2-1.

Step	Total activity (units)	Protein (ug)	Specific activity (units/ug)	Fold-purification
HSS	440,000	1,320,000	0.33	1.00
AS supe	400,000	524,000	0.76	2.30
Ph. sepharose	300,000	122,000	2.45	7.40
heparin	150,000	2,410	62.30	188.79
monoS #1	72,000	595	121.00	366.67
superose 6	15,000	65	230.77	699.30
monoQ FT	10,000	28	357.14	1082.24
monoS #2	4,500	5	900.00	2727.27

Figure 2-1:

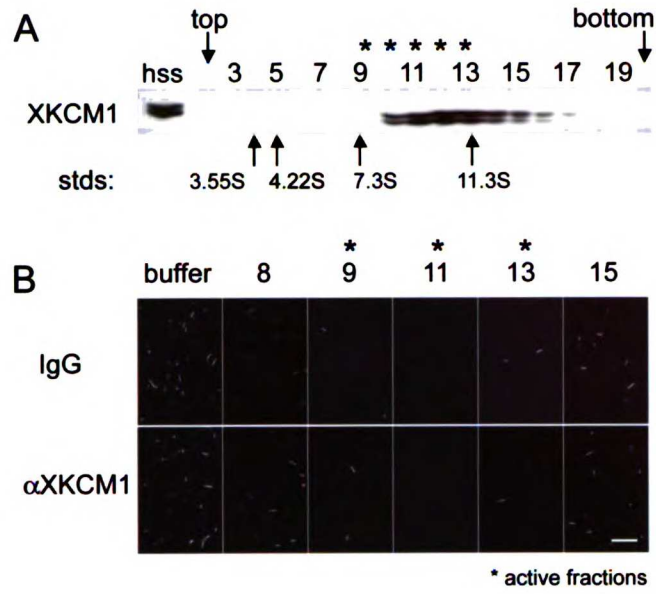


Figure 2-2:

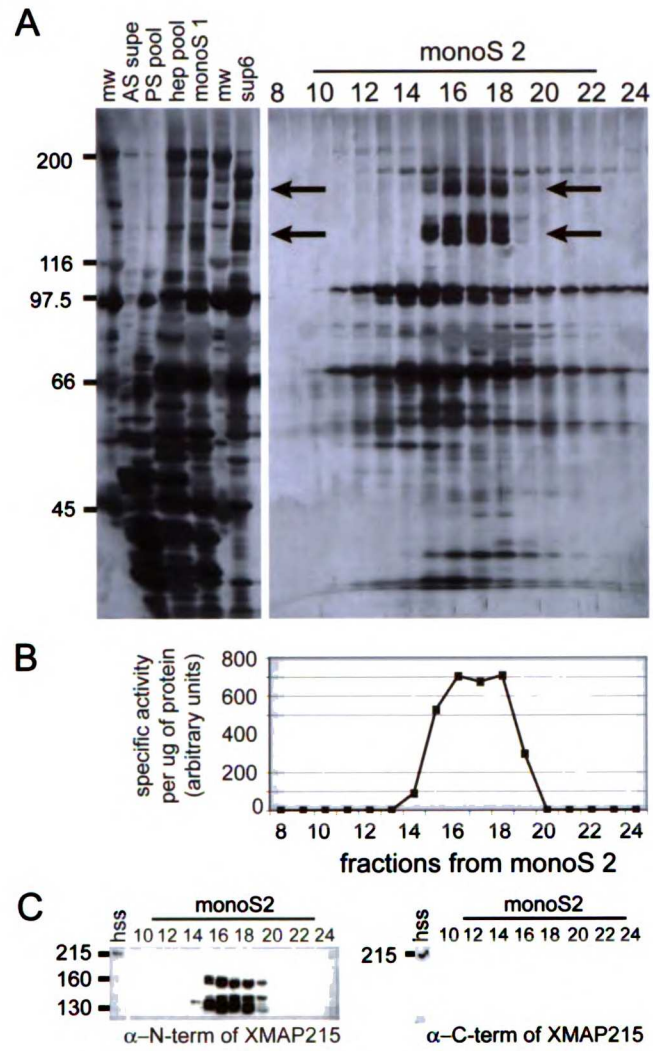


Figure 2-3:

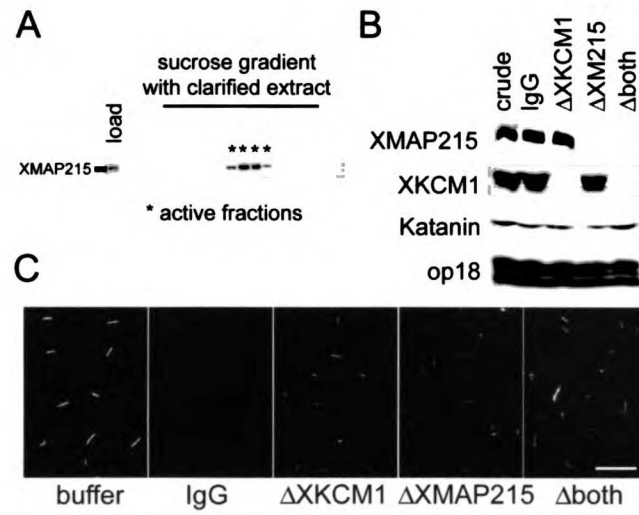


Figure 2-4:

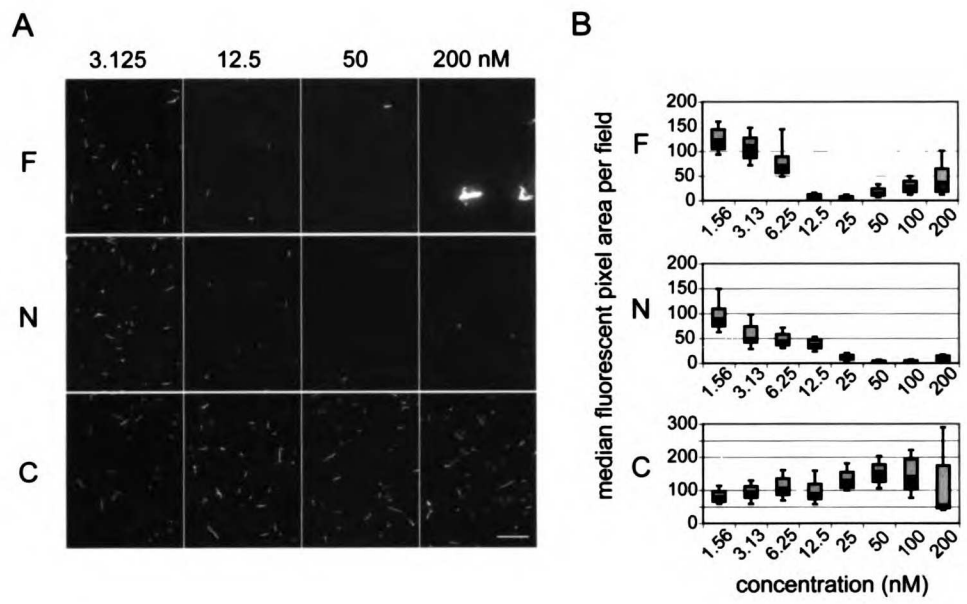


Fig. 2-5:

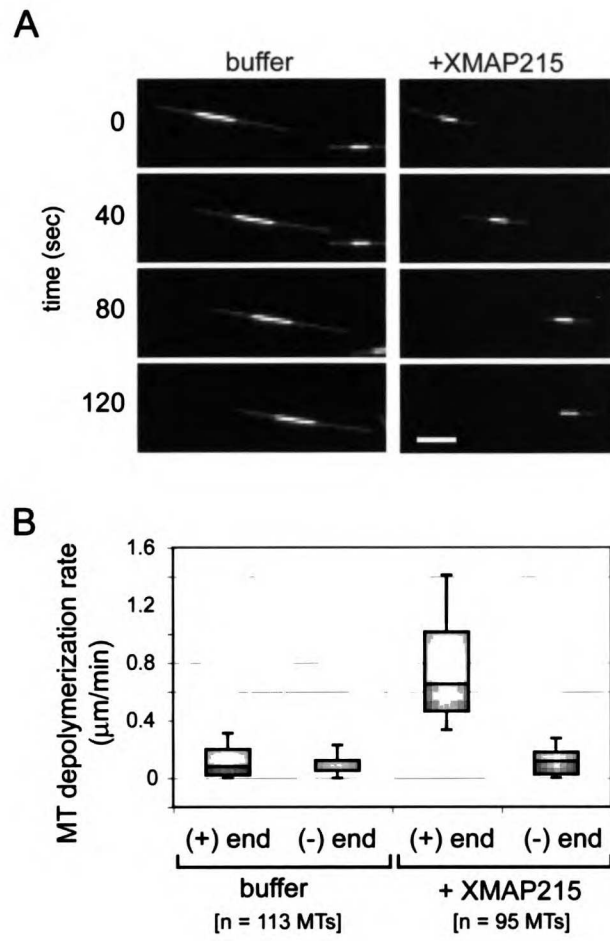




Figure 2-6:

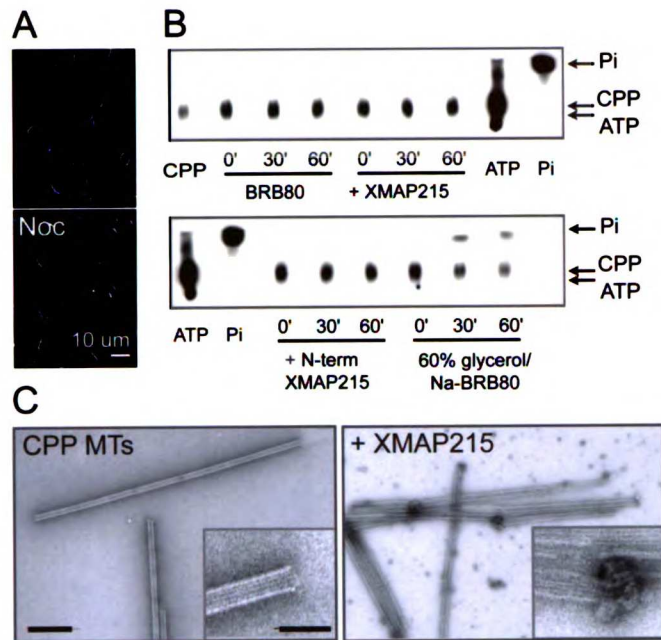


Figure 2-7:

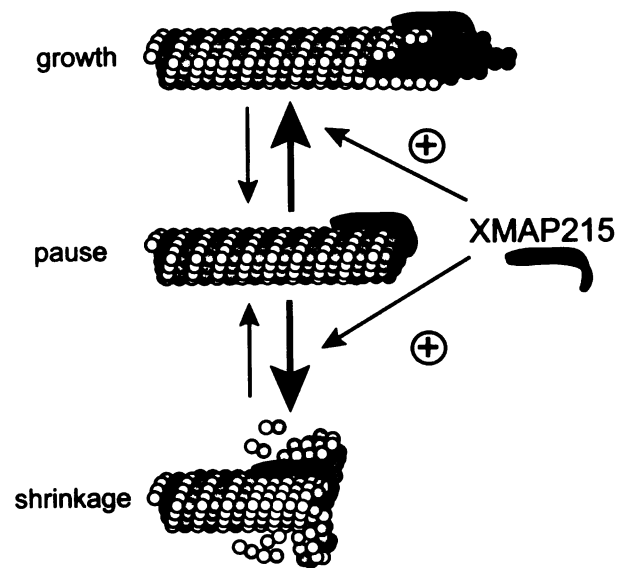


Figure S-1:

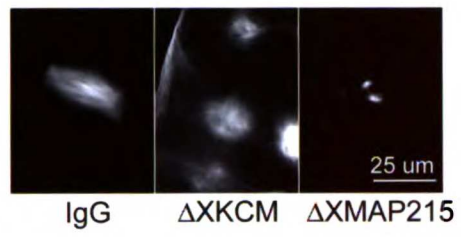
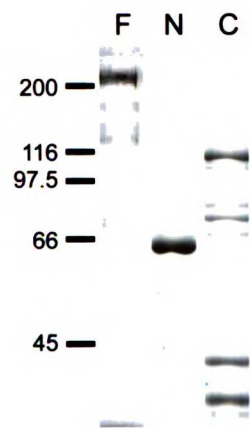


Figure S-2:



- Carr DB, Sesack SR (2000) Projections from the rat prefrontal cortex to the ventral tegmental area: target specificity in the synaptic associations with mesoaccumbens and mesocortical neurons. *J Neurosci* 20:3864-3873.
- Chavkin C, James IF, Goldstein A (1982) Dynorphin is a specific endogenous ligand of the kappa opioid receptor. *Science* 215:413-415.
- Chefer VI, Moron JA, Hope B, Rea W, Shippenberg TS (2000) Kappa-opioid receptor activation prevents alterations in mesocortical dopamine neurotransmission that occur during abstinence from cocaine. *Neuroscience* 101:619-627.
- Chen JC, Liang KW, Huang EY (2001) Differential effects of endomorphin-1 and -2 on amphetamine sensitization: neurochemical and behavioral aspects. *Synapse* 39:239-248.
- Chou TC, Lee CE, Lu J, Elmquist JK, Hara J, Willie JT, Beuckmann CT, Chemelli RM, Sakurai T, Yanagisawa M, Saper CB, Scammell TE (2001) Orexin (hypocretin) neurons contain dynorphin. *J Neurosci* 21:RC168.
- Christie MJ, Hack SP (2003) Emergence of delta-opioid receptor mediated presynaptic inhibition in preiaqueductal grey neurons after chronic morphine. Washington, DC: Society for Neuroscience.
- Cornish JL, Kalivas PW (2001) Cocaine sensitization and craving: differing roles for dopamine and glutamate in the nucleus accumbens. *J Addict Dis* 20:43-54.
- Cornish JL, Nakamura M, Kalivas PW (2001) Dopamine-independent locomotion following blockade of N-methyl-D-aspartate receptors in the ventral tegmental area. *J Pharmacol Exp Ther* 298:226-233.

- Corrigall WA, Coen KM, Adamson KL, Chow BL (1999) The mu opioid agonist DAMGO alters the intravenous self-administration of cocaine in rats: mechanisms in the ventral tegmental area. *Psychopharmacology (Berl)* 141:428-435.
- Corrigall WA, Coen KM, Adamson KL, Chow BL, Zhang J (2000) Response of nicotine self-administration in the rat to manipulations of mu-opioid and gamma-aminobutyric acid receptors in the ventral tegmental area. *Psychopharmacology (Berl)* 149:107-114.
- Cosgrove KP, Carroll ME (2002) Effects of bremazocine on self-administration of smoked cocaine base and orally delivered ethanol, phencyclidine, saccharin, and food in rhesus monkeys: a behavioral economic analysis. *J Pharmacol Exp Ther* 301:993-1002.
- Cowen MS, Lawrence AJ (1999) The role of opioid-dopamine interactions in the induction and maintenance of ethanol consumption. *Prog Neuropsychopharmacol Biol Psychiatry* 23:1171-1212.
- Dahlstroem A, Fuxe K (1964) Evidence for the Existence of Monoamine-Containing Neurons in the Central Nervous System. I. Demonstration of Monoamines in the Cell Bodies of Brain Stem Neurons. *Acta Physiol Scand* 62:SUPPL 232:231-255.
- Dalman FC, O'Malley KL (1999) Kappa-opioid tolerance and dependence in cultures of dopaminergic midbrain neurons. *J Neurosci* 19:5750-5757.
- Devine DP, Wise RA (1994) Self-administration of morphine, DAMGO, and DPDPE into the ventral tegmental area of rats. *J Neurosci* 14:1978-1984.

Devine DP, Leone P, Wise RA (1993a) Mesolimbic dopamine neurotransmission is increased by administration of mu-opioid receptor antagonists. *Eur J Pharmacol* 243:55-64.

Devine DP, Leone P, Pocock D, Wise RA (1993b) Differential involvement of ventral tegmental mu, delta and kappa opioid receptors in modulation of basal mesolimbic dopamine release: in vivo microdialysis studies. *J Pharmacol Exp Ther* 266:1236-1246.

Devine DP, Leone P, Carlezon WA, Jr., Wise RA (1993c) Ventral mesencephalic delta opioid receptors are involved in modulation of basal mesolimbic dopamine neurotransmission: an anatomical localization study. *Brain Res* 622:348-352.

Devine DP, Reinscheid RK, Monsma FJ, Jr., Civelli O, Akil H (1996) The novel neuropeptide orphanin FQ fails to produce conditioned place preference or aversion. *Brain Res* 727:225-229.

Di Chiara G (2000) Role of dopamine in the behavioural actions of nicotine related to addiction. *Eur J Pharmacol* 393:295-314.

Di Mascio M, Esposito E (1997) The degree of inhibition of dopaminergic neurons in the ventral tegmental area induced by selective serotonin reuptake inhibitors is a function of the density-power-spectrum of the interspike interval. *Neuroscience* 79:957-961.

Di Mascio M, Di Giovanni G, Di Matteo V, Esposito E (1999) Decreased chaos of midbrain dopaminergic neurons after serotonin denervation. *Neuroscience* 92:237-243.

- Fallon JH, Leslie FM, Cone RI (1985) Dynorphin-containing pathways in the substantia nigra and ventral tegmentum: a double labeling study using combined immunofluorescence and retrograde tracing. *Neuropeptides* 5:457-460.
- Feenstra MG (2000) Dopamine and noradrenaline release in the prefrontal cortex in relation to unconditioned and conditioned stress and reward. *Prog Brain Res* 126:133-163.
- Floresco SB, West AR, Ash B, Moore H, Grace AA (2003) Afferent modulation of dopamine neuron firing differentially regulates tonic and phasic dopamine transmission. *Nat Neurosci* 6:968-973.
- Fudge JL, Emiliano AB (2003) The extended amygdala and the dopamine system: another piece of the dopamine puzzle. *J Neuropsychiatry Clin Neurosci* 15:306-316.
- Garzon M, Pickel VM (2001) Plasmalemmal mu-opioid receptor distribution mainly in nondopaminergic neurons in the rat ventral tegmental area. *Synapse* 41:311-328.
- Giuliano F, Allard J (2001) Dopamine and sexual function. *Int J Impot Res* 13 Suppl 3:S18-28.
- Grace AA, Onn SP (1989) Morphology and electrophysiological properties of immunocytochemically identified rat dopamine neurons recorded in vitro. *J Neurosci* 9:3463-3481.
- Greenwell TN, Zangen A, Martin-Schild S, Wise RA, Zadina JE (2002) Endomorphin-1 and -2 immunoreactive cells in the hypothalamus are labeled by fluoro-gold injections to the ventral tegmental area. *J Comp Neurol* 454:320-328.

- Gysling K, Wang RY (1983) Morphine-induced activation of A10 dopamine neurons in the rat. *Brain Res* 277:119-127.
- Hamilton ME, Bozarth MA (1988) Feeding elicited by dynorphin (1-13) microinjections into the ventral tegmental area in rats. *Life Sci* 43:941-946.
- Harris GC, Aston-Jones G (2003) Critical role for ventral tegmental glutamate in preference for a cocaine-conditioned environment. *Neuropsychopharmacology* 28:73-76.
- Hokfelt T, Skirboll L, Rehfeld JF, Goldstein M, Markey K, Dann O (1980) A subpopulation of mesencephalic dopamine neurons projecting to limbic areas contains a cholecystinin-like peptide: evidence from immunohistochemistry combined with retrograde tracing. *Neuroscience* 5:2093-2124.
- Iwamoto ET (1985) Place-conditioning properties of mu, kappa, and sigma opioid agonists. *Alcohol Drug Res* 6:327-339.
- Jenck F, Bozarth M, Wise RA (1988) Contraversive circling induced by ventral tegmental microinjections of moderate doses of morphine and [D-Pen2, D-Pen5]enkephalin. *Brain Res* 450:382-386.
- Johnson SW, North RA (1992a) Two types of neurone in the rat ventral tegmental area and their synaptic inputs. *Journal of Physiology* 450:455-468.
- Johnson SW, North RA (1992b) Opioids excite dopamine neurons by hyperpolarization of local interneurons. *Journal of Neuroscience* 12:483-488.
- Johnson SW, Seutin V, North RA (1992) Burst firing in dopamine neurons induced by N-methyl-D-aspartate: role of electrogenic sodium pump. *Science* 258:665-667.



- Jones BE, Cuello AC (1989) Afferents to the basal forebrain cholinergic cell area from pontomesencephalic--catecholamine, serotonin, and acetylcholine--neurons. *Neuroscience* 31:37-61.
- Jones S, Kauer JA (1999) Amphetamine depresses excitatory synaptic transmission via serotonin receptors in the ventral tegmental area. *J Neurosci* 19:9780-9787.
- Joyce EM, Koob GF, Strecker R, Iversen SD, Bloom FE (1981) The behavioural effects of enkephalin analogues injected into the ventral tegmental area and globus pallidus. *Brain Res* 221:359-370.
- Kalivas PW, Taylor S, Miller JS (1985) Sensitization to repeated enkephalin administration into the ventral tegmental area of the rat. I. Behavioral characterization. *J Pharmacol Exp Ther* 235:537-543.
- Kalivas PW, Churchill L, Klitenick MA (1993) GABA and enkephalin projection from the nucleus accumbens and ventral pallidum to the ventral tegmental area. *Neuroscience* 57:1047-1060.
- Kalivas PW, Pierce RC, Cornish J, Sorg BA (1998) A role for sensitization in craving and relapse in cocaine addiction. *J Psychopharmacol* 12:49-53.
- Kelley AE, Stinus L, Iversen SD (1980) Interactions between D-ala-met-enkephalin, A10 dopaminergic neurones, and spontaneous behaviour in the rat. *Behav Brain Res* 1:3-24.
- Kelley AE, Cador M, Stinus L, Le Moal M (1989) Neurotensin, substance P, neurokinin-alpha, and enkephalin: injection into ventral tegmental area in the rat produces differential effects on operant responding. *Psychopharmacology (Berl)* 97:243-252.

- Kiyatkin EA (1988) Morphine-induced modification of the functional properties of ventral tegmental area neurons in conscious rat. *Int J Neurosci* 41:57-70.
- Klitenick MA, Wirtshafter D (1995) Behavioral and neurochemical effects of opioids in the paramedian midbrain tegmentum including the median raphe nucleus and ventral tegmental area. *J Pharmacol Exp Ther* 273:327-336.
- Klitenick MA, DeWitte P, Kalivas PW (1992) Regulation of somatodendritic dopamine release in the ventral tegmental area by opioids and GABA: an in vivo microdialysis study. *J Neurosci* 12:2623-2632.
- Koob GF (1992) Drugs of abuse: anatomy, pharmacology and function of reward pathways. *Trends Pharmacol Sci* 13:177-184.
- Lacey MG, Mercuri NB, North RA (1989) Two cell types in rat substantia nigra zona compacta distinguished by membrane properties and the actions of dopamine and opioids. *J Neurosci* 9:1233-1241.
- Lamonte N, Echo JA, Ackerman TF, Christian G, Bodnar RJ (2002) Analysis of opioid receptor subtype antagonist effects upon mu opioid agonist-induced feeding elicited from the ventral tegmental area of rats. *Brain Res* 929:96-100.
- Latimer LG, Duffy P, Kalivas PW (1987) Mu opioid receptor involvement in enkephalin activation of dopamine neurons in the ventral tegmental area. *J Pharmacol Exp Ther* 241:328-337.
- Leone P, Pocock D, Wise RA (1991) Morphine-dopamine interaction: ventral tegmental morphine increases nucleus accumbens dopamine release. *Pharmacol Biochem Behav* 39:469-472.

- Leyton M, Stewart J (1992) The stimulation of central kappa opioid receptors decreases male sexual behavior and locomotor activity. *Brain Res* 594:56-74.
- Leyton M, Rajabi H, Stewart J (1992) U-50,488H into A10 reduces haloperidol-induced elevations of accumbens dopamine. *Neuroreport* 3:1127-1130.
- Lindvall O, Bjorklund A, Divac I (1978) Organization of catecholamine neurons projecting to the frontal cortex in the rat. *Brain Res* 142:1-24.
- Lutfy K, Khaliq I, Carroll FI, Maidment NT (2002) Orphanin FQ/nociceptin blocks cocaine-induced behavioral sensitization in rats. *Psychopharmacology (Berl)* 164:168-176.
- Maccaferri G, Toth K, McBain CJ (1998) Target-specific expression of presynaptic mossy fiber plasticity. *Science* 279:1368-1370.
- Magendzo K, Bustos G (2003) Expression of amphetamine-induced behavioral sensitization after short- and long-term withdrawal periods: participation of mu- and delta-opioid receptors. *Neuropsychopharmacology* 28:468-477.
- Maidment NT, Chen Y, Tan AM, Murphy NP, Leslie FM (2002) Rat ventral midbrain dopamine neurons express the orphanin FQ/nociceptin receptor ORL-1. *Neuroreport* 13:1137-1140.
- Manabe T, Wyllie DJ, Perkel DJ, Nicoll RA (1993) Modulation of synaptic transmission and long-term potentiation: effects on paired pulse facilitation and EPSC variance in the CA1 region of the hippocampus. *Journal of Neurophysiology* 70:1451-1459.

- Mansour A, Burke S, Pavlic RJ, Akil H, Watson SJ (1996) Immunohistochemical localization of the cloned kappa 1 receptor in the rat CNS and pituitary. *Neuroscience* 71:671-690.
- Manzoni OJ, Williams JT (1999) Presynaptic regulation of glutamate release in the ventral tegmental area during morphine withdrawal. *J Neurosci* 19:6629-6636.
- Margolis EB, Hjelmstad GO, Bonci A, Fields HL (2003) Kappa-opioid agonists directly inhibit midbrain dopaminergic neurons. *J Neurosci* 23:9981-9986.
- Marinelli M, White FJ (2000) Enhanced vulnerability to cocaine self-administration is associated with elevated impulse activity of midbrain dopamine neurons. *J Neurosci* 20:8876-8885.
- Marinelli S, Vaughan CW, Schnell SA, Wessendorf MW, Christie MJ (2002) Rostral ventromedial medulla neurons that project to the spinal cord express multiple opioid receptor phenotypes. *J Neurosci* 22:10847-10855.
- Markram H, Wang Y, Tsodyks M (1998) Differential signaling via the same axon of neocortical pyramidal neurons. *Proc Natl Acad Sci U S A* 95:5323-5328.
- Mason BJ, Goodman AM, Dixon RM, Hameed MH, Hulot T, Wesnes K, Hunter JA, Boyeson MG (2002) A pharmacokinetic and pharmacodynamic drug interaction study of acamprosate and naltrexone. *Neuropsychopharmacology* 27:596-606.
- Mathe JM, Nomikos GG, Schilstrom B, Svensson TH (1998) Non-NMDA excitatory amino acid receptors in the ventral tegmental area mediate systemic dizocilpine (MK-801) induced hyperlocomotion and dopamine release in the nucleus accumbens. *J Neurosci Res* 51:583-592.

- McBride WJ, Murphy JM, Ikemoto S (1999) Localization of brain reinforcement mechanisms: intracranial self-administration and intracranial place-conditioning studies. *Behav Brain Res* 101:129-152.
- Mendez M, Leriche M, Calva JC (2001) Acute ethanol administration differentially modulates mu opioid receptors in the rat meso-accumbens and mesocortical pathways. *Brain Res Mol Brain Res* 94:148-156.
- Mercuri NB, Bonci A, Calabresi P, Stefani A, Bernardi G (1995) Properties of the hyperpolarization-activated cation current  $I_h$  in rat midbrain dopaminergic neurons. *Eur J Neurosci* 7:462-469.
- Meredith GE (1999) The synaptic framework for chemical signaling in nucleus accumbens. *Ann N Y Acad Sci* 877:140-156.
- Mitchell JB, Stewart J (1990a) Facilitation of sexual behaviors in the male rat associated with intra-VTA injections of opiates. *Pharmacol Biochem Behav* 35:643-650.
- Mitchell JB, Stewart J (1990b) Facilitation of sexual behaviors in the male rat in the presence of stimuli previously paired with systemic injections of morphine. *Pharmacol Biochem Behav* 35:367-372.
- Moore H, Rose HJ, Grace AA (2001) Chronic cold stress reduces the spontaneous activity of ventral tegmental dopamine neurons. *Neuropsychopharmacology* 24:410-419.
- Mucha RF, Herz A (1985) Motivational properties of kappa and mu opioid receptor agonists studied with place and taste preference conditioning. *Psychopharmacology (Berl)* 86:274-280.

- Murphy NP, Maidment NT (1999) Orphanin FQ/nociceptin modulation of mesolimbic dopamine transmission determined by microdialysis. *J Neurochem* 73:179-186.
- Nader K, van der Kooy D (1997) Deprivation state switches the neurobiological substrates mediating opiate reward in the ventral tegmental area. *J Neurosci* 17:383-390.
- Narayanan S, Lutfy K, Maidment N (2002) Sensitization to cocaine after a single intracerebral injection of orphanin FQ/nociceptin. *Behav Brain Res* 131:97-103.
- Neal CR, Jr., Mansour A, Reinscheid R, Nothacker HP, Civelli O, Watson SJ, Jr. (1999a) Localization of orphanin FQ (nociceptin) peptide and messenger RNA in the central nervous system of the rat. *J Comp Neurol* 406:503-547.
- Neal CR, Jr., Mansour A, Reinscheid R, Nothacker HP, Civelli O, Akil H, Watson SJ, Jr. (1999b) Opioid receptor-like (ORL1) receptor distribution in the rat central nervous system: comparison of ORL1 receptor mRNA expression with (125)I-[(14)Tyr]-orphanin FQ binding. *J Comp Neurol* 412:563-605.
- Noel MB, Wise RA (1995) Ventral tegmental injections of a selective mu or delta opioid enhance feeding in food-deprived rats. *Brain Res* 673:304-312.
- Norton CS, Neal CR, Kumar S, Akil H, Watson SJ (2002) Nociceptin/orphanin FQ and opioid receptor-like receptor mRNA expression in dopamine systems. *J Comp Neurol* 444:358-368.
- Nylander I, Vlaskovska M, Terenius L (1995) The effects of morphine treatment and morphine withdrawal on the dynorphin and enkephalin systems in Sprague-Dawley rats. *Psychopharmacology (Berl)* 118:391-400.

- Nylander I, Hyytia P, Forsander O, Terenius L (1994) Differences between alcohol-preferring (AA) and alcohol-avoiding (ANA) rats in the prodynorphin and proenkephalin systems. *Alcohol Clin Exp Res* 18:1272-1279.
- Overton PG, Clark D (1997) Burst firing in midbrain dopaminergic neurons. *Brain Res Brain Res Rev* 25:312-334.
- Pan ZZ (1998) mu-Opposing actions of the kappa-opioid receptor. *Trends in Pharmacological Sciences* 19:94-98.
- Paxinos G (1995) *The rat nervous system*, 2nd Edition. San Diego: Academic Press.
- Pettit HO, Ettenberg A, Bloom FE, Koob GF (1984) Destruction of dopamine in the nucleus accumbens selectively attenuates cocaine but not heroin self-administration in rats. *Psychopharmacology (Berl)* 84:167-173.
- Phillips AG, LePiane FG (1980) Reinforcing effects of morphine microinjection into the ventral tegmental area. *Pharmacol Biochem Behav* 12:965-968.
- Phillips AG, Broekkamp CL, Fibiger HC (1983) Strategies for studying the neurochemical substrates of drug reinforcement in rodents. *Prog Neuropsychopharmacol Biol Psychiatry* 7:585-590.
- Phillips PE, Stuber GD, Heien ML, Wightman RM, Carelli RM (2003) Subsecond dopamine release promotes cocaine seeking. *Nature* 422:614-618.
- Phillipson OT (1979) Afferent projections to the ventral tegmental area of Tsai and interfascicular nucleus: a horseradish peroxidase study in the rat. *J Comp Neurol* 187:117-143.
- Pickel VM, Joh TH, Reis DJ (1976) Monoamine-synthesizing enzymes in central dopaminergic, noradrenergic and serotonergic neurons. *Immunocytochemical*

- localization by light and electron microscopy. *J Histochem Cytochem* 24:792-306.
- Pickel VM, Joh TH, Reis DJ (1977) Regional and ultrastructural localization of tyrosine hydroxylase by immunocytochemistry in dopaminergic neurons of the mesolimbic and nigrostriatal systems. *Adv Biochem Psychopharmacol* 16:321-329.
- Pickel VM, Chan J, Sesack SR (1993) Cellular substrates for interactions between dynorphin terminals and dopamine dendrites in rat ventral tegmental area and substantia nigra. *Brain Res* 602:275-289.
- Ragnauth A, Ruegg H, Bodnar RJ (1997) Evaluation of opioid receptor subtype antagonist effects in the ventral tegmental area upon food intake under deprivation, glucoprivic and palatable conditions. *Brain Res* 767:8-16.
- Richards CD, Shiroyama T, Kitai ST (1997) Electrophysiological and immunocytochemical characterization of GABA and dopamine neurons in the substantia nigra of the rat. *Neuroscience* 80:545-557.
- Robinson TE, Berridge KC (1993) The neural basis of drug craving: an incentive-sensitization theory of addiction. *Brain Res Brain Res Rev* 18:247-291.
- Ronken E, Van Muiswinkel FL, Mulder AH, Schoffelmeer AN (1993) Opioid receptor-mediated inhibition of evoked catecholamine release from cultured neurons of rat ventral mesencephalon and locus coeruleus. *Eur J Pharmacol* 230:349-355.
- Rosin A, Lindholm S, Franck J, Georgieva J (1999) Downregulation of kappa opioid receptor mRNA levels by chronic ethanol and repetitive cocaine in rat ventral tegmentum and nucleus accumbens. *Neurosci Lett* 275:1-4.



- Rosin DL, Weston MC, Sevigny CP, Stornetta RL, Guyenet PG (2003) Hypothalamic orexin (hypocretin) neurons express vesicular glutamate transporters VGLUT1 or VGLUT2. *J Comp Neurol* 465:593-603.
- Saal D, Dong Y, Bonci A, Malenka RC (2003) Drugs of abuse and stress trigger a common synaptic adaptation in dopamine neurons. *Neuron* 37:577-582.
- Scanziani M, Gahwiler BH, Chrupka S (1998) Target cell-specific modulation of transmitter release at terminals from a single axon. *Proc Natl Acad Sci U S A* 95:12004-12009.
- Schenk S, Partridge B, Shippenberg TS (2001) Effects of the kappa-opioid receptor agonist, U69593, on the development of sensitization and on the maintenance of cocaine self- administration. *Neuropsychopharmacology* 24:441-450.
- Schultz W (1998) Predictive reward signal of dopamine neurons. *J Neurophysiol* 80:1-27.
- Seroogy KB, Danganan K, Lim S, Haycock JW, Fallon JH (1989) Ventral mesencephalic neurons containing both cholecystinin- and tyrosine hydroxylase-like immunoreactivities project to forebrain regions. *J Comp Neurol* 279:397-414.
- Sesack SR, Pickel VM (1992) Dual ultrastructural localization of enkephalin and tyrosine hydroxylase immunoreactivity in the rat ventral tegmental area: multiple substrates for opiate-dopamine interactions. *J Neurosci* 12:1335-1350.
- Shippenberg TS, Herz A (1987) Place preference conditioning reveals the involvement of D1-dopamine receptors in the motivational properties of mu- and kappa-opioid agonists. *Brain Res* 436:169-172.
- Shippenberg TS, Herz A (1988) Motivational effects of opioids: influence of D-1 versus D-2 receptor antagonists. *Eur J Pharmacol* 151:233-242.

- Shippenberg TS, Bals-Kubik R (1995) Involvement of the mesolimbic dopamine system in mediating the aversive effects of opioid antagonists in the rat. *Behav Pharmacol* 6:99-106.
- Shippenberg TS, Rea W (1997) Sensitization to the behavioral effects of cocaine: modulation by dynorphin and kappa-opioid receptor agonists. *Pharmacology, Biochemistry and Behavior* 57:449-455.
- Shippenberg TS, Bals-Kubik R, Herz A (1993) Examination of the neurochemical substrates mediating the motivational effects of opioids: role of the mesolimbic dopamine system and D-1 vs. D-2 dopamine receptors. *Journal of Pharmacology and Experimental Therapeutics* 265:53-59.
- Shippenberg TS, Chefer VI, Zapata A, Heidbreder CA (2001) Modulation of the behavioral and neurochemical effects of psychostimulants by kappa-opioid receptor systems. *Ann N Y Acad Sci* 937:50-73.
- Simon H, Le Moal M, Calas A (1979) Efferents and afferents of the ventral tegmental-A10 region studied after local injection of [<sup>3</sup>H]leucine and horseradish peroxidase. *Brain Res* 178:17-40.
- Singh J, Desiraju T (1988) Differential effects of opioid peptides administered intracerebrally in loci of self-stimulation reward of lateral hypothalamus and ventral tegmental area--substantia nigra. *NIDA Res Monogr* 87:180-191.
- Singh J, Desiraju T, Nagaraja TN, Raju TR (1994) Facilitation of self-stimulation of ventral tegmentum by microinjection of opioid receptor subtype agonists. *Physiol Behav* 55:627-631.

- Spanagel R, Herz A, Shippenberg TS (1990) The effects of opioid peptides on dopamine release in the nucleus accumbens: an in vivo microdialysis study. *Journal of Neurochemistry* 55:1734-1740.
- Spanagel R, Herz A, Shippenberg TS (1992) Opposing tonically active endogenous opioid systems modulate the mesolimbic dopaminergic pathway. *Proceedings of the National Academy of Sciences of the United States of America* 89:2046-2050.
- Speciale SG, Manaye KF, Sadeq M, German DC (1993) Opioid receptors in midbrain dopaminergic regions of the rat. II. Kappa and delta receptor autoradiography. *J Neural Transm Gen Sect* 91:53-66.
- Steffensen SC, Svingos AL, Pickel VM, Henriksen SJ (1998) Electrophysiological characterization of GABAergic neurons in the ventral tegmental area. *J Neurosci* 18:8003-8015.
- Stewart J (1984) Reinstatement of heroin and cocaine self-administration behavior in the rat by intracerebral application of morphine in the ventral tegmental area. *Pharmacol Biochem Behav* 20:917-923.
- Svingos AL, Garzon M, Colago EE, Pickel VM (2001) Mu-opioid receptors in the ventral tegmental area are targeted to presynaptically and directly modulate mesocortical projection neurons. *Synapse* 41:221-229.
- Swanson LW (1982) The projections of the ventral tegmental area and adjacent regions: a combined fluorescent retrograde tracer and immunofluorescence study in the rat. *Brain Res Bull* 9:321-353.
- Szewczak MR, Spoerlein MT (1986) Opiate-induced turning in rats after injection into the ventral tegmental area. *Pharmacol Biochem Behav* 25:959-965.

- Tanda G, Di Chiara G (1998) A dopamine-mu1 opioid link in the rat ventral tegmentum shared by palatable food (Fonzies) and non-psychostimulant drugs of abuse. *Eur J Neurosci* 10:1179-1187.
- Tsuji M, Nakagawa Y, Ishibashi Y, Yoshii T, Takashima T, Shimada M, Suzuki T (1996) Activation of ventral tegmental GABAB receptors inhibits morphine-induced place preference in rats. *Eur J Pharmacol* 313:169-173.
- Uhl GR, Goodman RR, Kuhar MJ, Childers SR, Snyder SH (1979) Immunohistochemical mapping of enkephalin containing cell bodies, fibers and nerve terminals in the brain stem of the rat. *Brain Res* 166:75-94.
- Van Bockstaele EJ, Pickel VM (1995) GABA-containing neurons in the ventral tegmental area project to the nucleus accumbens in rat brain. *Brain Res* 682:215-221.
- Vezina P, Kalivas PW, Stewart J (1987) Sensitization occurs to the locomotor effects of morphine and the specific mu opioid receptor agonist, DAGO, administered repeatedly to the ventral tegmental area but not to the nucleus accumbens. *Brain Res* 417:51-58.
- Viggiano D, Vallone D, Ruocco LA, Sadile AG (2003) Behavioural, pharmacological, morpho-functional molecular studies reveal a hyperfunctioning mesocortical dopamine system in an animal model of attention deficit and hyperactivity disorder. *Neurosci Biobehav Rev* 27:683-689.
- Wang B, Luo F, Ge X, Fu A, Han J (2003) Effect of 6-OHDA lesions of the dopaminergic mesolimbic system on drug priming induced reinstatement of extinguished morphine CPP in rats. *Beijing Da Xue Xue Bao* 35:449-452.

- Xi ZX, Stein EA (2002a) GABAergic mechanisms of opiate reinforcement. *Alcohol* 37:485-494.
- Xi ZX, Stein EA (2002b) Blockade of ionotropic glutamatergic transmission in the ventral tegmental area reduces heroin reinforcement in rat. *Psychopharmacology (Berl)* 164:144-150.
- Yoshida M, Yokoo H, Mizoguchi K, Kawahara H, Tsuda A, Nishikawa T, Tanaka M (1992) Eating and drinking cause increased dopamine release in the nucleus accumbens and ventral tegmental area in the rat: measurement by in vivo microdialysis. *Neurosci Lett* 139:73-76.
- Yoshida M, Yokoo H, Tanaka T, Mizoguchi K, Emoto H, Ishii H, Tanaka M (1993) Facilitatory modulation of mesolimbic dopamine neuronal activity by a mu-opioid agonist and nicotine as examined with in vivo microdialysis. *Brain Res* 624:277-280.
- You ZB, Herrera-Marschitz M, Terenius L (1999) Modulation of neurotransmitter release in the basal ganglia of the rat brain by dynorphin peptides. *J Pharmacol Exp Ther* 290:1307-1315.
- Yung WH, Hausser MA, Jack JJ (1991) Electrophysiology of dopaminergic and non-dopaminergic neurones of the guinea-pig substantia nigra pars compacta in vitro. *J Physiol* 436:643-667.
- Zangen A, Ikemoto S, Zadina JE, Wise RA (2002) Rewarding and psychomotor stimulant effects of endomorphin-1: anteroposterior differences within the ventral tegmental area and lack of effect in nucleus accumbens. *J Neurosci* 22:7225-7233.

Zheng F, Johnson SW (2002) Group I metabotropic glutamate receptor-mediated enhancement of dopamine cell burst firing in rat ventral tegmental area in vitro. *Brain Res* 948:171-174.

Zheng F, Grandy DK, Johnson SW (2002) Actions of orphanin FQ/nociceptin on rat ventral tegmental area neurons in vitro. *Br J Pharmacol* 136:1065-1071.

## **Appendix: Abbreviations**

AMYG	amygdala
AP	action potential
DA	dopamine
DOP	$\delta$ opioid
DYN	dynorphin
EM	endomorphin
ENK	enkephalin
EPSC	excitatory postsynaptic current
GABA	gamma-aminobutyric acid
GIRK	G-protein coupled inwardly rectifying potassium channel
IPSP	inhibitory postsynaptic potential
ISI	interspike interval
KOP	$\kappa$ opioid
KOR	$\kappa$ opioid receptor
MFB	medial forebrain bundle
mPFC	medial prefrontal cortex
MOP	$\mu$ opioid
MOR	$\mu$ opioid receptor
NAc	nucleus accumbens
N/OFQ	nociceptin/orphanin FQ
ORL1	opioid receptor like
PPR	paired pulse ratio

<b>sEPSC</b>	<b>spontaneous excitatory postsynaptic current</b>
<b>TH</b>	<b>tyrosine hydroxylase</b>
<b>VP</b>	<b>ventral pallidum</b>
<b>VTA</b>	<b>ventral tegmental area</b>



## **Chapter 3**

### **Molecular Mechanism of XMAP215**

**XMAP215 Stimulates Nucleotide Exchange in  
the Microtubule Lattice**

Mimi Shirasu-Hiza\* and Timothy J. Mitchison<sup>§</sup>

\*Department of Biochemistry, University of California, San Francisco

<sup>§</sup>Department of Cell Biology, Harvard Medical School, Boston

## **Abstract**

XMAP215, an important regulator of microtubule dynamics, has been shown to increase both polymerization and depolymerization rates *in vitro*. We proposed previously that XMAP215 might act as an “anti-pause factor”, destabilizing a semi-stable microtubule end structure or pause state. Currently, it is believed that microtubule behavior is determined by the nucleotide content of its end subunits. Here we explore the possibility that XMAP215 regulates microtubule behavior by affecting its nucleotide content, specifically by catalyzing nucleotide exchange of tubulin subunits within the microtubule lattice.

## **Introduction**

XMAP215 is an evolutionarily conserved protein regulator of microtubule dynamics, with homologues in most eukaryotic organisms (reviewed in (Ohkura et al., 2001)). As described in Chapter 2, we identified XMAP215 as a microtubule destabilizing factor in *Xenopus* egg extract using conventional chromatography and a visual assay. XMAP215 had previously been identified as a major microtubule stabilizing factor from *Xenopus* egg extract (Gard and Kirschner, 1987). The apparently contradictory behavior of XMAP215, able to increase both polymerization and depolymerization rates (Vasquez et al., 1994), led us to propose that XMAP215 might act as an anti-pause factor, destabilizing a semi-stable third state predicted to exist between growth and shrinkage (Tran et al., 1997). But what does this mean on the molecular level? Microtubule dynamics and structure appear to be determined by the nucleotide content of tubulin subunits at the end of the microtubule; XMAP215 appears to affect both microtubule

dynamics and structure. We set out to investigate whether XMAP215 causes those changes in dynamics and structure by directly affecting the nucleotide content of tubulin subunits at the end of the microtubule.

The nucleotide content of other GTPases, like heterotrimeric G proteins and small ras-like GTPases, is typically regulated by three classes of proteins: GAPs (or GTP activating proteins) that stimulate nucleotide hydrolysis; GDIs (or GTP dissociation inhibitors) that inhibit nucleotide release; and GEFs (or GTP exchange factors) that stimulate nucleotide release. Tubulin is an unusual GTPase: unlike heterotrimeric G proteins and small ras-like GTPases, tubulin is not part of a signal transduction cascade and has a structurally divergent GTP binding pocket (Nogales et al., 1999). Does tubulin have any GAPs, GDIs, or GEFs? In the microtubule lattice, structural evidence supports the idea that tubulin acts as its own GAP and GDI, with residues from the  $\alpha$  tubulin of one subunit catalyzing hydrolysis in the  $\beta$  tubulin of the adjacent subunit and blocking exchange at that site (Nogales, 2000; Nogales et al., 1999). In solution, the dimer sequestering and catastrophe factor op18 appears to act as both GAP and GDI (Amayed et al., 2000; Larsson et al., 1999), possibly because it forms a complex of two tubulin heterodimers and one op18 molecule (Curmi et al., 1997; Jourdain et al., 1997) and thus allows tubulin to act as a GAP and GDI on itself. So far, no GEF has been identified either for tubulin dimers in solution (which have rapid exchange rates on the order of seconds) (Brylawski and Caplow, 1983); or for tubulin dimers within the microtubule lattice (which are not thought to exchange) (Caplow et al., 1984; Carlier and Pantaloni, 1981; Weisenberg et al., 1976); or for tubulin dimers with exposed E-sites at the microtubule plus end, which can exchange within at least an hour (Mitchison, 1993).

We first tested whether XMAP215 might act as a GAP for tubulin subunits in polymerized microtubules. As described in Chapter 2, *in vitro* assays of XMAP215 revealed that it is able to depolymerize microtubules stabilized by GMPCPP, a slowly-hydrolyzable guanine nucleotide analogue. We demonstrated that XMAP215 did not accomplish this by increasing the rate of GMPCPP hydrolysis. We next considered the possibility that XMAP215 acts as a GEF, or nucleotide exchange factor. GEFs for other small GTPases, though structurally divergent, appear to have a common mechanism: stabilizing the nucleotide-free (or “apo”) state of their target G protein (reviewed in (Cherfils and Chardin, 1999)). Because our CPP MT depolymerizing assay is performed with little or no nucleotide in solution, we postulated that XMAP215 might depolymerize CPP MTs by displacing the nucleotide in end subunits and creating “apotubulin” subunits, which is predicted to result in depolymerization (Caplow and Shanks, 1995). This model makes two predictions: 1) addition of excess CPP in solution should inhibit depolymerization of CPP MTs by XMAP215; and 2) XMAP215 should increase the rate of exchange between nucleotide in solution and nucleotide in the microtubule lattice. In this thesis chapter, we test these two predictions and briefly describe other experiments that may provide further test this model for the mechanism of XMAP215.

## **Materials and methods**

### *In vitro* assay for CPP MT depolymerization

Purified, recombinant full-length XMAP215 has been previously characterized (Kinoshita et al., 2001; Shirasu-Hiza et al., 2003) and was a generous gift from K. Kinoshita, D. Drechsel, and A. Hyman. Bovine brain tubulin was labeled with

tetramethyl- or X-rhodamine (Molecular Probes) as previously described (Hyman et al., 1991) and was used to prepare GMPCPP-stabilized microtubules (CPP MTs) using standard procedures (Caplow et al., 1994; Hyman et al., 1992). Concentration of tubulin (1:4, labeled:unlabeled) during polymerization was 0.25 mg/ml (2.5  $\mu$ M) and GMPCPP concentration was 125  $\mu$ M. After polymerization at 37°C for 60', MTs were removed from the water bath and placed to cool at room temperature for 5-15'. For each reaction, 0.5  $\mu$ l of polymerized CPP MTs was added to 10  $\mu$ l of buffer or buffer plus XMAP215, for a final tubulin concentration of 125 nM. Buffer used was either BRB80 (80 mM K-PIPES, pH 6.8, 1 mM MgCl<sub>2</sub>, 1 mM EGTA) or CSF-XB (100 mM KCl, 50 mM sucrose, 10 mM K-HEPES, pH 7.7, 5 mM EGTA, 2 mM MgCl<sub>2</sub>, 0.1 mM CaCl<sub>2</sub>); results were equivalent for both buffer conditions. Samples were taken at 15 min for reactions performed in CSF-XB and 30 min for BRB80. For visual analysis, one  $\mu$ l of each reaction was fixed with 2  $\mu$ l of 80% glycerol/0.1% glutaraldehyde. Images were acquired on an upright Nikon E-600 or E-800 microscope equipped with a cooled charge-coupled device camera (Princeton Instruments, Trenton, NJ) using MetaMorph software (Universal Imaging, West Chester, PA).

#### *Radioactively-labeled GMPCPP exchange assay*

[ $\gamma$ -<sup>32</sup>P] GMPCPP was synthesized from GMPCP and [ $\gamma$ -<sup>32</sup>P] ATP. 2 u of nucleotide diphosphate kinase (Sigma), 15  $\mu$ l of 1 mM GMPCP in BRB80, 15  $\mu$ l of [ $\gamma$ -<sup>32</sup>P] ATP were incubated at room temperature for 6 hours. The reaction was spun for 15 min in a microfuge and the supernatant was filtered through a 10K cut-off filter. 0.1  $\mu$ l of each reaction products was analyzed by thin-layer chromatography (TLC) using PEI-cellulose

plates (Baker-Flex) run in 1.0 M LiCl and detected using a phosphorimager (Biorad Molecular Imager FX) and Quantity One v.4.1.1 software. Standards (1  $\mu$ l each of 10 mM GMPCPP, ATP stocks) were run in parallel and detected using a handheld UV lamp.

$[\gamma\text{-}^{32}\text{P}]$  GMPCPP was used to monitor GMPCPP incorporation into pre-polymerized CPP MTs. 4  $\mu$ l of CPP MTs, polymerized as described above, were added to 40  $\mu$ l BRB80 containing 100  $\mu$ M GMPCPP and 0.1  $\mu$ M  $[\gamma\text{-}^{32}\text{P}]$  GMPCPP. We then added buffer or 30 nM full-length, recombinant XMAP215 in the presence of 50  $\mu$ M nocodazole or equivalent volume of DMSO. Reactions were incubated at room temperature. At 0, 30, and 60 min, 13  $\mu$ l samples were removed from each reaction and layered on 100  $\mu$ l of 40% glycerol/BRB80 cushion, then spun in a Beckman TLA100 table-top ultracentrifuge rotor for 15 min at 90K, 25°C. For each sample, supernatant was removed and discarded; cushion was washed 3 times with BRB80; and pellet was washed 3-4 times with BRB80. Each pellet was resolubilized by addition of 10  $\mu$ l denaturing buffer (8 M urea, 20 mM Tris-HCl, pH 7.0, 5 mM EDTA). Free  $^{32}\text{P}$ i was separated from  $[\gamma\text{-}^{32}\text{P}]$  GMPCPP by TLC on PEI-cellulose using 1.4 M LiCl, after first pre-running (post-load) each TLC plate with ddH<sub>2</sub>O to get rid of excess salt, urea, and glycerol in each sample. Radioactive GMPCPP was detected using a Molecular Imager FX phosphorimager (Biorad) and Quantity One v.4.1.1 software.

## Results

### *CPP MT depolymerization by XMAP215 is inhibited by exogenous GMPCPP*

XMAP215 was shown in Chapter 2 to depolymerize GMPCPP-stabilized microtubules (“CPP MTs”) in an *in vitro* assay containing little or no nucleotide in solution. If

XMAP215 acts as a GEF for tubulin subunits in the lattice, it may promote CPP MT depolymerization in our assay by catalyzing the formation of apotubulin subunits, which are thought to dissociate rapidly from the microtubule (Caplow and Shanks, 1995). Since these apotubulin subunits might be prevented from dissociating by rebinding GMPCPP, we predicted that XMAP215-catalyzed depolymerization would be inhibited by the presence of excess GMPCPP. To test this, we added buffer or 1 mM GMPCPP to rhodamine-labeled CPP MTs in the absence or presence of XMAP215. After fifteen minutes, fixed time points were visually examined by fluorescence microscopy (figure 1). In the absence of XMAP215, CPP MTs were stable over the time course of the experiment and were not affected by 1 mM GMPCPP. In the presence of 30 nM XMAP215, CPP MTs rapidly depolymerized. This depolymerization was significantly inhibited by the presence of 1 mM GMPCPP. Since XMAP215 contains no known GTP binding motif, we believe that excess GMPCPP is binding to microtubules in this assay and preventing depolymerization by reversing the formation of apotubulin subunits.

*XMAP215 increases the rate and amount of nucleotide exchange in CPP MTs*

We next set out to measure directly the rate of GMPCPP exchange into CPP MTs in the absence and presence of XMAP215. We were unable to use many of the assays conventionally used to measure bulk nucleotide exchange like FRET or fluorescence anisotropy. Because tubulin dimer in solution has a high exchange rate, low levels of microtubule depolymerization might result in high levels of apparent nucleotide exchange. For this reason, we decided to isolate microtubule polymer from tubulin dimer using a microtubule spin-down assay, monitoring nucleotide exchange with



radioactively-labeled GMPCPP.

Using this assay, we tested the rate of radioactively-labeled GMPCPP incorporation into CPP MTs in the presence or absence of XMAP215. In brief, we polymerized CPP MTs for one hour at 37°C and then diluted them 20-fold into buffer containing 100  $\mu$ M GMPCPP and a small amount of gamma-labeled radioactive GMPCPP. The concentration of cold GMPCPP in solution was kept low to maximize the relative proportion of radioactively labeled GMPCPP. We then added either buffer or 30 nM XMAP215. Samples from each reaction were removed at 0 min, 15 min, and 30 min and spun through glycerol cushions. Microtubule pellets were washed, resolubilized, and measured for radioactive GMPCPP. As seen in figure 2A, there was more radioactive GMPCPP in the microtubule pellet at both the 30 minute and 60 minute time points in the presence of XMAP215. Thus, XMAP215 stimulated both the rate and to lesser extent the amount of GMPCPP incorporation into pre-polymerized CPP MTs.

This increase in nucleotide exchange rate might also be the result of XMAP215-catalyzed tubulin dimer dissociation, nucleotide exchange in solution, and rapid reassociation. In order to measure nucleotide exchange of tubulin subunits in the microtubule lattice, we needed to prevent rebinding of any dissociated tubulin subunits. For this reason, we tested nucleotide exchange rate in the presence of 50  $\mu$ M nocodazole, a potent tubulin sequestering drug. This concentration of nocodazole prevents CPP MT polymerization (data not shown). The total amount of incorporation in each sample was less than was observed in samples without nocodazole. However, as seen in figure 2B, XMAP215 still increased the rate of incorporation relative to buffer control.

In order to test if this nucleotide exchange is restricted to  $\beta$  tubulin subunits

exposed at microtubule plus ends, we quantitated the relative fraction of tubulin subunits in the microtubule pellet that exchanged their nucleotide. We first quantitated the amount of labeled CPP in each sample using a titration of known labeled CPP samples. Using the proportion of labeled to unlabeled CPP, we were able to quantitate the total amount of nucleotide exchange represented in each sample. Since the total amount of polymer in these samples was unfortunately too small to be measured directly by Coomassie-stained SDS-PAGE analysis, we estimated the amount of microtubule polymer in each sample to be 80% of the initial polymer based on previous yields from similar microtubule spin-down experiments. Assuming one non-exchangeable site per tubulin dimer, we calculated the percentage of nucleotide exchange for each sample (figure 2C). In buffer alone, nucleotide exchange was 1.8%, 3.6%, and 10.7% for 0, 30, and 60 minutes incubation. When XMAP215 was added, nucleotide exchange was 1.1%, 12.9%, and 13.8% for the same time points. In the presence of nocodazole, nucleotide exchange in buffer alone was 0.8%, 1.1%, and 6.5% and, in XMAP215-treated samples, 0.7%, 7.3%, and 5.5%.

Microtubules are between 2 and 20  $\mu\text{m}$  long in our samples (see figure 1, bar). Assuming a tubulin dimer length of  $\sim 8$  nm (Nogales et al., 1999), tubulin subunits with exposed E sites at plus ends should comprise 0.4 to 0.04 % of total exchangeable sites. Though it is possible that our samples are enriched in tiny microtubules less than 2  $\mu\text{m}$  long, we have not seen any evidence for this by electron microscopy. Therefore, in both control and XMAP215 samples, the total amount of incorporation appeared to be greater than could be explained by nucleotide exchange solely at the tips of CPP MT plus ends.

## Discussion

In this chapter, we have presented evidence demonstrating that XMAP215 increased the rate of incorporation of GMPCPP from solution into pre-polymerized CPP MTs. This suggests that XMAP215 may act as a guanine nucleotide exchange factor for tubulin subunits in the microtubule lattice, a model which potentially explains many of the diverse and contradictory activities observed *in vitro* (Shirasu-Hiza et al., 2003; Vasquez et al., 1994).

In this model, XMAP215 causes CPP MT depolymerization in the absence of exogenous GMPCPP by catalyzing the transient formation and dissociation of apotubulin subunits. XMAP215 increases shrinkage rate in dynamic microtubules by the same mechanism. The increased growth rate observed in *in vitro* assays may also be explained by this model, if the presence of excess GTP and high concentrations of tubulin dimer results in the rebinding of GTP by apotubulin subunits and stabilization of the microtubule end long enough to allow association of more GTP-tubulin subunits. It is difficult to reconcile the observed decrease in rescue frequency with this model. Currently we do not understand the mechanism of rescue on a structural or chemical level. It is possible that once depolymerization is triggered at the microtubule end, protofilament curling breaks interprotofilament bonds in such a way that they do not reassociate, even if GTP is exchanged into end subunits. There is some evidence *in vivo* that curled protofilaments break off before phases of rapid microtubule polymerization, perhaps allowing synchronization of microtubule protofilaments (Tirnauer et al., 2002). The model of XMAP215 as a nucleotide exchange factor will hopefully lend insight into

some of these unsolved questions about the mechanism of microtubule dynamic instability.

The work presented here indicates a promising direction of research. However, there are significant concerns which must be addressed in future experiments. First, each result requires more rigorous quantitation of microtubule polymer. We are currently working out conditions for a glass filter assay that would allow such quantitation as well as higher resolution time-points. In brief, samples containing fluorescently or radioactively labeled microtubules are applied to glass fiber filters on a vacuum manifold. Soluble tubulin, buffer, and nucleotide flow through and microtubules remain caught on the filter. Using this assay, we will be able to quantitate the result that GMPCPP inhibits XMAP215 depolymerization of CPP MTs. Furthermore, using this assay instead of the microtubule spin-down assay will allow us to take faster time points, normalize labeled CPP samples with microtubule polymer, and also determine the exact fraction of polymer subunits undergoing exchange.

Second, it is not clear if nocodazole completely blocks tubulin dimer reassociation. A simple experiment to test this assumption would involve adding Alexa488 (green)-labeled tubulin dimer to a reaction containing rhodamine-labeled CPP MTs, XMAP215, GMPCPP, and nocodazole. Fluorescence microscopy or glass filter analysis should reveal whether this new labeled tubulin incorporates into pre-polymerized CPP MTs in the presence of XMAP215 and 50  $\mu$ M nocodazole.

Third, we would like to determine the location of tubulin subunits in the microtubule lattice that undergo XMAP215-stimulated nucleotide exchange. The answer has significant implications both for the model of XMAP215 mechanism and for the

mechanism of microtubule dynamics. XMAP215 has been shown to act specifically on microtubule plus ends. Is this because XMAP215 only catalyzes nucleotide exchange at the plus end or because changes in nucleotide content only affect plus end dynamics? Furthermore, it is not known whether the nucleotide content of many, or a few, subunits at the end of a microtubule determines its dynamic behavior. Does XMAP215 catalyze exchange only in tubulin subunits at the very end of the microtubule or in subunits deeper in the microtubule lattice? To visualize the sites of exchange, we plan to synthesize a fluorescently-labeled GMPCPP for use in a nucleotide incorporation assay with XMAP215. We are currently exploring different fluorescent nucleotide derivatives. Though a technically difficult experiment, this assay would allow us to locate sites of exchange and provide strong evidence in support of our model.

### **Acknowledgements**

We are grateful to Kazu Kinoshita, David Drechsel, and Tony Hyman for their gift of purified recombinant XMAP215 protein. We also thank Zach Perlman and Justin Yarrow for their comments and thoughtful intellectual support. This project was supported by NIH grant (GM39565) to T.J.M.

### **References**

Amayed, P., M.F. Carrier, and D. Pantaloni. 2000. Stathmin slows down guanosine diphosphate dissociation from tubulin in a phosphorylation-controlled fashion. *Biochemistry*. 39:12295-302.

- Brylawski, B.P., and M. Caplow. 1983. Rate for nucleotide release from tubulin. *J Biol Chem.* 258:760-3.
- Caplow, M., B.P. Brylawski, and R. Reid. 1984. Mechanism for nucleotide incorporation into steady-state microtubules. *Biochemistry.* 23:6745-52.
- Caplow, M., R.L. Ruhlen, and J. Shanks. 1994. The free energy for hydrolysis of a microtubule-bound nucleotide triphosphate is near zero: all of the free energy for hydrolysis is stored in the microtubule lattice. *J Cell Biol.* 127:779-88.
- Caplow, M., and J. Shanks. 1995. Induction of microtubule catastrophe by formation of tubulin-GDP and apotubulin subunits at microtubule ends. *Biochemistry.* 34:15732-41.
- Carrier, M.F., and D. Pantaloni. 1981. Kinetic analysis of guanosine 5'-triphosphate hydrolysis associated with tubulin polymerization. *Biochemistry.* 20:1918-24.
- Cherfils, J., and P. Chardin. 1999. GEFs: structural basis for their activation of small GTP-binding proteins. *Trends Biochem Sci.* 24:306-11.
- Curmi, P.A., S.S. Andersen, S. Lachkar, O. Gavet, E. Karsenti, M. Knossow, and A. Sobel. 1997. The stathmin/tubulin interaction in vitro. *J Biol Chem.* 272:25029-36.
- Gard, D.L., and M.W. Kirschner. 1987. A microtubule-associated protein from *Xenopus* eggs that specifically promotes assembly at the plus-end. *J Cell Biol.* 105:2203-15.
- Hyman, A., D. Drechsel, D. Kellogg, S. Salsler, K. Sawin, P. Steffen, L. Wordeman, and T. Mitchison. 1991. Preparation of modified tubulins. *Methods Enzymol.* 196:478-85.

- Hyman, A.A., S. Salser, D.N. Drechsel, N. Unwin, and T.J. Mitchison. 1992. Role of GTP hydrolysis in microtubule dynamics: information from a slowly hydrolyzable analogue, GMPCPP. *Mol Biol Cell*. 3:1155-67.
- Jourdain, L., P. Curmi, A. Sobel, D. Pantaloni, and M.F. Carlier. 1997. Stathmin: a tubulin-sequestering protein which forms a ternary T2S complex with two tubulin molecules. *Biochemistry*. 36:10817-21.
- Kinoshita, K., I. Arnal, A. Desai, D.N. Drechsel, and A.A. Hyman. 2001. Reconstitution of physiological microtubule dynamics using purified components. *Science*. 294:1340-3.
- Larsson, N., B. Segerman, B. Howell, K. Fridell, L. Cassimeris, and M. Gullberg. 1999. Op18/stathmin mediates multiple region-specific tubulin and microtubule-regulating activities. *J Cell Biol*. 146:1289-302.
- Mitchison, T.J. 1993. Localization of an exchangeable GTP binding site at the plus end of microtubules. *Science*. 261:1044-7.
- Nogales, E. 2000. Structural insights into microtubule function. *Annu Rev Biochem*. 69:277-302.
- Nogales, E., M. Whittaker, R.A. Milligan, and K.H. Downing. 1999. High-resolution model of the microtubule. *Cell*. 96:79-88.
- Ohkura, H., M.A. Garcia, and T. Toda. 2001. Dis1/TOG universal microtubule adaptors - one MAP for all? *J Cell Sci*. 114:3805-12.
- Shirasu-Hiza, M., P. Coughlin, and T. Mitchison. 2003. Identification of XMAP215 as a microtubule-destabilizing factor in *Xenopus* egg extract by biochemical purification. *J Cell Biol*. 161:349-58.

- Tirnauer, J.S., S. Grego, E.D. Salmon, and T.J. Mitchison. 2002. EB1-Microtubule Interactions in *Xenopus* Egg Extracts: Role of EB1 in Microtubule Stabilization and Mechanisms of Targeting to Microtubules. *Mol Biol Cell*. 13:3614-26.
- Tran, P.T., R.A. Walker, and E.D. Salmon. 1997. A metastable intermediate state of microtubule dynamic instability that differs significantly between plus and minus ends. *J Cell Biol*. 138:105-17.
- Vasquez, R.J., D.L. Gard, and L. Cassimeris. 1994. XMAP from *Xenopus* eggs promotes rapid plus end assembly of microtubules and rapid microtubule polymer turnover. *J Cell Biol*. 127:985-93.
- Weisenberg, R.C., W.J. Deery, and P.J. Dickinson. 1976. Tubulin-nucleotide interactions during the polymerization and depolymerization of microtubules. *Biochemistry*. 15:4248-54.

### **Figure legends**

*Figure 1: Depolymerization of CPP MTs by XMAP215 in vitro is inhibited by GMPCPP in solution*

Rhodamine-labeled GMPCPP-stabilized microtubules were treated with buffer (top two panels) or XMAP215 (bottom two panels) in the absence or presence of 1 mM GMPCPP for 15 minutes before being fixed for visual analysis. Bar, 10  $\mu$ m.

*Figure 2: XMAP215 increased the rate of radioactively-labeled GMPCPP incorporation into pre-polymerized CPP MTs*



(A) CPP MTs were treated with buffer or XMAP215 in a buffer containing 100  $\mu$ M GMPCPP and a small amount of radioactively labeled GMPCPP, in the absence (top panel) or presence (bottom panel) of 50  $\mu$ M nocodazole. Samples were taken at 0, 30, and 60 min for spin-down and quantitation of radioactivity. Arrow indicates GMPCPP position by thin-layer chromatography.

(B) Quantitation of the percentage of nucleotide exchange is shown here. The total amount of radioactivity per sample was calculated by comparison with titrations of known quantities. Knowing the ratio of radioactively-labeled GMPCPP to total GMPCPP, we calculated the total nucleotide incorporation. Assuming 80% tubulin yield after pelleting and one non-exchangeable site per dimer, we calculated the percentage of nucleotide exchange for each sample.

Figure 3-1:

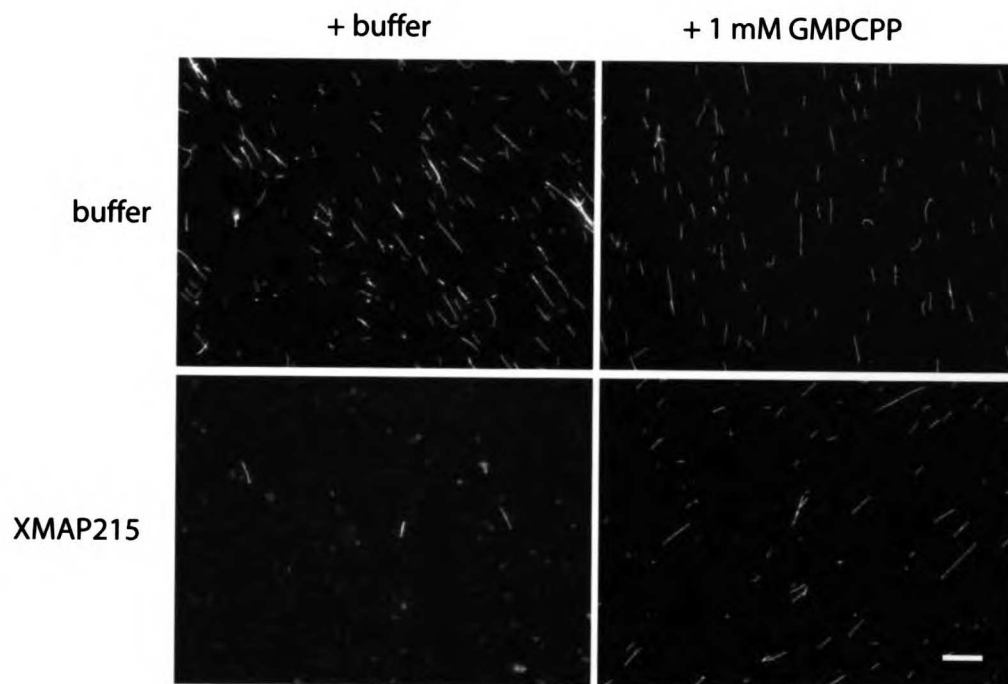
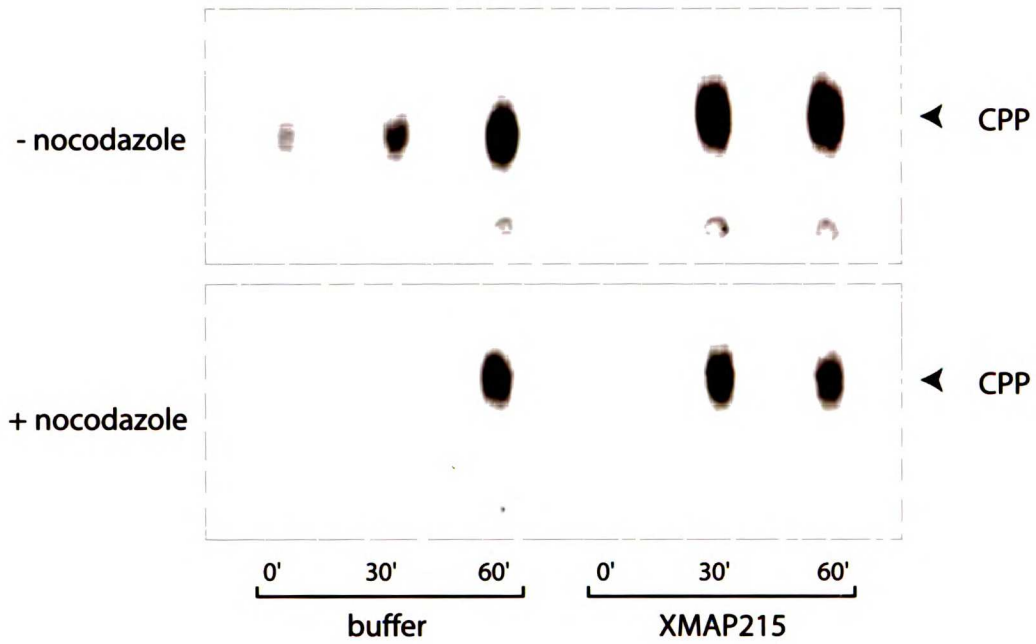
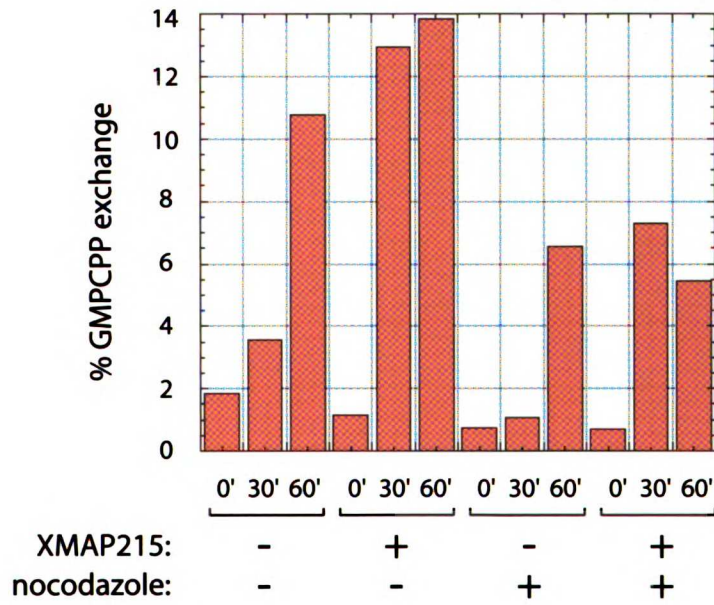


Figure 3-2:

A



B



## **Appendix I**

### **Microtubule Dynamics in Xenopus Egg Extract**

This appendix has been reproduced from the *Microscopy Research and Technique*, 1999, Mar 15;44(6):435-45. © 1999 Wiley-Liss, Inc.

I wrote the review in this appendix with Ann Yonetani and Dr. Claire Walczak. Ann Yonetani also produced all the figures, with comments from myself and Dr. Walczak.

# Microtubule Dynamics in *Xenopus* Egg Extracts

MIMI SHIRASU<sup>1</sup>\*, ANN YONETANI<sup>1</sup>, AND CLAIRE E. WALCZAK<sup>2</sup>\*

<sup>1</sup>Department of Cell Biology, Harvard Medical School, Boston MA 02115

<sup>2</sup>Medical Sciences Program, Indiana University, Bloomington, IN 47405

**KEY WORDS** microtubule; proteins; cell cycle; cellular function

**ABSTRACT** The organization and function of microtubules change dramatically during the cell cycle. At the onset of mitosis, a radial array of microtubules is broken down and reorganized into a bipolar spindle. This event requires changes in the dynamic behavior of individual microtubules. Through the use of *Xenopus laevis* egg extracts, a number of proteins affecting microtubule behavior have been identified. Recently, progress has also been made towards understanding how the activities of such microtubule-affecting proteins are regulated in a cell cycle-dependent manner. It is hoped that understanding how microtubule behavior is controlled during the cell cycle in vitro may illuminate the role of microtubule dynamics in various cellular processes. *Microsc. Res. Tech.* 44:000-000, 1999. © 1999 Wiley-Liss, Inc.

## INTRODUCTION

Underlying basic cellular functions, including intracellular transport and chromosome segregation, is a network of cytoskeletal polymers called microtubules. During interphase in animal cells, microtubules emanate from a single microtubule-organizing center (MTOC) found near the nucleus and form an astral array extending to the cell periphery. These microtubules are long and sparse relative to those found in mitotic cells. During mitosis, newly-duplicated MTOCs separate, and the microtubules associated with them form a bipolar spindle, which is responsible for segregating chromosomes to daughter cells. Bipolar spindles are built from a dense population of short and highly dynamic microtubules (Fig. 1). The means by which microtubules undergo this dramatic transformation during the cell cycle is an important cell biological problem; this review will focus on recent progress towards understanding this phenomenon through the use of *Xenopus* egg extracts.

Microtubules are hollow filaments, 25 nm in diameter, composed of alpha/beta tubulin heterodimers. Unlike equilibrium polymers, microtubules in steady-state undergo stochastic transitions between phases of polymerization and depolymerization. The transition from polymerization to depolymerization is called "catastrophe", and the transition from depolymerization to polymerization is termed "rescue" (Fig. 2). This behavior is known as "dynamic instability" (Mitchison and Kirschner, 1984). Microtubules exhibit inherent polarity in their dynamic behavior at each end of the polymer. One end (the "plus" end) polymerizes at a faster rate than the other (the "minus" end) (Walker et al., 1988). In most cell types, microtubules are strictly organized with respect to this polarity; microtubule minus ends are found proximal to the MTOC and plus ends found distal, at the cell periphery.

Using purified tubulin, measurements of microtubule behavior in vitro show significant differences from measurements in vivo (reviewed in Desai and Mitchison, 1997). In vitro, increasing concentrations of tubu-

lin lead to increased rates of polymerization and decreased rates of catastrophe (Walker et al., 1988). In vivo, the rate of polymerization is much higher than expected for the concentration of tubulin in the cytoplasm but is nevertheless associated with a high rate of catastrophe (reviewed in Cassimeris, 1993). Clearly, microtubule-affecting proteins exist in vivo which account for these differences and play an important role in modulating the behavior and organization of microtubules in cells. Of particular interest are those proteins that promote the dramatic changes in microtubule dynamics during the transition from interphase to mitosis.

Microtubules can be observed in cells in many ways (reviewed in Inoue and Salmon, 1995). Historically, fibers were first seen by electron microscopy, but their preservation varied with different fixation techniques. It was not until the advent of polarized light microscopy that birefringent fibers could be observed reliably in living cells. Polarized light studies could demonstrate that this fibrous array undergoes dynamic rearrangement during the cell cycle and is extremely labile to low temperature and anti-mitotic drugs such as colchicine. However, use of this technique was restricted to the observation of microtubules within dense, highly organized structures such as the mitotic spindle. Improvement in fixation techniques for electron microscopy as well as the development of immunofluorescence microscopy allowed initial observations to be made about microtubule dynamics. However, it is important to realize the limitations of deducing dynamic behavior from fixed samples. Currently, time-lapse video microscopy in live cells, using GFP-labeled tubulin, microinjection of fluorescently-labeled tubulin, or video-enhanced differential interference contrast (VE-DIC) microscopy, allows direct observation of the dynamics of individual microtubules (Cassimeris et al., 1988; Gelfand and

\*These authors contributed equally to this work.

\*Correspondence to: Claire E. Walczak, Medical Sciences Program, Indiana University, Jordan Hall 306, Bloomington, IN 47405. E-mail: cwalczak@indiana.edu

Received 24 September 1998; accepted in revised form 3 November 1998

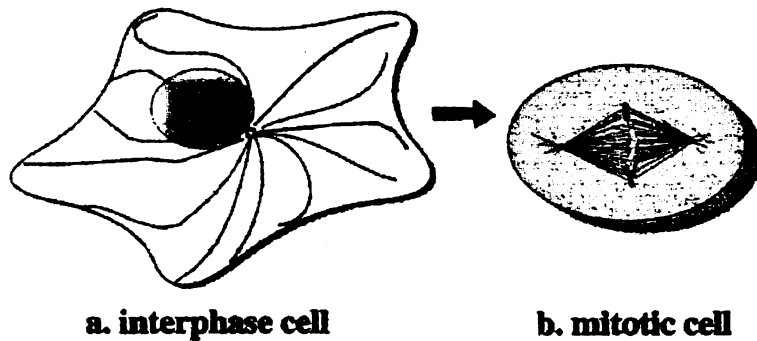


Fig. 1. Microtubule morphology changes dramatically during the cell cycle. (a) In an interphase animal cell, microtubules are found in a radial array around the microtubule-organizing center (MTOC). Microtubules are long and sparse and have a wavy appearance. (b) During mitosis, microtubules are organized into a symmetrical bipolar spindle. Condensed chromosomes are aligned in pairs at the central metaphase plate before being separated and pulled towards opposite spindle poles.

Bershadsky, 1991; Stearns, 1995; Walker et al., 1988). These techniques have their own drawbacks; for example, cells are perturbed by microinjection and by photodamage generated from fluorescent probes. DIC microscopy, while a sensitive and non-invasive technique, is limited by sample thickness. DIC allows high-resolution visualization of microtubules within the relatively flat peripheral sections of interphase cells, but microtubules in the central parts of the cell and in rounded mitotic cells are more difficult to observe. As a result, *in vivo* measurements of microtubule dynamics by this method have been restricted to microtubule plus ends found in thin regions near the cell periphery.

Cytoplasmic extracts of *Xenopus* eggs (as well as other amphibian and marine invertebrates) have proven to be extremely useful in studying MT dynamics, lending themselves more readily to microscopic techniques than do intact cells. Perhaps more importantly, extracts are biochemically tractable. Egg extracts are often a rich source of native protein for biochemical fractionation. Because embryos undergo a series of very rapid cell divisions following fertilization, eggs are stockpiled with proteins involved in cell division including those involved in reorganizing the microtubule cytoskeleton.

*Xenopus* egg extracts are well suited for the study of MT dynamics for two reasons. First, *Xenopus* egg extracts offer the advantage of a synchronized and controllable cell cycle. Studies of cell cycle progression in *Xenopus* egg extracts have shown that the maturation promoting factor (MPF), which induces mitosis and meiosis, corresponds to the active protein kinase cdc2 complexed with cyclin B (Lohka, et al., 1988). MPF activity (as monitored by H1 kinase activity) is high in metaphase and low in interphase. By controlling the activity of MPF, experimentalists can manipulate *Xenopus* egg extracts to be stably arrested in either interphase or mitosis (Murray, 1991). This makes it possible to purify native proteins in particular cell cycle states (i.e. phosphorylated or complexed).

Second, these highly concentrated frog extracts are capable of recapitulating complex changes in MT dynamics, which occur during cell cycle progression, such as those required for mitotic spindle assembly. These extracts can then be manipulated in ways which would be extremely difficult (if not impossible) in whole cells. For example, inhibition of specific proteins by antibody

addition or immunodepletion is technically simpler in extracts than in cells, where such procedures require microinjection or gene expression. Pure protein can also be added back to immunodepleted extracts, demonstrating that depletion phenotypes are specific to the protein of interest. In this way, the effects on MT dynamics produced by perturbing a particular protein can be determined during each stage of the cell cycle (Desai et al., 1998).

In order to observe real-time MT dynamics in crude extracts, it is necessary to visualize the microtubules by addition of fluorescently-labeled tubulin, which incorporates into endogenous microtubules. For observation by DIC, the extract must first be clarified of refractile particles such as membrane vesicles. Clarified extracts (also called high-speed supernatants or HSS) retain their cell cycle state and, though incapable of bipolar spindle formation, will polymerize microtubules from a nucleating substrate. Common microtubule-nucleating substrates for both crude and clarified extracts include purified centrosomes and axonemes. Reagents such as taxol and DMSO stabilize microtubules and can induce the formation of organized microtubule arrays in *Xenopus* extracts (Verde et al., 1991); however, these reagents obviously perturb MT dynamics and are thus unsuitable for studying physiological dynamics.

In this review, we focus on changes in MT dynamics during the cell cycle. Precise determination of MT dynamic parameters in interphase and mitotic *Xenopus* extracts constituted a major step toward understanding how microtubules undergo the dramatic structural rearrangement during the interphase-to-mitosis transition. *Xenopus* egg extracts have also been central to the identification and characterization of many microtubule-affecting proteins, some of which may be key players in mediating the differences between interphase and mitotic MT dynamics. Finally, we review current investigation into links between the cell-cycle machinery (like cdc2/cyclinB kinase) and MT dynamics.

#### CHANGES IN MTS WITH CELL CYCLE PROGRESSION

In the transition from interphase to mitosis, structural rearrangement of microtubules is accompanied by changes in polymer length, number, and turnover rate. Microtubules in mitosis are shorter on average than microtubules in interphase and the total number

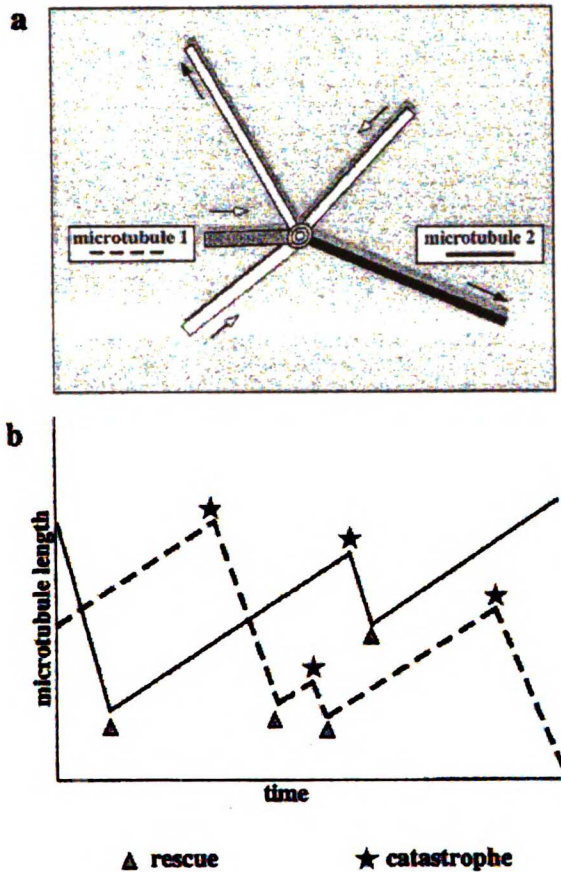


Fig. 2. Dynamic behavior of microtubule polymers. (a) Schematic representation of centrosome-nucleated microtubules as viewed by VE-DIC microscopy. The behavior of individual microtubules are independent of each another, with some polymerizing and others depolymerizing at any given time. (b) Graph representing the length of two particular microtubules as a function of time. Transitions (rescue and catastrophe) between phases of polymerization and depolymerization are stochastic.

of microtubules increases (Zhai and Borisy, 1994; Zhai et al., 1995). Mitotic cells also display a higher rate of microtubule turnover than do interphase cells, as shown by the rapid incorporation of labeled tubulin into cellular microtubule structures as well as the rapid recovery of fluorescence after photobleaching (Salmon et al., 1984; Saxton et al., 1984). In newt lung cells, for example, microtubules are several times shorter, four times as numerous, and turn over two to three orders of magnitude faster in the mitotic spindle than in the interphase array (Cassimeris et al., 1988; Wadsworth and Salmon, 1986).

Understanding these changes in population morphology required the precise determination of changes in MT dynamics. Theoretically, altering any of the four parameters of MT dynamics (polymerization, depolymerization, catastrophe, and rescue) might account for a transition from long, stable microtubules to short,

dynamic ones. Microtubules in mitosis could polymerize more slowly or depolymerize more quickly than they do in interphase. Alternatively, microtubules in mitosis could spend more time depolymerizing than they do polymerizing, which might result from an increase in catastrophe rate or a decrease in rescue rate.

Early studies of MT dynamics in extracts measured the lengths of microtubules which had been fixed at successive time-points (Verde et al., 1990). This type of analysis could not distinguish between changes in each dynamic parameter and gave only net polymerization and depolymerization rates. Microtubules were shown to exhibit a lower rate of net growth in mitosis relative to interphase (Verde et al., 1990). This was interpreted as a lower rate of polymerization in mitosis and led to two early hypotheses on cell-cycle regulation of MT dynamics. The first hypothesis proposed that the increase in microtubule nucleation sites during mitosis might be sufficient to deplete the cytoplasm of tubulin dimer (Mitchison and Kirschner, 1984). Because polymerization is a bimolecular reaction, polymerization rate decreases with decreased tubulin concentration. It was postulated that this would result in short, dynamic polymers. The second hypothesis was influenced by studies on neuronal microtubule-associated proteins (MAPs), proteins which bind and stabilize microtubules, thereby increasing their polymerization rate (Drechsel et al., 1992; Pryer et al., 1992). It was proposed that decreased assembly rates and stability in mitosis may be due to phosphorylation of these MAPs, which inhibits their binding to microtubules and prevents them from promoting microtubule polymerization (reviewed in McNally, 1996).

However, real-time analysis of MT dynamics (Belmont et al., 1990) showed that in *Xenopus* egg extracts the transition from interphase to mitosis is characterized by a change in catastrophe rate. The rate of polymerization was not decreased in mitotic extracts relative to interphase; in fact, both polymerization and depolymerization rates were slightly higher in mitosis. The major difference between the two cell cycle states was a 5- to 10-fold increase in catastrophe rate during mitosis. It was later shown that this increased catastrophe rate is specifically triggered by cyclinB-associated cdc2 kinase (MPF); addition of cyclinA-associated cdc2 kinase to interphase extracts did not affect catastrophe frequencies (Verde et al., 1992).

Is this change in catastrophe rate enough to account for the increase in MT turnover observed during mitosis? Verde et al. (1992) discussed a mathematical model for microtubule dynamics previously studied by T. Hill (1985). This model relates the average length of stiff, non-interacting polymers in an infinite, homogenous medium (like microtubules in *Xenopus* egg extracts) to the four parameters of dynamic instability. Given experimentally-determined rates for each dynamic parameter, the model predicts an average microtubule length which correlates amazingly well with measured microtubule lengths.

The Hill model predicts that minimal changes in transition frequencies (catastrophe or rescue) will have far greater effect on average MT length than corresponding changes in polymerization or depolymerization rates but does not predict whether catastrophe or rescue is the dominant parameter. In *Xenopus* extracts,

increased catastrophe rate appears to be primarily responsible for increased MT turnover in mitosis. However, a study by Gliksman et al. (1992) showed that, in sea urchin egg extracts treated with phosphatase inhibitors, a similar effect could be produced by decreased rescue rate. The regulation of catastrophe versus rescue events may be cell-type specific.

The Hill analysis also makes no assumptions about the molecular mechanisms underlying specific changes in MT dynamic parameters. Phosphorylation of MAPs and subsequent decreases in their affinity for microtubules do not lead to decreased polymerization rates in *Xenopus* egg extracts. However, it is possible that, during mitosis, this decrease in MAP affinity makes microtubules more sensitive to other destabilizing activities, such as a mitotic catastrophe factor.

Though this type of Hill analysis has been extremely useful, it is limited to the four classic dynamic parameters. There are several, more complex, types of microtubule behavior seen in both mitotic cells and mitotic *Xenopus* extracts: increased microtubule nucleation, microtubule severing, and poleward microtubule flux. These types of microtubule behavior are frequently overlooked in analyses of MT dynamics but may be important for microtubule function during mitosis and therefore warrant mention here. Microtubule nucleation is clearly cell-cycle regulated and, while it does not lead to a depletion of tubulin monomer as originally proposed, it is probably important for formation of a bipolar spindle. Microtubule severing has only recently been observed in tissue culture cells, and its function remains unknown. Poleward microtubule flux is defined as the coordinated movement of microtubule subunits in the mitotic spindle toward spindle poles. Pharmacological studies in *Xenopus* extracts have suggested that flux may drive chromosome movement during anaphase A (Desai et al., 1998); however, flux appears to play a more minor role in chromosome segregation in tissue culture cells (Mitchison and Salmon, 1992).

Quantitative measurements of MT dynamics vary between different cell types and between cells and extracts. It should be noted that precise dynamics measurements may even vary from one extract preparation to the next. Microtubule behavior may also be affected by techniques involving addition of exogenous (often bovine) and/or modified tubulin, dilution with buffer, and clarification by centrifugation, and extreme care should be taken in noting these differences during comparisons of results from independent studies.

In a recent paper by Parsons and Salmon (1997), data is presented which describes MT dynamics in a clarified HSS extracts, as visualized by DIC. No exogenous, fluorescently-labeled tubulin, which is known to have effects on MT dynamics, was added to the extract. Dynamic measurements in these extracts were significantly different from those made in crude extracts by Belmont and Verde (Belmont et al., 1990; Verde et al., 1992). Both polymerization and depolymerization rates were much higher in interphase and depolymerization significantly higher in mitosis. More disturbingly, both mitotic and interphase extracts had extremely low catastrophe frequencies. Does this mean that the high rates of catastrophe seen in crude mitotic extracts was somehow an artifact generated by the addition of

exogenous tubulin? Addition of bovine brain tubulin to these highly-clarified mitotic extract was not sufficient to restore catastrophe frequencies to those seen in crude mitotic extracts. This result implies that high catastrophe frequencies are not an artifact due to exogenous tubulin. In this system, high-speed centrifugation appears to remove an important factor that directly or indirectly induces microtubule catastrophe. The identification of this catastrophe-promoting factor will be an important area of future research.

While measurements of MT dynamics in extracts cannot be taken as literal interpretations of cellular MT dynamics, the relative changes in these dynamics can provide valuable insight into how the transition between interphase and mitotic MT dynamics may be mediated. In being able to perturb this system, assess changes in microtubule lengths and lifetimes, and determine which MT dynamic parameters are responsible for those changes, investigators have a unique window into the inner workings of the cell. In this way, utilization of *Xenopus* egg extracts has led to the identification and characterization of some of the most important proteins so far discovered to modulate MT dynamics.

#### PROTEIN MODULATORS OF MICROTUBULE DYNAMICS

Microtubule effectors can be divided into three classes: 1) proteins that affect MT dynamics, as defined by the four dynamic parameters (polymerization, depolymerization, rescue, or catastrophe); 2) proteins that affect the number of polymer ends; and 3) proteins that bind microtubules and rearrange them into higher order structures. We will emphasize proteins in the first class. Proteins belonging to the last category, including many kinesin-related motor proteins, have been well-studied in *Xenopus* egg extracts; however, they have been discussed in several recent reviews and will not be covered here (reviewed in Barton and Goldstein, 1996; Vale and Fletterick, 1997).

Mathematical modeling of theoretical polymer dynamics by Hill (1985), as well as computer simulation studies by Gliksman et al. (1993), predict that small changes in transition frequencies (catastrophe and rescue) could have rapid and dramatic effects on polymer populations. Cellular factors which mediate such changes in microtubule behavior have long been sought and, in the last several years, a number of these proteins have been identified in *Xenopus* egg extracts.

#### XMAPs (Xenopus Microtubule-Associated Proteins)

Gard and Kirschner (1987) observed that *Xenopus* extracts contained an activity which greatly stimulated microtubule assembly. Purification of the protein responsible for this activity resulted in the identification of XMAP215. Using a fixed timepoint assay, purified XMAP215 protein was found to accelerate tubulin polymerization at microtubule plus-ends, resulting in longer but, paradoxically, less stable microtubules. Subsequently, real-time analysis revealed that the effect of this protein on microtubule dynamics was complex. In vitro, XMAP215 increases MT polymerization rate by an order of magnitude, causes a three-fold increase in depolymerization rate, and nearly elimi-



nates rescue (Vasquez et al., 1994). Because the increase in polymerization rate is greater than the effects on depolymerization and rescue, the net effect of XMAP215 is to promote MT assembly; however, this net assembly is associated with increased MT turnover.

XMAP215 was the first MAP found to increase MT turnover. A human homologue of the protein TOG has recently been identified and found to have similar effects on microtubules (Charrasse et al., 1998). Without immunodepletion data, the physiological function of XMAP215 remains unclear. Its activity may be modulated in vivo by interaction with other MAPs and MT-affecting proteins. However, it is likely that the activity of factors like XMAP215 contribute to the high rate of microtubule turnover observed in vivo, relative to solutions of pure tubulin. XMAP215 might also be involved in regulating MT dynamics during mitosis, when polymer concentration is maintained at interphase levels even though turnover rate is greatly increased.

In contrast to XMAP215, most known MAPs decrease, rather than increase, MT turnover. Two *Xenopus* MAPs of this kind were recently isolated and characterized by Karsenti and coworkers (Andersen et al., 1994; Andersen and Karsenti, 1997b). The effects of the purified proteins on microtubule dynamics were assayed by monitoring the behavior of centrosome-nucleated microtubules with VE-DIC microscopy. XMAP230 and XMAP310 were both found to have stabilizing effects on microtubules, but each acts by a different mechanism. XMAP230 caused a significant decrease in catastrophe rate; XMAP310, on the other hand, had the primary effect of increasing rescue rate. These studies demonstrate the importance of real-time observation since the mechanisms by which these two MAPs act would likely have been indistinguishable in fixed timepoint assays.

Studies of *Xenopus* as well as neuronal MAPs have demonstrated that these proteins are important modulators of microtubule behavior. However, the collective effect of these *Xenopus* MAPs is not sufficient to account for the dramatic increase in microtubule turnover observed during mitosis. In particular, none of the known *Xenopus* MAPs increases the rate of microtubule catastrophe.

#### Catastrophe factors

**Op18/Stathmin.** After making the initial observation in frog extracts that microtubule catastrophe rate increased several-fold during mitosis, Belmont and Mitchison (1996) set out to purify microtubule-destabilizing activities present in extracts. One protein factor, which they isolated from thymus extracts, was identical to a previously characterized leukemia-associated oncoprotein called Op18 or stathmin. Op18 had initially been identified as a protein whose expression was highly induced in some tumor cells, and its phosphorylation was characterized extensively (Sobel, 1991). The physiological function of the protein, however, remained unclear until Op18 was identified as a catastrophe-inducing factor.

Immunodepletion of Op18 from *Xenopus* egg extracts resulted in increased microtubule length and density in sperm centrosome-nucleated asters. Readdition of pure protein to the depleted extract restored microtubule

polymer to normal levels (Belmont and Mitchison, 1996). The role of Op18 in the mitotic spindle, however, remains elusive. Immunodepletion of the protein caused excessive microtubule polymerization during the early stages of spindle assembly, but normal bipolar spindles were ultimately formed (Andersen et al., 1997a).

Op18 was also shown to interact with tubulin dimers. A tubulin-sequestering protein might be predicted to increase microtubule catastrophe rate by decreasing growth rate as a consequence of depleting soluble tubulin dimers. Whether or not Op18 acts in this way is an unresolved issue; Belmont and Mitchison (1996) maintain that the protein acts catalytically whereas Jourdain et al. (1997) support a sequestering role.

**XKCM1.** The *Xenopus* kinesin-like protein XKCM1 was identified during a screen for kinesin-like motor proteins which might be involved in spindle assembly (Walczak et al., 1996). Immunodepletion from extracts showed that XKCM1 was necessary for spindle assembly and, surprisingly, modulated MT dynamics. In the absence of XKCM1 protein, microtubule asters were ten times larger than in mock-depleted extracts, implying that XKCM1 acts to destabilize microtubules. Studies using the purified enzyme showed that it was capable of promoting microtubule catastrophes in an ATP-dependent manner (Desai et al. submitted). This result was a landmark in microtubule motor studies, showing definitively for the first time that motor-like molecules can affect the behavior of the microtubules to which they bind. The molecular mechanism by which XKCM1 acts to induce end-wise microtubule disassembly is currently the subject of active investigation.

#### Proteins affecting filament number: MT severing and nucleation

*Xenopus* extracts have brought about the characterization of proteins which affect other notable aspects of microtubule behavior. These proteins modulate bulk microtubule behavior by affecting the number of microtubule ends available to shrink or grow. This second category of proteins includes a microtubule severing protein and a microtubule nucleating factor, both of which have been characterized in *Xenopus*.

**Katanin.** Katanin was identified as an activity which causes fragmentation of microtubules in *Xenopus* egg extracts (McNally and Thomas, 1998; Vale, 1991). When purified and cloned from sea urchin egg extracts, it was found to be a heterodimeric molecule, composed of a p60 and p80 subunit (Hartman et al., 1998; McNally and Vale, 1993). Katanin's severing activity is dependent on ATP hydrolysis but how the enzyme utilizes the energy of nucleotide hydrolysis to disrupt the microtubule lattice remains unknown.

Though several possibilities have been proposed, the in vivo function of microtubule severing has yet to be determined. Severing may be involved in the rapid disassembly of the microtubule cytoskeleton at the onset of mitosis. Also, release of microtubules from centrosomal nucleating sites has been documented in mitotic *Xenopus* extracts (Belmont et al., 1990). This observation may be important in understanding the phenomenon of polewards microtubule flux, which must allow disassembly at microtubule minus ends at spindle poles. Indeed, McNally et al. (1996) have recently shown katanin to be centrosome-associated.

**$\lambda$ -tubulin.** Control of microtubule nucleation is another means by which cells can modulate cytoskeletal morphology. Due to the kinetic barrier to nucleation, microtubules do not nucleate spontaneously in the cytoplasm but assemble at distinct nucleating sites such as the centrosome. The microtubule-nucleating capacity of centrosomes has been shown to increase significantly during mitosis (Kuriyama and Borisy, 1981). *Xenopus* egg extracts have been a fruitful *in vitro* system for the study of centrosome microtubule nucleation, most notably in investigating the structure and function of  $\gamma$ -tubulin-containing complexes (Zheng, et al., 1995).

Since its discovery,  $\gamma$ -tubulin was hypothesized to play a role in microtubule nucleation (reviewed in Pereira and Schiebel, 1997). A homologue of alpha and beta tubulin, it localizes to sites of microtubule nucleation. Inhibition of  $\gamma$ -tubulin function *in vivo* or in extracts abolishes nucleation activity at centrosomes (Felix et al., 1994; Stearns et al., 1991; Stearns and Kirschner, 1994). Native  $\gamma$ -tubulin has been purified from *Xenopus* egg extracts in the form of a ring-shaped complex ( $\gamma$ -TuRC) (Zheng et al., 1995). In isolated centrosomes, similar ring structures containing  $\gamma$ -tubulin have been visualized within the pericentriolar material at the base of associated microtubules (Moritz et al., 1995). The purified  $\gamma$ -TuRC has been shown to promote microtubule assembly *in vitro* and the complex is found associated with microtubule minus ends (Zheng et al., 1995). These studies showed convincingly that  $\gamma$ -tubulin is a central component of microtubule nucleating structures and perhaps templates the assembly of tubulin subunits at these sites.

#### LINKING THE CELL CYCLE TO CHANGES IN MT DYNAMICS

In the absence of protein synthesis, addition of purified *cdc2/cyclinB* kinase to interphase *Xenopus* egg extracts is sufficient to induce mitotic MT dynamics (Verde et al., 1990). Inhibition of *cdc2* kinase activity by the general kinase inhibitor DMAP completely inhibits this transition, indicating that phosphorylation is important for modulating microtubule behavior. Phosphatase inhibitors like okadaic acid and I-2 have also been used to show that dephosphorylating activities are also important. Different classes of phosphatases appear to play distinct roles in the cell-cycle regulation of MT dynamics. For example, protein phosphatase type 2A (PP2A) helps to modulate metaphase dynamics and protein phosphatase type 1 (PP1) seems to be involved in prophase and anaphase dynamics (Tournebize et al., 1997).

Purified MAP kinase has also been shown to be capable of inducing changes in microtubule dynamics similar to those elicited by addition of exogenous *cdc2* kinase when added to *Xenopus* egg extracts. Inhibition of MAP kinase activity either by immunodepletion from extracts or via microinjection of inhibitory MAP kinase phosphatase into *Xenopus* tissue culture cells interfered with the mitotic spindle assembly checkpoint after treatment with nocodazole (Wang et al., 1997; Takenaka et al., 1997). The kinase substrates directly responsible for these changes in microtubule behavior and spindle organization remain to be elucidated.

Some microtubule-affecting proteins have been shown to be substrates for these kinases and phosphatases. Though many microtubule effectors have been characterized in *Xenopus* extracts, the cell cycle-dependent regulation of their activities has often turned out to be much more complicated than a simple "on/off" switch triggered by the absence or presence of phosphorylation.

#### MT stabilizing proteins

The activities of a number of neuronal MAPs have been shown to be regulated by phosphorylation in a cell-cycle dependent manner. Mitotic phosphorylation of XMAP230 appears to inhibit its ability to stabilize microtubules (Andersen et al., 1994). Many MAPs contain potential *cdc2* phosphorylation sites and purified *cdc2* kinase has been shown to phosphorylate a number of these *in vitro*. However, the effects of *cdc2*-cyclin kinase on MT dynamics is likely to involve additional downstream signaling molecules. For example, MAP kinase has also been shown to target microtubule-associated proteins and, like *cdc2/cyclinB* kinase, its addition to interphase *Xenopus* extracts can induce mitotic MT dynamics (Gotoh et al., 1991).

The newest players in cellular MAP regulation are the recently-identified MARK kinases. MARK kinase has been shown to phosphorylate several different MAPs *in vitro* and cause their dissociation from microtubules. Overexpression of MARK in tissue culture cells results in hyperphosphorylation of MAPs and dramatically disrupts the microtubule cytoskeleton (Drewes et al., 1997). A *Xenopus* homologue has not yet been identified.

#### Proteins which affect MT dynamics

**Op18.** The cell cycle-regulated phosphorylation of Op18 was intensely studied even before its role in modulating microtubule dynamics was discovered. During mitosis, Op18 is phosphorylated at multiple residues, including two *cdk2* consensus sites. Belmont, et al. (1996) postulated that this catastrophe factor might be activated by mitotic phosphorylation, leading to increased catastrophe rates and the establishment of mitotic MT dynamics. This model was consistent with the increase in Op18 expression and phosphorylation seen in rapidly dividing tumor cells.

Since then, however, work on Op18 has led to a different perspective on its cell cycle regulation. Studies in human tissue culture cells indicate that *cdk*-mediated serine phosphorylation, rather than activating Op18, actually inhibits its microtubule destabilization activity (Marklund et al., 1996). This implies, paradoxically, that this catastrophe factor is highly phosphorylated and therefore inactive during mitosis. Two other serines which are phosphorylated by an unidentified kinase could, in theory, modulate or antagonize the effect of cyclin-dependent kinase modifications; however, recent evidence seems to indicate that Op18 is not in fact a major regulator of global MT dynamics in mitosis. For example, depletion of Op18 from mitotic egg extracts induces only a slight decrease in catastrophe rate, certainly not to interphase levels (Tournebize et al., 1997).

Andersen et al. (1997a) propose that local inactivation of Op18 near chromosomes might promote microtu-

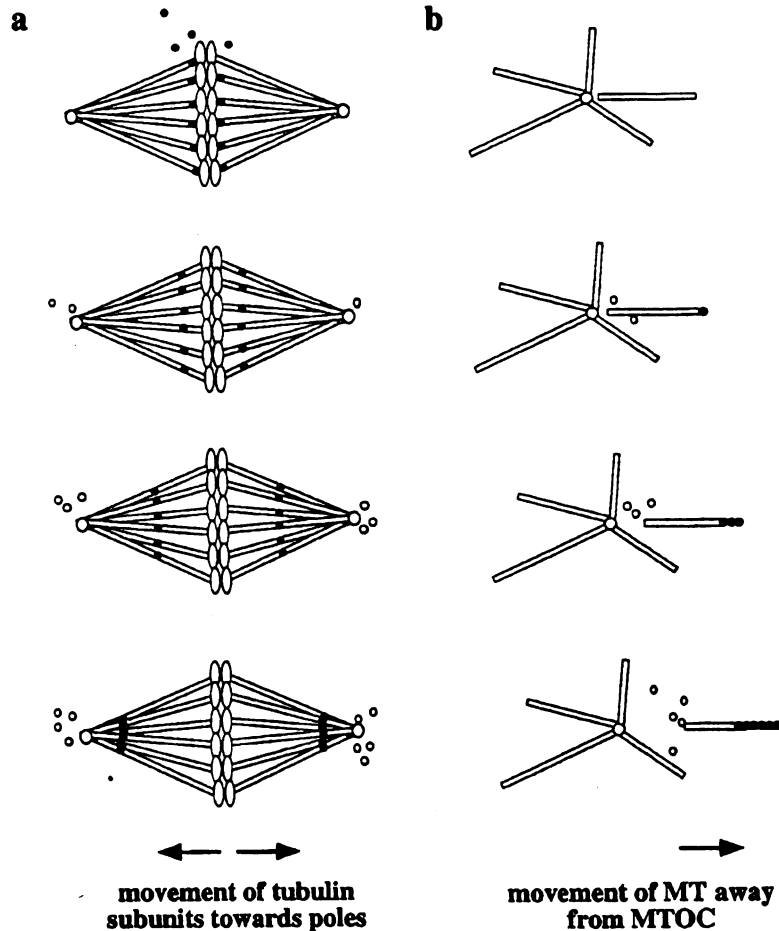


Fig. 3. Poleward microtubule flux (a) versus microtubule treadmilling (b). (a) Tubulin subunits of spindle microtubules move poleward over time. Net polymerization at MT plus ends is coordinated with net depolymerization at MT minus ends at spindle poles. Note that tubulin subunits move poleward (dark circles) and MT ends appear fixed; force is required to translocate the MT lattice toward the pole. (b) The microtubule on the right side of this interphase array has been released from its MTOC. This particular free microtubule undergoes plus-end polymerization and minus-end depolymerization. Tubulin subunits remain stationary and, due to shrinkage of the minus end and growth of the plus end, the microtubule translocates toward the cell periphery, in the direction of polymerization.

bule-chromatin interactions during spindle assembly. Hyperphosphorylation of Op18 was shown to be dependent on the presence of chromatin; however, the effect of this hyperphosphorylation on MT dynamics has not been clearly demonstrated. This chromatin-induced hyperphosphorylation may be due to a chromatin-associated kinase; alternatively, the chromatin could contain a factor which inhibits Op18 dephosphorylation. In support of the latter, Op18 hyperphosphorylation was also shown to be induced, in the absence of chromatin, by addition of 0.5  $\mu$ M okadaic acid. This concentration of okadaic acid inhibits type 2A phosphatases but not type 1 phosphatases, implying that PP2A may mediate chromatin-induced inhibition of Op18.

This is not the only downstream effect of okadaic acid. Addition of okadaic acid to spindle assembly reactions resulted in abnormal spindles with very long microtubules—an effect not seen with Op18 depletion (Tournebise et al., 1997). Okadaic acid may inhibit another phosphatase important for MT dynamics or, alternatively, PP2A may control more than one microtubule regulator.

**XKCM1.** XKCM1 is a phosphoprotein, but it has not yet been determined whether this phosphorylation differs between interphase and mitotic extracts nor if the catastrophe-inducing activity of XKCM1 is cell cycle-regulated (Walczak, unpublished results). Baculovirus-expressed XKCM1 protein used in the *in vitro* experiments characterizing the enzyme's activity was purified predominantly from interphase cells, suggesting that XKCM1 is capable of promoting microtubule destabilization throughout the cell cycle (Desai and Walczak, unpublished results). If so, it is possible that microtubules are somehow less susceptible to XKCM1-mediated destabilization in interphase than in mitosis. For example, the association of MAPs may inhibit binding of XKCM1 to interphase microtubules or stabilize microtubules against XKCM1 activity.

While XKCM1 is clearly a major promoter of MT catastrophe, it has not been shown whether immunodepletion from mitotic extracts is sufficient to reduce the rate of catastrophe down to interphase levels. XKCM1 may have a more specific role in mitosis, controlled by its localization. For both XKCM1 and its

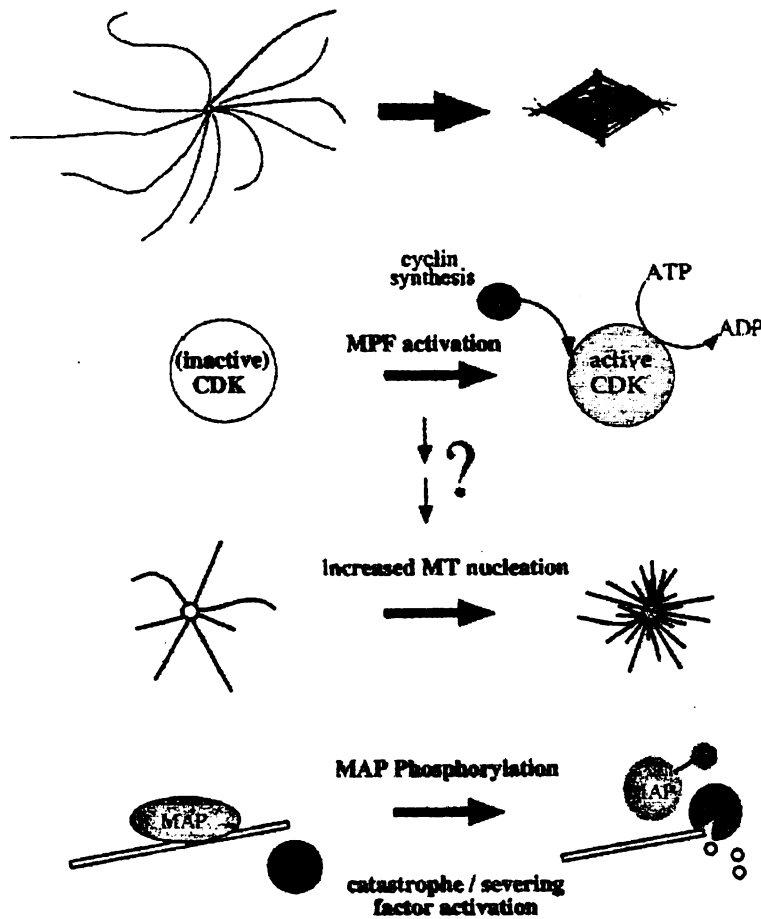


Fig. 4. Overview of several molecular mechanisms involved in changing microtubule morphology/dynamics from interphase to mitosis. The onset of mitosis requires activation of cyclin-dependent kinases, which directly or indirectly participate in the activation of nucleation-promoting factors, the inactivation of MT-stabilizing MAPs, and the induction of catastrophe factors, as well as other proteins which may affect MT dynamics.

human homologue MCAK, a fraction of the protein appears to localize to kinetochores (Wordeman and Mitchison, 1995). It is interesting to speculate that this protein may function to promote microtubule disassembly at kinetochores during anaphase and/or be involved in mediating interactions between kinetochores and microtubules (Maney, et al., 1998).

#### Other types of microtubule behavior

Three types of microtubule behavior that do not fall strictly into the classic categories of MT dynamics were described earlier: microtubule nucleation, microtubule severing, and poleward microtubule flux. Though little is known about the cell-cycle regulation of these activities, there is evidence to support the existence of such regulation.

**Microtubule nucleation.** Ring-shaped complexes containing  $\gamma$ -tubulin are now widely accepted to be microtubule nucleation sites at the centrosome. The increase in microtubule number at the centrosome during mitosis may be due to an increase in the number of these sites or regulation of their microtubule-

nucleating activity. There is no evidence to date distinguishing between these two possibilities.

**Microtubule severing.** Katanin, the most well-characterized of the three known microtubule-severing proteins, is postulated to be cell-cycle regulated; however, there is little evidence to support this (Vale, 1991). Determination of its regulation may give insight into its physiological function. Microtubule severing could help to increase the number of microtubules in mitosis by increasing the number of ends available for polymerization; alternatively, severing could promote rapid disassembly of microtubules in prophase by increasing the number of ends available for depolymerization. MT severing has also been postulated to be involved in the release of microtubules from centrosomes (McNally and Thomas, 1998).

**Poleward microtubule flux.** Poleward flux, the coordinated movement of tubulin subunits within spindle microtubules toward spindle poles, requires three events: net polymerization at microtubule plus ends, net depolymerization at microtubule minus ends, and translocation of the microtubule lattice toward the

poles (Fig. 3) (Mitchison, 1989). Poleward flux appears to be a cell-cycle regulated phenomenon, though this has been examined in a limited number of cell types. In mitotic spindles of somatic cells, microtubule bundles connecting chromosomes to spindle poles (kinetochores) exhibit poleward flux (Mitchison and Salmon, 1992). In mitotic *Xenopus egg* extracts, bipolar spindles as well as simpler centrosome and/or chromatin-free structures have been observed to exhibit poleward flux (Sawin and Mitchison, 1991; Sawin and Mitchison, 1994). Poleward flux does not appear to exist in interphase microtubule arrays, though it is technically more difficult to detect poleward flux in sparse interphase structures.

In several types of interphase cells, a similar but distinct phenomenon called "microtubule treadmill" has recently been observed (Fig. 3) (Rodionov and Borisy, 1997). Microtubules which are released from the centrosome appear to translocate towards the cell periphery by a "treadmill" mechanism, undergoing net polymerization at their plus ends (distal to the centrosome) and net depolymerization at their minus ends (proximal to the centrosome) (Waterman-Storer and Salmon, 1997). In these cases, microtubules still attached to centrosomes do not seem to exhibit poleward flux.

It is not known whether treadmill and poleward flux occur by similar mechanisms; no molecular components responsible for either phenomena have been identified. Treadmilling is a single microtubule event whereas flux is a population dynamic; in treadmill, the microtubule is free and translocates in the direction of polymerization whereas in poleward flux microtubules are fixed within a complex structure and tubulin subunits move toward the pole (Fig. 3). However, they do have one element in common: minus end dynamics. The minus ends of centrosome-anchored microtubules in interphase appear to be stably capped and do not exhibit any dynamic behavior. The minus-end depolymerization seen in both treadmill and poleward flux indicates that these microtubule ends must be free to depolymerize, even those in the mitotic spindle. In fact, EM studies of mitotic spindles in several cell types have shown that many spindle microtubules do not terminate in the pericentriolar material (Mastrorarde et al., 1993). MT minus ends have been described as the "dark side of microtubule dynamics" (Desai and Mitchison, 1997). Most research on MT dynamics, especially *in vivo*, has focused on MT plus ends; much less is known about the dynamics and regulation of minus ends, which are difficult to visualize. It is now clear that insight into minus end dynamics, particularly at the centrosome, will be crucial for understanding complex microtubule behavior in cells.

### CONCLUSION

The behavior of microtubules *in vivo* differs significantly from the dynamics of pure tubulin *in vitro*. An elaborate system of protein modulators exists to regulate MT dynamics both temporally (throughout the cell cycle) and spatially (in different parts of the cell). During mitosis, for example, specific subpopulations of microtubules (astral or cytoplasmic microtubules, spindle microtubules, kinetochore microtubules, and

interzone microtubules) behave very differently from each other. Why does the cell expend considerable energy and employ so many proteins to maintain this complex, dynamic microtubule cytoskeleton?

We can only speculate on the biological functions of dynamic instability *in vivo*. This unique polymer behavior may facilitate the rapid rearrangement of microtubules during the interphase to mitosis transition. Dynamic instability has also been proposed to increase the efficiency by which microtubules probe cytoplasmic space (Holy and Leibler, 1994); this would be particularly important during mitosis, when microtubules must rapidly find and capture very small target zones, the kinetochores of individual chromosomes. Disruption of MT dynamics in many cell types will trigger mitotic arrest even after kinetochore capture, indicating a function for dynamic instability in later stages of mitosis. Types of MT dynamics like poleward flux and inhibition of plus end polymerization appear to assist in the segregation of chromosomes at anaphase. It is likely that MT dynamics play an important role in other processes which have yet to be identified.

Many complex *in vivo* MT dynamics can be reconstituted in *Xenopus egg* extracts, allowing the characterization of a number of important microtubule-affecting proteins. We have described a few of these proteins and recent progress made toward investigating their spatial and temporal regulation (Fig. 4). Through this kind of work, which dissects the molecular mechanisms behind different types of MT dynamics, we understand the roles of these dynamics in specific subcellular processes; only then will we begin to answer the question, "Why dynamic instability?"

### ACKNOWLEDGMENTS

The authors thank Arshad Desai and Jack Taunton for help in writing and editing this manuscript; and Joel Hiza, Lennie Feldman, Justin Yarrow, Terry Lechler, and Aneil Mallavarapu for advice and support. We also thank Tim Mitchison and the rest of the Mitchison lab for scientific discussions that were an important basis for our views of this field.

### REFERENCES

- Andersen SS, Ashford AJ, Tournebise R, Gavet O, Sobel A, Hyman AA, Karsenti E. 1997a. Mitotic chromatin regulates phosphorylation of Stathmin/Op18. *Nature* 389:640-643.
- Andersen SS, Buendia B, Dominguez JE, Sawyer A, Karsenti E. 1994. Effect on microtubule dynamics of XMAP230, a microtubule-associated protein present in *Xenopus laevis* eggs and dividing cells. *J Cell Biol* 127:1289-1299.
- Andersen SS, Karsenti E. 1997b. XMAP310: a *Xenopus* rescue-promoting factor localized to the mitotic spindle. *J Cell Biol* 139:975-983.
- Barton N, Goldstein LSB. 1996. Going mobile: microtubule motors and chromosome segregation. *Proc Natl Acad Sci USA* 93:1735-1742.
- Belmont LD, Hyman AA, Sawin KE, Mitchison TJ. 1990. Real-time visualization of cell cycle-dependent changes in microtubule dynamics in cytoplasmic extracts. *Cell* 62:579-589.
- Belmont L, Mitchison TJ, Deacon H. 1996. Catastrophic revelations about Op18/stathmin. *Trends Biochem Sci* 21:197-198.
- Belmont LD, Mitchison TJ. 1996. Identification of a protein that interacts with tubulin dimers and increases the catastrophe rate of microtubules. *Cell* 84:623-631.
- Cassimeris L. 1993. Regulation of microtubule dynamic instability. *Cell Motil Cytoskeleton* 26:275-281.
- Cassimeris L, Pryer NK, Salmon ED. 1988. Real-time observations of

- microtubule dynamic instability in living cells. *J Cell Biol* 107:2223–2231.
- Charrasse S, Schroeder M, Gauthier-Rouviere C, Ango F, Cassimeris L, Gard DL, Larroque C. 1998. The TOGp protein is a new human microtubule-associated protein homologous to the *Xenopus* XMAP215. *J Cell Sci* 111:1371–1383.
- Desai A, Maddox PS, Mitchison TJ, Salmon ED. 1998. Anaphase A chromosome movement and poleward spindle microtubule flux occur at similar rates in *Xenopus* extract spindles. *J Cell Biol* 141:703–713.
- Desai A, Mitchison TJ. 1997. Microtubule polymerization dynamics. *Annu Rev Cell Dev Biol* 13:83–117.
- Desai A, Murray A, Mitchison TJ, Walczak CE. 1998. The use of *Xenopus* egg extracts to study mitotic spindle assembly and function in vitro. *Meth In Cell Biol* 61:385–412.
- Desai A, Verma S, Mitchison TJ, Walczak CE. 1999. Kin I kinesins are microtubule-destabilizing enzymes. *Cell* 96:69–78.
- Drechsel DN, Hyman AA, Cobb MH, Kirschner MW. 1992. Modulation of the dynamic instability of tubulin assembly by the microtubule-associated protein tau. *Mol Biol Cell* 3:1141–1154.
- Drewes G, Biernat J, Preuss U, Mandelkow EM. 1997. MARK, a novel family of protein kinases that phosphorylate microtubule-associated proteins and trigger microtubule disruption. *Cell* 89:297–308.
- Felix MA, Antony C, Wright M, Maro B. 1994. Centrosome assembly in vitro: role of gamma-tubulin recruitment in *Xenopus* sperm aster formation. *J Cell Biol* 124:19–31.
- Gard DL, Kirschner MW. 1987. A microtubule-associated protein from *Xenopus* eggs that specifically promotes assembly at the plus-end. *J Cell Biol* 105:2203–2215.
- Gelfand VI, Bershadsky AD. 1991. Microtubule dynamics: mechanism, regulation, and function. *Annu Rev Cell Biol* 7:93–116.
- Gliksman NR, Parsons SF, Salmon ED. 1992. Okadaic acid induces interphase to mitotic-like microtubule dynamic instability by inactivating rescue. *J Cell Biol* 119:1271–1276.
- Gliksman NR, Skibbens RV, Salmon ED. 1993. How the transition frequencies of microtubule dynamic instability (nucleation, catastrophe, and rescue) regulate microtubule dynamics in interphase and mitosis: analysis using a Monte Carlo computer simulation. *Mol Biol Cell* 4:1035–1050.
- Gotoh Y, Nishida E, Matsuda S, Shiina N, Kosako H, Shiohara K, Akiyama, T, Ohta, K, Sakai H. 1991. In vitro effects on microtubule dynamics of purified *Xenopus* M phase-activated MAP kinase. *Nature* 349:251–254.
- Hartman JJ, Mahr J, McNally K, Okawa K, Iwamatsu A, Thomas S, Cheesman, S, Heuser J, Vale RD, McNally FJ. 1998. Katanin, a microtubule-severing protein, is a novel AAA ATPase that targets to the centrosome using a WD40-containing subunit. *Cell* 93:277–287.
- Hill TL. 1985. Theoretical problems related to the attachment of microtubules to kinetochores. *Proc Natl Acad Sci USA* 82:4404–4408.
- Holy TE, Leibler S. 1994. Dynamic instability of microtubules as an efficient way to search in space. *Proc Natl Acad Sci USA* 91:5682–5685.
- Inoue S, Salmon ED. 1995. Force generation by microtubule assembly/disassembly in mitosis and related movements. *Mol Biol Cell* 6:1619–1640.
- Jourdain L, Curmi P, Sobel A, Pantaloni D, Carlier MF. 1997. Stathmin: a tubulin-sequestering protein which forms a ternary T2S complex with two tubulin molecules. *Biochemistry* 36:10817–10821.
- Kuriyama R, Borisov GG. 1981. Microtubule-nucleating activity of centrosomes in Chinese hamster ovary cells is independent of the centriole cycle but coupled to the mitotic cycle. *J Cell Biol* 91:822–826.
- Lohka MJ, Hayes MK, Maller JL. 1988. Purification of maturation-promoting factor, an intracellular regulator of early mitotic events. *Proc Natl Acad Sci USA* 85:3009–3013.
- Maney T, Hunter AW, Wagenback M, Wordeman L. 1998. Mitotic centromere-associated kinesin is important for anaphase chromosome segregation. *J Cell Biol* 142:787–801.
- Marklund U, Larsson N, Gradin HM, Brattsand G, Gullberg M. 1996. Oncoprotein 18 is a phosphorylation-responsive regulator of microtubule dynamics. *Embo J* 15:5290–5298.
- Mastroratte DN, McDonald KL, Ding R, McIntosh JR. 1993. Interpolar spindle microtubules in PTK cells. *J Cell Biol* 123:1475–1489.
- McNally FJ. 1996. Modulation of microtubule dynamics during the cell cycle. *Curr Opin Cell Biol* 8:23–29.
- McNally FJ, Okawa K, Iwamatsu A, Vale RD. 1996. Katanin, the microtubule-severing ATPase, is concentrated at centrosomes. *J Cell Sci* 109:561–567.
- McNally FJ, Thomas S. 1998. Katanin is responsible for the M-phase microtubule-severing activity in *Xenopus* eggs. *Mol Biol Cell* 9:1847–1861.
- McNally FJ, Vale RD. 1993. Identification of katanin, an ATPase that severs and disassembles stable microtubules. *Cell* 75:419–429.
- Mitchison T, Kirschner M. 1984. Dynamic instability of microtubule growth. *Nature* 312:237–242.
- Mitchison TJ. 1989. Polewards microtubule flux in the mitotic spindle: evidence from photoactivation of fluorescence. *J Cell Biol* 109:637–652.
- Mitchison TJ, Salmon ED. 1992. Poleward kinetochore fiber movement occurs during both metaphase and anaphase-A in newt lung cell mitosis. *J Cell Biol* 119:569–582.
- Moritz M, Braunfeld MB, Sedat JW, Alberts B, Agard DA. 1995. Microtubule nucleation by gamma-tubulin-containing rings in the centrosome. *Nature* 378:638–640.
- Murray AW. 1991. Cell cycle extracts. *Meth. Cell Biol* 36:581–605.
- Parsons SF, Salmon ED. 1997. Microtubule assembly in clarified *Xenopus* egg extracts. *Cell Motil Cytoskeleton* 36:1–11.
- Pereira G, Schiebel E. 1997. Centrosome-microtubule nucleation. *J Cell Sci* 110:295–300.
- Pryer NK, Walker RA, Skeen VP, Bourns BD, Soboleiro MF, Salmon ED. 1992. Brain microtubule-associated proteins modulate microtubule dynamic instability in vitro. Real-time observations using video microscopy. *J Cell Sci* 103:965–976.
- Rodionov VI, Borisov GG. 1997. Microtubule treadmill in vivo. *Science* 275:215–218.
- Salmon ED, Leslie RJ, Saxton WM, Karow ML, McIntosh JR. 1984. Spindle microtubule dynamics in sea urchin embryos: analysis using a fluorescein-labeled tubulin and measurements of fluorescence redistribution after laser photobleaching. *J Cell Biol* 99:2165–2174.
- Sawin KE, Mitchison TJ. 1991. Poleward microtubule flux in mitotic spindles assembled in vitro. *J Cell Biol* 112:941–954.
- Sawin KE, Mitchison TJ. 1994. Microtubule flux in mitosis is independent of chromosomes, centrosomes, and antiparallel microtubules. *Mol Biol Cell* 5:217–226.
- Saxton WM, Stemple DL, Leslie RJ, Salmon ED, Zavortink M, McIntosh JR. 1984. Tubulin dynamics in cultured mammalian cells. *J Cell Biol* 99:2175–2186.
- Sobel A. 1991. Stathmin: a relay phosphoprotein for multiple signal transduction? *Trends Biochem Sci* 16:301–305.
- Stearns T. 1995. Green fluorescent protein. The green revolution. *Curr Biol* 5:262–264.
- Stearns T, Evans L, Kirschner M. 1991. Gamma-tubulin is a highly conserved component of the centrosome. *Cell* 65:825–836.
- Stearns T, Kirschner M. 1994. In vitro reconstitution of centrosome assembly and function: the central role of gamma-tubulin. *Cell* 76:623–637.
- Tanemaka K, Gotoh Y, Nishida E. 1997. MAP kinase is required for the spindle assembly checkpoint but is dispensable for the normal M-phase entry and exit in *Xenopus* egg cell cycle extracts. *J Cell Biol* 136:1091–1097.
- Tournebise R, Andersen SS, Verde F, Doree M, Karsenti E, Hyman AA. 1997. Distinct roles of PP1 and PP2A-like phosphatases in control of microtubule dynamics during mitosis. *Embo J* 16:5537–5549.
- Vale RD. 1991. Severing of stable microtubules by a mitotically activated protein in *Xenopus* egg extracts. *Cell* 64:827–839.
- Vale RD, Fletterick R J. 1997. The design plan of kinesin motors. *Annu Rev Cell Dev Biol* 13:745–777.
- Vasquez RJ, Gard DL, Cassimeris L. 1994. XMAP from *Xenopus* eggs promotes rapid plus end assembly of microtubules and rapid microtubule polymer turnover. *J Cell Biol* 127:985–993.
- Verde F, Berrez JM, Antony C, Karsenti E. 1991. Taxol-induced microtubule asters in mitotic extracts of *Xenopus* eggs: requirement for phosphorylated factors and cytoplasmic dynein. *J Cell Biol* 112:1177–1187.
- Verde F, Dogterom M, Stelzer E, Karsenti E, Leibler S. 1992. Control of microtubule dynamics and length by cyclin A- and cyclin B-dependent kinases in *Xenopus* egg extracts. *J Cell Biol* 118:1097–1108.
- Verde F, Labbe JC, Doree M, Karsenti E. 1990. Regulation of microtubule dynamics by cdc2 protein kinase in cell-free extracts of *Xenopus* eggs. *Nature* 343:233–238.
- Wadsworth P, Salmon ED. 1986. Analysis of the treadmill model during metaphase of mitosis using fluorescence redistribution after photobleaching. *J Cell Biol* 102:1032–1038.

- Walczak CE, Mitchison TJ, Desai A. 1996. XKCM1: a *Xenopus* kinesin-related protein that regulates microtubule dynamics during mitotic spindle assembly. *Cell* 84:37-47.
- Walker RA, O'Brien ET, Pryer NK, Soboeiro MF, Voter WA, Erickson, H.P, Salmon ED. 1988. Dynamic instability of individual microtubules analyzed by video light microscopy: rate constants and transition frequencies. *J Cell Biol* 107:1437-1448.
- Wang XM, Zhai Y, Ferrell JE. 1997. A role for mitogen-activated protein kinase in the spindle assembly checkpoint in XTC cells. *J Cell Biol* 137:433-443.
- Waterman-Storer CM, Salmon ED. 1997. Microtubule dynamics: treadmilling comes around again. *Curr Biol* 7:R369-372.
- Wordeman L, Mitchison TJ. 1995. Identification and partial characterization of mitotic centromere-associated kinesin, a kinesin-related protein that associates with centromeres during mitosis. *J Cell Biol* 128:95-104.
- Zhai Y, Borisy, G.G. 1994. Quantitative determination of the proportion of microtubule polymer present during the mitosis-interphase transition. *J Cell Sci* 107:881-890.
- Zhai Y, Kronebusch PJ, Borisy GG. 1995. Kinetochore microtubule dynamics and the metaphase-anaphase transition. *J Cell Biol* 131:721-734.
- Zheng Y, Wong ML, Alberts B, Mitchison T. 1995. Nucleation of microtubule assembly by a gamma-tubulin-containing ring complex. *Nature* 378:578-583.

## **Appendix II**

### **Dynamics of the Mitotic Spindle – Potential Therapeutic Targets**

This appendix has been reproduced from *Progress in Cell Cycle*, Vol. 5, Chapter 35, 349-360 (2003), Meijer, L., Jezequel, A., and Roberge, M., eds.

I wrote the review in this appendix with Zach Perlman and David Miyamoto. Zach Perlman also produced all the figures, with comments from myself and David Miyamoto.



## Dynamics of the mitotic spindle - potential therapeutic targets

David T. Miyamoto<sup>1,‡</sup>, Zachary E. Perlman<sup>1,‡</sup>, Timothy J. Mitchison<sup>1,‡</sup>, and Mimi Shirasu-Hiza<sup>1</sup>

<sup>‡</sup> These authors contributed equally to this work.

The dynamic nature of microtubules underlies many of the most basic activities of the cell. The establishment of cell polarity, cell differentiation, and cell division all require microtubules and make use of their intrinsic capacity for rapid structural rearrangement. In interphase cells, microtubules radiate outward from the MTOC (Microtubule Organizing Center) and act as relatively static "railroad tracks" for vesicles and protein cargoes. Upon entering mitosis, the cell dismantles and rebuilds this radial array into a bipolar mitotic spindle that carries out the segregation of sister chromatids. Precise regulation of microtubule dynamics underpins the elaborate series of structural rearrangements necessary for this dramatic transformation to occur properly (1).

These same dynamic rearrangements make the mitotic spindle a vulnerable target for drugs that interfere with cell cycle progression. Inhibition of this cell division machinery underlies the clinical treatment of many human diseases characterized by excessive cell proliferation. As discussed in Chapter 12, small molecules that affect microtubule dynamics are one of the most effective classes of anti-mitotic therapeutics, possibly because perturbation of microtubule dynamics in the spindle leads to a prolonged mitotic arrest, followed by cell death.

One problem with direct inhibitors of tubulin is their lack of specificity for dividing cells. Microtubules provide important structural and transport functions in neurons and other non-mitotic cells. Drugs that target the microtubule cytoskeleton without discriminating between dividing and non-dividing cells may thus cause undesired toxicity in living organisms. For example, the microtubule stabilizing drug paclitaxel causes peripheral neuropathy, which is thought to result from perturbation of the microtubule network in post-mitotic neurons (2). It is natural to ask whether we can target mitotic cells more specifically, perhaps by inhibiting proteins that play a large role in mitosis but not interphase.

In this chapter, we ask from a cell biology perspective whether proteins that regulate microtubule dynamics and organization in the spindle might make

good targets for inhibiting cell division. We begin by reviewing the fundamentals of microtubule dynamics and the stereotyped physical rearrangements essential to the function of the mitotic spindle. The bulk of this chapter is then devoted to reviewing microtubule regulating proteins that may be of particular interest in screens for cell cycle inhibitors.

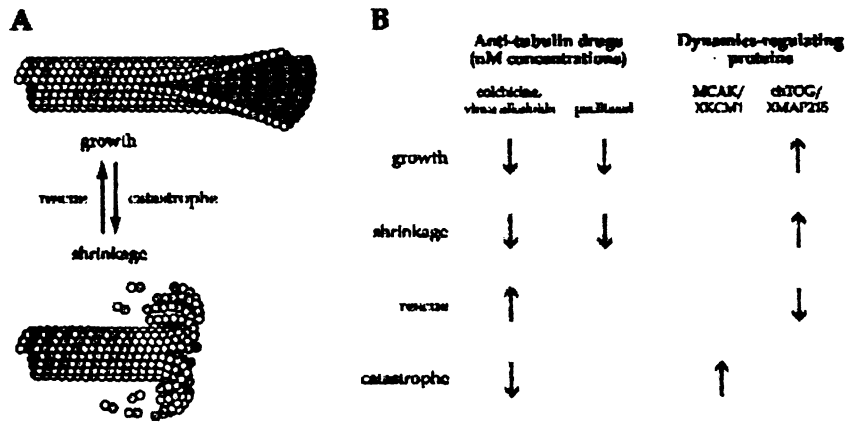
### MICROTUBULE DYNAMICS AND SPINDLE ASSEMBLY

**The polymerization dynamics of microtubules are essential to their function.**

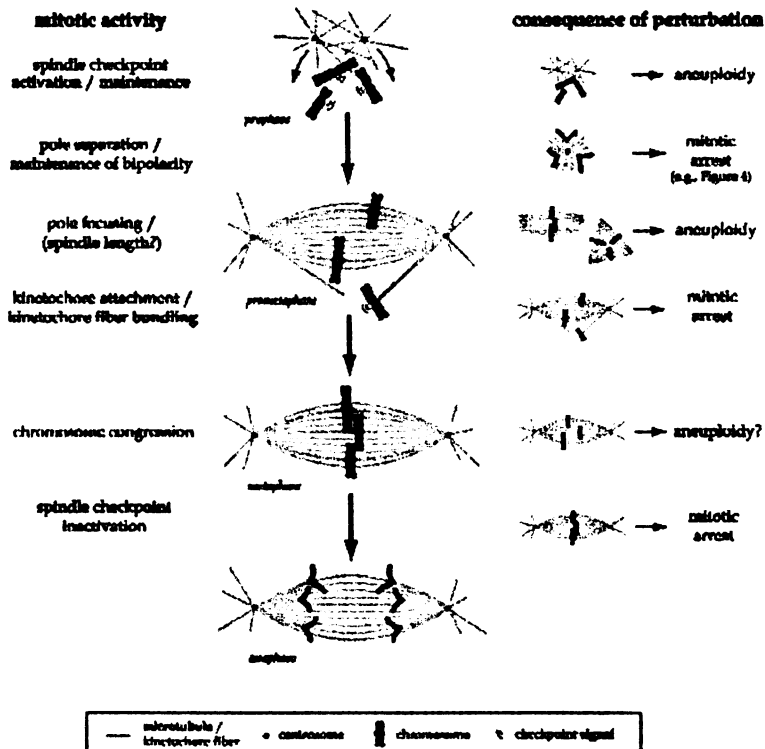
For a comprehensive review of microtubule dynamics, see (3). Briefly, microtubules are composed of  $\alpha$ -/  $\beta$ -tubulin heterodimers, which hydrolyze GTP during polymerization. Unlike typical equilibrium polymers, microtubules never reach steady-state length and instead exhibit a behavior termed "dynamic instability" — that is, stochastic transitions between phases of growth and shrinkage. The four classic parameters of microtubule dynamics are growth rate, shrinkage rate, catastrophe frequency, and rescue frequency (Figure 1A). As depicted, polymerization is correlated with the formation of protofilament sheets at the growing end of the microtubule and depolymerization with a "ram's horn" conformation of curled protofilaments. The two ends of microtubules have different dynamic characteristics. The "plus end" polymerizes more rapidly than the "minus end." It is not clear how or whether protein regulators of microtubule dynamics affect microtubule minus ends, which *in vivo* are usually embedded in the MTOC or pericentrosomal material. In this review, we focus on plus end dynamic behavior.

**Protein regulators of microtubule dynamics are potential targets for cell cycle inhibitors.**

*In vivo*, protein regulators of microtubule dynamics play a key role in transforming the long, stable microtubules of interphase into the short, dynamic microtubules of the mitotic spindle. Direct measurement of microtubule dynamics in different systems have demonstrated that the most significant change in dynamics is either an increase in catastrophe frequen-



**Figure 1.** A. Four parameters are conventionally measured to describe microtubule dynamics. Microtubules typically undergo stochastic transitions (rescue, catastrophe) between phases of polymerization and depolymerization (growth, shrinkage). B. Tubulin inhibitors and microtubule-associated proteins affect the dynamics of microtubules. In contrast to the high (>1 μM) concentrations of anti-tubulin drug typically used in cell biological studies, nanomolar concentrations of anti-tubulin drugs inhibit microtubule dynamics without changing total microtubule polymer mass (7, 122). These nanomolar concentrations approximately correspond to the effective plasma concentrations in patients during chemotherapy (123). Two microtubule dynamics regulating proteins that have been well characterized *in vitro* are shown for comparison.



**Figure 2.** Many distinct activities are required between chromosome condensation and sister chromatid separation. The central column depicts the morphological changes of the spindle during mitotic progression, the left column describes the sequence of some of the biochemical activities underlying these rearrangements, and the right column describes the consequences reported for inhibition of some of the involved proteins.

cy (4), a decrease in rescue frequency (5), or, in the case of mammalian tissue culture cells, both (6). Direct anti-tubulin drugs like paclitaxel or vinca alkaloids can inhibit cell cycle progression by altering microtubule dynamics, even at concentrations too low to affect total polymer mass (7) (Figure 1B). Accordingly, inhibiting some of the proteins that regulate microtubule dynamics *in vivo* (3) might be expected to result in mitotic arrest. As will be discussed, such inhibitors might also act in synergy with tubulin inhibitors.

**Many microtubule-regulating proteins are essential for mitotic progression.**

In addition to regulators of microtubule dynamics, many other proteins have been shown to be involved in spindle assembly and function. These include motor proteins, enzymes which use the energy of ATP hydrolysis to move along microtubules; nucleating factors, which stimulate the polymerization of new microtubules; and structural proteins, which do not appear to have any enzymatic activity but which are necessary for spindle structure (8).

In Figure 2, we outline the complex microtubule rearrangements that occur in mitosis and depict the predicted consequence of inhibiting some proteins involved in these events. Prior to nuclear envelope breakdown, the pair of centrosomes at the center of the MTOC begins to separate until the metaphase inter-polar distance is achieved. The upregulation of dynamic instability at mitosis allows microtubule plus ends to explore the volume of the cell. A microtubule that comes in contact with a kinetochore will be stabilized and will be incorporated into a bundle of microtubules termed the kinetochore fiber. Kinetochore fibers transmit force to move chromosomes and allow the trafficking of structural and signaling proteins between kinetochores and poles. Minus ends are held together at the poles, giving rise to the characteristic fusiform shape of the mitotic spindle. The intrinsic bipolarity of the mitotic spindle enables it to push and pull on sister chromatids in two opposite directions, resulting in the migration of bioriented chromosomes to the metaphase plate at the center of the spindle and allowing equal partitioning of chromosomes to the two daughter cells. A spindle checkpoint exists to ensure that this sister chromatid separation does not occur until all chromosomes are properly oriented at the metaphase plate. Some of the proteins we will discuss are involved in this error checking mechanism and communicate with the signaling proteins discussed in Chapter 43. Upon sister chromatid separation, the chromosomes are moved towards the poles, the poles are moved further apart, and a cleavage furrow forms to separate the cytoplasm and give two daughter cells.

**Many of the proteins responsible for microtubule rearrangements during mitosis may be interesting potential targets for cell cycle inhibitors.**

Some of the proteins that regulate microtubule rearrangements in mitosis are listed in Table 1. Since the action of anti-microtubule drugs seems to involve prolonged activation of the spindle checkpoint, our

discussion will highlight those proteins that have been shown to cause mitotic arrest when perturbed and therefore might be potential anti-mitotic drug targets. It should be kept in mind that most of the cell biology data upon which we rely are based on depletion or deletion studies and that small molecule inhibition of a protein may be more likely to phenocopy a dominant negative mutation.

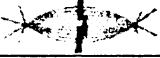




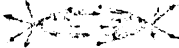





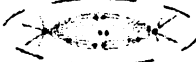
We will also review some proteins for which inhibition does not trigger the spindle checkpoint, but which are essential for function of the mitotic apparatus. There may be some risk associated with the inhibition of some of these proteins, since their perturbation may give rise to aneuploidy, which has been proposed to be an oncogenic mechanism (9). For example, as will be discussed, inhibition or depletion of some microtubule dynamics regulators and some mitotic kinesins leads to defective chromosome segregation. This is perhaps because many of these proteins are important both for spindle structure and spindle checkpoint function.

The proteins in this chapter are divided into microtubule destabilizers, microtubule stabilizers, and mitotic motors. In discussing each protein, we attempt to highlight the effects of its inhibition on cell cycle progression, provide information on its *in vitro* activity, present evidence for its function in mitotic and interphase cells, and discuss potential strategies that may be used to screen for small molecule inhibitors. In general, assays that already exist for dynamics regulators or motor proteins can often be scaled up for high-throughput screening with relative ease. A number of simple assays are well-established for the measurement of nucleotide hydrolysis rates under equilibrium or nonequilibrium conditions; these assays might be used to measure ATPase motor activity (10) or the GTPase activity of microtubule polymerization. Alternatively, cell-based screens for the phenotypic outcome of mitotic arrest may yield inhibitors that would be difficult to obtain *in vitro* - for example, in the case of proteins with relatively low ATPase activity. Some proteins might also be subject to cell cycle-specific regulation or require cellular co-factors difficult to supply in an *in vitro* assay.

**MICROTUBULE DYNAMICS REGULATORS: DESTABILIZERS**

Microtubule destabilizers constitute an important class of potential anti-mitotic targets. Paclitaxel, by analogy, blocks microtubule destabilization, resulting in excessive stabilization and mitotic block (Chapter 33). Inhibiting a catastrophe-inducing protein that is upregulated during mitosis might target mitotic cells more specifically. The importance of the precise regulation of microtubule dynamics in mitosis is underscored by the observation that at least one destabilizing protein, Op18, is upregulated in cancer cells.

However, genetic and functional depletion data present a pessimistic forecast for microtubule destabilizers as targets for cell cycle inhibitors. Inhibition of microtubule destabilization leads more often to abnormal chromosome segregation than to mitotic arrest.

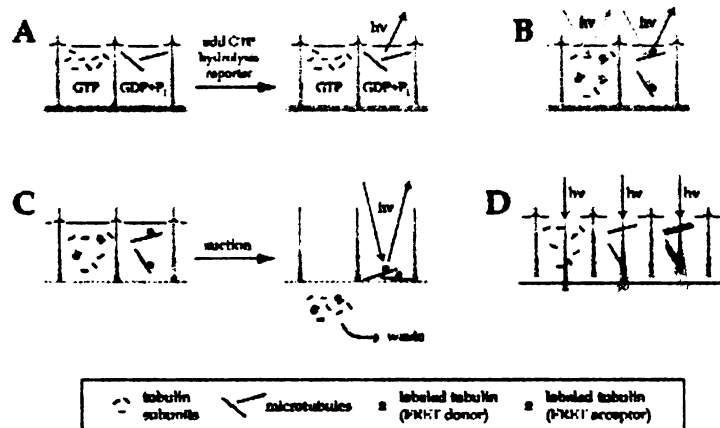
Destabilizers	Key Homologues	Metaphase Localization	Metaphase Function	Inhibition gives Mitotic Arrest?
				
MCAK [KNL6] (80 kDa)	KIF2A/2C ( <i>Mm</i> ); XKCM1[XKIF2] ( <i>Xl</i> )		MT catastrophe	N
Op18 [stathmin,p18, p19, prosolin, metablastin] (18 kDa)	Op18 ( <i>Mm</i> , <i>Xl</i> )		?	N
Katanin (60 kDa/80 kDa)	katanin ( <i>Mm</i> , <i>Dm</i> , <i>Xl</i> , <i>Spu</i> ); Mei1/2 ( <i>Ce</i> ); Erh3/Fra2[Atktn] ( <i>At</i> )		MT severing at poles?	N
<b>Stabilizers</b>				
ChTOG (218 kDa)	XMAP215 ( <i>Xl</i> ); Msp2( <i>Dm</i> ); Zyg9 ( <i>Ce</i> ); Stu2 ( <i>Sc</i> ); Dis1/Mtc1[Alp14] ( <i>Spo</i> )		MT growth MT rescue	Y?
EB1 (35 kDa)	EB1 ( <i>Mm</i> , <i>Xl</i> ); Bim1 ( <i>Sc</i> )		MT growth ? MT targeting ?	N
<b>plus end motors</b>				
Eg5 [KNL1,KSP] (120 kDa) [BimC family]	KIF11 ( <i>Mm</i> ); Eg5[KNL1] ( <i>Xl</i> ) KLP61F/KRP136 ( <i>Dm</i> ) Cin8/Kip1 ( <i>Sc</i> ); Cut7 ( <i>Spo</i> )		pole separation	Y
Hklp2 (160 kDa)	Xklp2 ( <i>Xl</i> ); KRP180 ( <i>Spu</i> )		pole separation ?	N
MKLP1 [CHO1] (100 kDa)	KIF23 ( <i>Mm</i> ); CHO1 ( <i>Cg</i> , <i>Xl</i> ); Pavarotti ( <i>Dm</i> ); Zen4 ( <i>Ce</i> )		?	Y?
CENP-E (312 kDa)	CENP-E ( <i>Xl</i> ); CENP-meta ( <i>Dm</i> )		kinetochore attachment	Y
<b>minus end motors</b>				
HSET [KNL2] (75/80 kDa) [Kar3 family]	KIFC1/C4/C5A ( <i>Mm</i> ) CHO2 ( <i>Cg</i> ); XCTK2 ( <i>Xl</i> ); Ncd ( <i>Dm</i> ); Kar3 ( <i>Sc</i> ); Klp2/Pkl1 ( <i>Spo</i> ); KLP4 ( <i>An</i> )		pole focusing spindle length? K-fiber bundling? intraspindle trafficking?	N
Cytoplasmic Dynein (~2 MDa)	dynein ( <i>eukaryotes</i> ...)		pole focusing kinetochore attachment cortical attachment intraspindle trafficking checkpoint inactivation	Y

**Table 1. Some potential drug targets in the spindle.** Square brackets denote alternate naming conventions, slashes denote homologues within same organism. Localization and Function columns reflect observations in mammalian cells if known, and *Xenopus* egg extract otherwise. The Mitotic Arrest column gives the end result of inhibition. *Mm*=*Mus musculus*; *Cg*=*Cricetulus griseus*; *Xl*=*Xenopus laevis*; *Dm*=*Drosophila melanogaster*; *Ce*=*Caenorhabditis elegans*; *Spu*=*Strongylocentrotus purpuratus*; *Sc*=*Saccharomyces cerevisiae*; *Spo*=*Schizosaccharomyces pombe*; *An*=*Aspergillus nidulans*; *At*=*Arabidopsis thalianus*.

We might speculate that this is because endogenous microtubule destabilizers may influence microtubules only at specific times or places. Another possibility is that many of these dynamics regulators may have a direct role in the spindle checkpoint mechanism.

Although inhibitors of a microtubule regulating protein may not cause mitotic arrest, they might act synergistically with anti-tubulin drugs. For example, inhibition of Op18, a destabilizer that will be discussed in this section, does not cause mitotic arrest but does appear to make cells more sensitive to the anti-mitotic effects of low doses of paclitaxel (11).

We discuss three destabilizers in depth: XKCM1, katanin, and Op18. Destabilizers that we do not discuss in detail include EF-1 $\alpha$ , for which a reported microtubule severing activity is now widely believed to be an artifactual consequence of bundling activity (12); ELP70, reported to decrease polymerization rate and increase catastrophe frequency (13); and tubulin folding co-factor D, a reported tubulin-sequestering protein whose mitotic implications remain unclear (14). For each of the proteins we discuss below, *in vivo* or *in vitro* screens assaying the polymerization state of microtubules are reasonable options, although anecdotal



**Figure 3.** Several assays that measure the activity of microtubule regulators can be adapted to a high throughput format in multi-well plates. Many assays make use of the well established protocols for fluorescent labeling of purified tubulin (for protocols, see <http://mitchison.med.harvard.edu/Protocols.htm>). Depicted here are cross-sections of two or more wells in which microtubule polymerization state is reported by: **A.** GTP hydrolysis; **B.** fluorescence resonance energy transfer (FRET); **C.** microtubules separated from tubulin subunits by filtration; or **D.** light scattering. As depicted, the light scattering can also be used to assay for microtubule bundling activity.

evidence suggests that the overwhelming majority of positives will end up being drugs that directly stabilize microtubules. *In vitro* assays amenable to high-throughput screening include those relying on GTP hydrolysis, FRET (fluorescence resonance energy transfer) between tubulin monomers, light scattering, and determination of polymer concentration by filtration assays (Figure 3). Where possible, we suggest alternative screens that exploit characteristics specific to each protein.

**MCAK (XKCM1) is a catastrophe factor involved in spindle assembly, but its inhibition does not lead to mitotic arrest.**

The mitotic Kin I kinesins have central motor domains and induce microtubule catastrophe. The best-studied members of this family are MCAK (mammalian centromere-associated kinesin) and its homologue XKCM1 (*Xenopus* kinesin central motor 1) (15, 16). In most systems, these proteins localize prominently to centromeres (17), though XKCM1 also shows general spindle microtubule localization (18). XKCM1 is believed to be responsible for high mitotic catastrophe rates in *Xenopus* egg extracts, and immunodepletion from that system results in long stable microtubules and total inhibition of spindle assembly (18).

However, inhibition of MCAK in cultured hamster ovary cells does not result in mitotic arrest. Instead, these cells assemble normal-looking spindles and undergo defective chromosome segregation (19). The lack of obvious changes in microtubule polymerization and distribution may be due to MCAK's specific localization to the centromere, where microtubule depolymerization appears to be important for chromosome movement, either in congression to the metaphase plate or during anaphase segregation. Small-molecule inhibitors of

MCAK might also affect non-mitotic cells, since MCAK appears to be active throughout the cell cycle (20).

With all these caveats, MCAK remains one of the more important microtubule destabilizers discovered to date and would probably be one of the simplest to screen *in vitro*. As will be discussed, kinesins represent a particularly tractable class of screening targets. Practical advantages of MCAK include the fact that baculovirus-expressed, active protein can easily be purified from Sf9 cells (16). The protein has high specific activity and can induce catastrophe in taxol-stabilized microtubules, which are easier to work with than dynamic microtubules.

**Katanin is a well-characterized microtubule severing protein complex with no clear mitotic role.**

The name of this p60/p80 protein complex as "katanin" is derived from - Japanese for "sword" - because it severs microtubules along their lengths (21). The complex localizes to centrosomes throughout the cell cycle (22) and current evidence suggests that katanin severs microtubules at the centrosome to allow microtubule redistribution or disassembly.

A katanin inhibitor would not be likely to produce mitotic arrest. In mammalian tissue culture cells, inhibition of katanin's severing activity does not affect spindle assembly and function (23). Katanin inhibitors might also have adverse effects on postmitotic cells, particularly neurons (24), where the complex appears to have a role in microtubule distribution. Mutations in a katanin-related human protein (spastin) are associated with a neuronal disease, hereditary spastic paraplegia (25).

For screening purposes, the *in vitro* microtubule severing assay used to purify katanin would not be easily adapted to a high-throughput screening format and katanin inhibition does not have a phenotype

strong enough for screening in tissue culture cells. However, the ATPase activity of katanin might be exploited in a high-throughput assay. Another assay is suggested by the observation that mutation of katanin homologues inhibits proper development and cell wall biosynthesis in plants (26, 27) and disrupts meiosis in *C. elegans* (28). If one were interested in inhibiting cell development in plants or fertility in worms (*i.e.*, for anti-helminthic drugs), phenotypic screens using those organisms might potentially uncover a katanin inhibitor.

**Op18 is a catastrophe factor that also sequesters tubulin monomers, and its inactivation is required for cell cycle progression.**

This oncoprotein of 18 kD is upregulated in several types of cancer (29) and undergoes complex phosphoregulation at multiple sites, both in response to extracellular signals (30) and during the cell cycle (29). Op18 is mostly cytoplasmic throughout the cell cycle, although it is enriched at spindle poles during mitosis (31). The protein has two distinct microtubule-destabilizing domains, one that promotes catastrophe and one that sequesters tubulin monomers (32). Op18 is expressed in most dividing cells as well as neurons, where it appears to be involved in differentiation (33).

While it is tempting to view Op18 as a link between upregulated microtubule destabilization and the increased cell proliferation seen in tumorigenesis, the majority of work to date implicates a role for Op18 activity in interphase, not mitosis (20). Inhibition of Op18 using either RNAi (11) or antibody microinjection (34) does not result in mitotic arrest. Intriguingly, however, cells subjected to both Op18 RNAi and paclitaxel treatment were arrested at lower doses of paclitaxel than control cells, indicating that inhibition of Op18 may sensitize cells to mitotic arrest by paclitaxel (32).

It is possible that activators of Op18 or inhibitors of Op18 inactivation might be effective anti-mitotics. Phosphorylation and inactivation of Op18 have been shown to be required for proper cell cycle progression (29). The reasons for this are not clear, although they are presumed to be due to effects on microtubule dynamics. As an example of the latter, Op18 inactivation has been hypothesized to have a role in microtubule stabilization near chromatin (35, 36). A recent report further suggests that Op18 dephosphorylation and activation may be necessary for spindle disassembly and exit from mitosis (37). Though it is currently difficult to predict whether or not inhibitors or activators of Op18 would constitute effective anti-mitotics, the complex regulation and behavior of this protein in cells is clearly interesting and potentially relevant to anti-cancer research.

The co-crystal structure of Op18 and tubulin suggests that it might be difficult to disrupt their interaction with a small molecule, since the two proteins interact through a very large interface (38). Alternatively, one could screen for drugs that cause changes in the phosphorylation state of Op18.

## MICROTUBULE DYNAMICS REGULATORS: STABILIZERS

Most stabilizing MAPs (microtubule-associated proteins) would not be expected to be ideal targets for anti-mitotic drugs. During mitosis, MAPs are generally phosphorylated, which is associated with both decreased microtubule binding affinity and decreased stabilizing activity (39). Inhibition of these proteins would therefore probably not affect mitotic cell cycle progression. However, drugs that activate MAPs or inhibit MAP phosphorylation might inappropriately stabilize microtubules during mitosis and induce mitotic arrest themselves or enhance the effects of microtubule stabilizing drugs like paclitaxel. In human tissue culture cells, transfection of the microtubule stabilizer MAP4 with mutated putative cdc2 phosphorylation sites leads to slowed cell cycle progression and increased microtubule stability (40). Cdc2 is a general cell cycle regulator, but the existence of the microtubule-specific kinase MARK (MAP/microtubule affinity-regulating kinase, also called par-1) suggests that more specific inhibition may be possible (41). Inhibition of a kinase like MARK might have the further advantage of simultaneously activating many MAPs of potentially redundant function.

Though we recognize the potential for microtubule stabilizing proteins as drug targets, we discuss only one, ch-TOG, in detail. Of the known microtubule-stabilizing proteins, ch-TOG has the best-characterized mitotic phenotype. Ch-TOG/XMAP215 appears to play a complex and important role in mitosis, counterbalancing the microtubule destabilizer MCAK/XKCM1 (42). In fact, it was recently demonstrated that combining appropriate concentrations of XMAP215 and XKCM1 alone is sufficient to produce *in vitro* microtubule dynamics quantitatively similar to those seen *in vivo* (43).

Other stabilizers that may play a role in mitosis include EB1, a plus end-binding protein that affects mitotic dynamics and spindle positioning in yeast (44); APC (adenomatous polyposis coli), a plus end-binding protein often mutated in colon cancer that binds EB1 and enhances its polymerization activity (45); and orbit, mutation of which in *Drosophila* results in spindle assembly defects and polyploidy (46). The human homologues of orbit, the CLASPs (Clip-170 Associated Proteins), have not been examined for a role in mitosis. These are all potentially interesting proteins and we eagerly await further information on their role in mitosis.

**ch-TOG increases microtubule growth and dynamics and its inhibition may result in mitotic arrest.**

ch-TOG (colonic hepatic tumor overexpressed gene) and its well-characterized homologue XMAP215 (*Xenopus* microtubule-associated protein of 215 kD) appear to play key roles in mitosis by stabilizing microtubules. ch-TOG differs from simple stabilizers in making microtubules not only longer but also more dynamic (47). ch-TOG localizes to centrosomes during mitosis in most model organisms. In some organisms, like *Xenopus* and *Drosophila*, the protein also localizes

more generally to spindle microtubules (48, 49) and in others, like fission and budding yeast, appears to be enriched on microtubules near the kinetochores (50-52). It has been hypothesized that ch-TOG stabilizes short nascent microtubules at the centrosome, thus spatially restricting microtubule growth to the poles and possibly playing a role in spindle pole focusing.

Ch-TOG may be an attractive target for anti-mitotic drugs for several reasons. First, from genetic and functional depletion data available in frog, fly, yeast, and worm, we know that ch-TOG plays an important and complex role in spindle assembly. The two most common phenotypes of ch-TOG inhibition are short, destabilized microtubules and defects in spindle pole formation (53). Its localization to poles is apparently important for function—mutations in proteins that localize ch-TOG such as D-TACC (54) or *ncd* (55) result in phenotypes consistent with microtubule destabilization. Second, mutations in at least one homologue, mini-spindles in *Drosophila*, lead to mitotic arrest (49). A small-molecule inhibitor of this ch-TOG might further be valuable as a tool for understanding the etiology of the colonic and hepatic cancers in which the protein is overexpressed (56).

Like most MAPs, XMAP215 is phosphorylated in mitosis and more active in interphase (39). However, although interphase microtubule defects occur in plant and yeast ch-TOG mutations (57, 58), interphase defects have not been reported upon inhibition in animal cells. It is possible that inhibition of the interphase activity of ch-TOG results in centrosome duplication defects or abnormalities in centrosome structure that become apparent only in mitosis.

High-throughput screens for inhibitors of ch-TOG *in vitro* might make use of the same assays of microtubule polymerization described earlier for destabilizers. *In vivo* assays are also possible (screening for short microtubules or small spindles) but would undoubtedly yield a large number of drugs that target tubulin.

#### MICROTUBULE MOTOR PROTEINS

Control of microtubule dynamics alone is not sufficient to organize microtubules into a bipolar mitotic spindle. Microtubule motor proteins, structural proteins, and microtubule nucleating proteins are also necessary for the complex rearrangements underlying spindle assembly and function. For a number of reasons, we believe that motors are particularly amenable to inhibition by small molecules. First, inhibitors of enzymatic activity have historically been easier to find than inhibitors of protein-protein interactions (for a rare counterexample, see (59).) It may thus be easier to block the ATPase activity of motor proteins than the protein-protein interactions involved in structural protein function and microtubule nucleation. Second, the global conformational changes intrinsic to motor function may increase the probability of finding allosteric inhibitors — that is, small molecules that act by stabilizing a particular conformation and thereby prevent motion necessary for the function of the motor (for

examples of this principle in a variety of proteins, see (60-63)). Finally, as will be discussed, small molecules have already been found that prevent the motor activity of the kinesin Eg5 without affecting the activity of other kinesins. This demonstrates that although the motor domain is highly conserved, it can be specifically inhibited.

The inhibition of many mitotic motors results in mitotic arrest (Table 1 and Figure 2). Of particular interest are motors responsible for spindle pole separation and maintenance of spindle bipolarity. When these motors are inhibited, spindle poles collapse together, resulting in a monoaster, a radial array of microtubules. This phenotype is often accompanied by mitotic arrest. Two motors implicated in spindle bipolarity, Eg5 and Xklp2, are reviewed below. Inhibition of the motors responsible for kinetochore attachment, kinetochore fiber formation, or spindle checkpoint inactivation can also lead to mitotic arrest. We discuss in detail two such motors, CENP-E and cytoplasmic dynein.

As mentioned in the introduction, there is some risk associated with targeting the activities of the mitotic spindle. Disruption of some mitotic motors involved in spindle assembly may give rise to aneuploidy without mitotic arrest (Figure 2). For example, we discuss below the motor protein HSET, a kinesin involved in spindle pole focusing. Inhibition of this protein results in sparse bipolar spindles or multipolar microtubule arrays, both of which can result in chromosome missegregation.

The motors of this section are grouped according to the direction in which they appear to walk along microtubules *in vitro*. Eg5, Xklp2, MKLP1 and CENP-E are all plus end-directed kinesins. In addition to their other functions, each appears to mediate the interaction of antiparallel microtubules in metaphase or anaphase. HSET and cytoplasmic dynein are both minus end-directed motors help to focus spindle poles. In assessing these motors as potential anti-mitotic drug targets, we review their roles in mitosis and interphase and highlight the effects of their inhibition on mitotic progression.

#### Eg5 is required for spindle bipolarity and its inhibition leads to mitotic arrest.

Eg5, a member of the BimC (blocked in mitosis) family of plus end-directed kinesins, is a key motor in the establishment of spindle bipolarity (64). These BimC proteins form bipolar homotetramers with motor domains positioned on opposite ends of a central rod, suggesting an ability to crosslink and slide apart antiparallel microtubules (65). Eg5 localizes to spindle microtubules and is involved in spindle pole separation and production of the bipolar spindle in many organisms including humans (66). Microinjection of inhibitory antibodies into HeLa cells results in monoasters and mitotic arrest (67, 68).

Based on our current understanding, we would not expect an inhibitor of Eg5 to affect interphase cells. The presence of Eg5 in post-mitotic neurons has led to speculation that Eg5 and other mitotic motor proteins may play roles in axonal elongation and retraction (69,

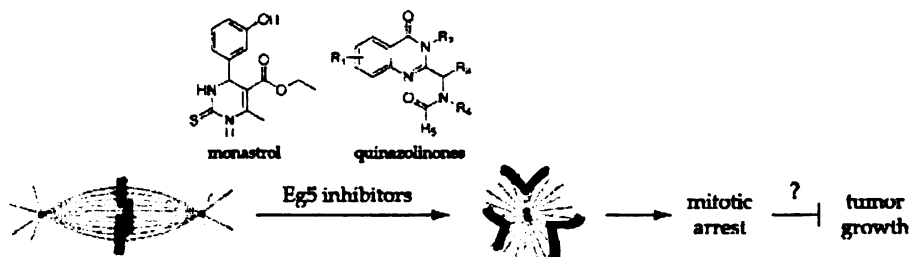


Figure 4. Small molecule inhibitors of Eg5 result in monoastral mitotic figures and mitotic arrest.

70). However, no functional evidence has yet been published to support this hypothesis. Eg5 itself appears to be tightly regulated through the cell cycle. In interphase cells, Eg5 is diffusely cytoplasmic and a conserved putative site of phosphorylation by the mitotic kinase cdc2 appears to be necessary for localization to the mitotic spindle (66, 67).

A number of specific small molecule inhibitors of Eg5 have been identified using high-throughput screens (71, 72). In some mammalian cells, these inhibitors cause monoasters very similar to those seen upon antibody inhibition. The first of these compounds was found in a three step screen (71). A high throughput assay detecting cell cycle-dependent nucleolin phosphorylation was initially used to identify compounds that increase the mitotic index of mammalian cells. Visual assays were then performed on the hits from this primary assay to eliminate compounds that perturb tubulin polymerization *in vitro*. Finally, fluorescence microscopy was used to visualize the effects of the remaining compounds on spindle morphology in mammalian cells. The signature phenotype of Eg5 inhibition was observed for a 1,4-dihydropyrimidine-based compound (Figure 4) which was confirmed to inhibit Eg5 in an *in vitro* microtubule gliding assay. This compound, monastrol, does not inhibit the *in vitro* motility of conventional kinesin and does not disrupt the cellular localization of lysosomes or the Golgi in interphase cells, indicating that the kinesins involved in the localization of these organelles are not perturbed.

Recent meeting abstracts report the identification of a broad class of quinazolinone Eg5 inhibitors (Figure 4) (72). One of these, a 2-(aminomethyl) quinazolinone, appears to have broad spectrum activity against murine solid tumors and human colon tumor xenografts without causing peripheral neuropathy in mice, and the researchers plan to bring this compound to clinical trials (73). These results suggest that an Eg5 inhibitor can inhibit mitosis without causing undesired side effects in interphase cells even at the organismal level.

**Hk1p2 may be required for bipolarity, but its inhibition may not lead to mitotic arrest.**

The human homologue, Hk1p2, of the plus end-directed *Xenopus* kinesin-like protein Xk1p2 (74) remains poorly characterized (75). Xk1p2 is concentrated on centrosomes throughout the cell cycle, while the

sea urchin homologue KRP180 localizes along astral microtubules in interphase and to the spindle midzone during mitosis (74, 76).

Initial data suggested that Xk1p2 is involved in spindle pole separation and the establishment of spindle bipolarity. A putative dominant negative Xk1p2 truncation construct prevented spindle pole separation in *Xenopus* egg extracts (74). Both this construct and inhibitory antibodies led to dramatic inward collapse of the spindle poles in sea urchin embryos (76). However, immunodepletion of Xk1p2 from *Xenopus* egg extracts does not perturb cycled spindle assembly (77) and allows normal bipolar spindles to form around chromatin beads (78). Given these contradictory results, it is difficult to assess the role of Xk1p2 in the establishment or maintenance of spindle bipolarity.

The majority of sea urchin embryos in the above inhibition studies proceed into anaphase with normal timing, suggesting that Xk1p2 may not be a good antimitotic drug target even if it does play a role in spindle bipolarity (76).

**MKLP1 has a poorly understood role in mitosis, but its inhibition has been reported to cause mitotic arrest.**

Early work on this family of plus end-directed kinesins suggested a role in anaphase spindle elongation. However, the bulk of genetic evidence points to an important role in cytokinesis. Human MKLP1 (mammalian kinesin-like protein 1) is localized to centrosomes and nuclei during interphase, to the midzone microtubules during anaphase, and eventually at the midbody during telophase. *In vitro*, it can bundle and slide apart antiparallel microtubules in an ATP-dependent fashion (79).

Inhibition of MKLP1 in mammalian cells and sea urchin embryos by antibody microinjection causes mitotic arrest with apparently normal metaphase spindles (80, 81). However, in subsequent genetic studies, disruption or deletion of the *C. elegans* and *Drosophila* homologues did not cause mitotic arrest and instead led to failures in cytokinesis, giving rise to multinucleate cells (82, 83). This discrepancy has not been resolved, although an intriguing recent report shows that at least two alternative splice products exist in the mitotic cell and may have different inhibition phenotypes (84).



Inhibitors of MKLP1 may disrupt the structure and function of some specialized postmitotic cells. Several interphase functions have been identified for MKLP1, including the formation of major processes in podocytes and the establishment of dendritic identity in neurons (85, 86). In both cases, MKLP1 helps to establish an antiparallel microtubule array in these specialized cellular processes. If MKLP1 is pursued as an anti-mitotic drug target, the phenotypes of metaphase arrest or multinucleate cells observed with its inhibition might readily lend themselves to image-based phenotypic screening. The *in vitro* bundling activity of MKLP1 might also be exploited for high-throughput screening using a light scattering assay (Figure 3).

**CENP-E is necessary for chromosome alignment and spindle checkpoint signaling, and its inhibition leads to mitotic arrest.**

This kinesin-like centromere-associated protein is a plus end-directed kinesin with a second microtubule-binding site in addition to that of the motor domain (87-89). CENP-E associates with kinetochores upon nuclear envelope breakdown and remains there until anaphase, when it rapidly relocates to the midzone (87, 90).

We believe that CENP-E is a particularly attractive candidate drug target. Inhibition of CENP-E (in mammalian cells) results in a strong mitotic arrest, as demonstrated by antibody microinjection or antisense experiments (91, 92). CENP-E has been implicated in a number of important spindle events. It is necessary for bioriented attachment of chromosomes and subsequent alignment of chromosomes at the metaphase plate (88, 91, 93, 94). A direct functional role for CENP-E in these processes is further supported by *in vitro* studies demonstrating that CENP-E can couple chromosome movement to microtubule depolymerization (90). As discussed in Chapter 43, CENP-E also interacts with spindle checkpoint proteins at the kinetochore and appears to be an essential component of the checkpoint, although the detailed mechanism of its function remains unclear (91, 95). Finally, additional anaphase function is suggested by its paired microtubule binding sites and the changes in its phosphorylation and localization at anaphase onset (89, 90). Adding to its attractiveness as a potential drug target, CENP-E does not appear to have any role in interphase or postmitotic cells, and it is degraded at the end of mitosis (87).

In addition to the conventional screens for motor activity, an interesting possible screening strategy may be suggested by the observation that CENP-E has a CAAX box and is farnesylated. Since farnesyl transferase inhibitors often arrest cells in mitosis with misaligned chromosomes, it is possible that CENP-E is one of the true targets of this actively pursued class of anti-tumor agents (96, 97).

**HSET is necessary for spindle pole focusing, and its inhibition does not result in mitotic arrest.**

HSET (human spleen, embryonic tissue and testes) is a member of the Kar3p (*karyogamy* defects during mating) family of minus end-directed motors. This

family appears to play a highly conserved role in spindle pole focusing and spindle length determination. In eukaryotes, this protein localizes to spindle poles and spindle microtubules (98-101) and electron microscopy suggests that HSET localizes between microtubules in parallel bundles (101).

Inhibition of HSET does not induce mitotic arrest or any obvious spindle defects in mammalian cells (101). This differs from the spindle pole defects and chromosome segregation problems resulting from inhibition of the best-characterized metazoan homologue, the *Drosophila* protein Ncd (*Non-claret disjunction*, after its role in chromosome disjunction and proximity to the claret locus.) Interestingly, inhibition of Kar3p family members in human, fruit fly and fungus rescues the loss of spindle bipolarity that accompanies inhibition of Eg5 (101-103). No interphase role has been shown for members of this family, although they remain present throughout the cell cycle (104, 105).

HSET may have a from a cross-linking function or may play a role in trafficking of spindle components. Ncd has recently been shown to be necessary for the polar localization of the *Drosophila* ch-TOG homologue Msp5 (55), which might suggest that HSET inhibition might synergize with inhibition of ch-TOG.

**Cytoplasmic dynein has multiple roles in mitosis, and its inhibition leads to mitotic arrest.**

Cytoplasmic dynein in mammalian cells is a complex of two heavy chains, three intermediate chains, and four light chains (106), with multiple isoforms of each chain present in most model organisms (107). The complex is so named to distinguish it from flagellar dynein. The genetic or biochemical differences distinguishing cytoplasmic and flagellar dynein remain poorly understood. The functional cytoplasmic dynein complex appears to require association with another large complex, the *dynein activator* dynactin (108).

Cytoplasmic dynein deserves attention as a potential drug target because its inhibition results in mitotic arrest (109). Dynein is essential in higher eukaryotic mitosis and its inhibition results in mitotic arrest. The complex localizes at the nuclear envelope in early prophase in mammalian cells, and later at the cortex and on spindle poles, microtubules, and kinetochores in a wide range of organisms (110). In mammalian cells, dynein has been shown to be necessary for multiple events in mitosis, including spindle positioning, pole focusing, proper localization of pole and kinetochore components, and the delocalization of spindle checkpoint proteins after proper attachment of kinetochores to microtubules. It is also implicated in the poleward movement of chromosomes during spindle assembly and anaphase (111-116).

Cytoplasmic dynein is also important in interphase cells, playing major roles in ER and Golgi trafficking and assembly (111). However, dynein null yeast are viable, showing only mild spindle positioning and chromosome separation defects (117). At the organismal level, dynein is likely to play a number of

important developmental roles tied to spindle positioning (118) and vesicle transport (111). Another risk of targeting cytoplasmic dynein is that inhibition of flagellar dynein results in infertility, respiratory disorders, and *situs invertus* (119). The development of dynein as a therapeutic target may require better understanding of its differential regulation in the cell.

Since recombinant expression of a functional dynein-dynactin complex may prove difficult, *in vitro* screens will likely require biochemically purified complex. The ATPase activity of dynein purified from bovine brain was reported to have a  $V_{max}$  an order of magnitude lower than that of conventional kinesin (120), so an *in vitro* ATPase assay will require sensitive detection. Cell-based phenotypic assays may prove necessary in the search for dynein inhibitors.

#### CONCLUSION

The mitotic spindle is a complex, dynamic structure. The morphogenesis and organization of which we are just beginning to understand at the molecular level. The success of paclitaxel and the vinca alkaloids as anti-mitotic drugs highlights the vulnerability of the spindle as a drug target. The possibility that inhibitors of proteins that regulate microtubule dynamics and organization may also be effective anti-mitotics remains largely unexplored.

Predicting the clinical efficacy or toxicity of targeting these proteins is impossible from basic cell biology, but we can point to certain properties that suggest their potential as viable drug targets. Many of the proteins we have discussed in this chapter are regulated or degraded by the cell cycle machinery, suggesting that these may allow specific targeting of dividing cells. Inhibition of many of these proteins in a number of model systems results in a mitotic arrest promisingly similar to that obtained by anti-mitotic drugs that directly target microtubules.

Inhibition of other proteins discussed in this chapter does not lead to mitotic arrest. However, as has been suggested in the case of Op18, inhibitors of these proteins may act in synergy with anti-tubulin drugs. Such a synergy might both produce more effective mitotic arrest and lower the individual doses required for therapeutic efficacy, minimizing adverse effects. The strategy of combination therapy has been successfully applied to the treatment of bacterial infection, HIV, and many types of cancer (121).

Throughout this chapter, we have attempted to assess the potential of microtubule regulators as candidate drug targets by examining their known functions in mitosis and highlighting the effects of their inhibition on cell cycle progression. As the example of Eg5 shows, improvements in our understanding of the cell biology of mitosis continue to suggest new targets for anti-mitotic drugs.

#### ACKNOWLEDGEMENTS

We thank Ann Yonetani, Alina Vrabioiu, and Zoltan Maliga for reviewing this manuscript. We are

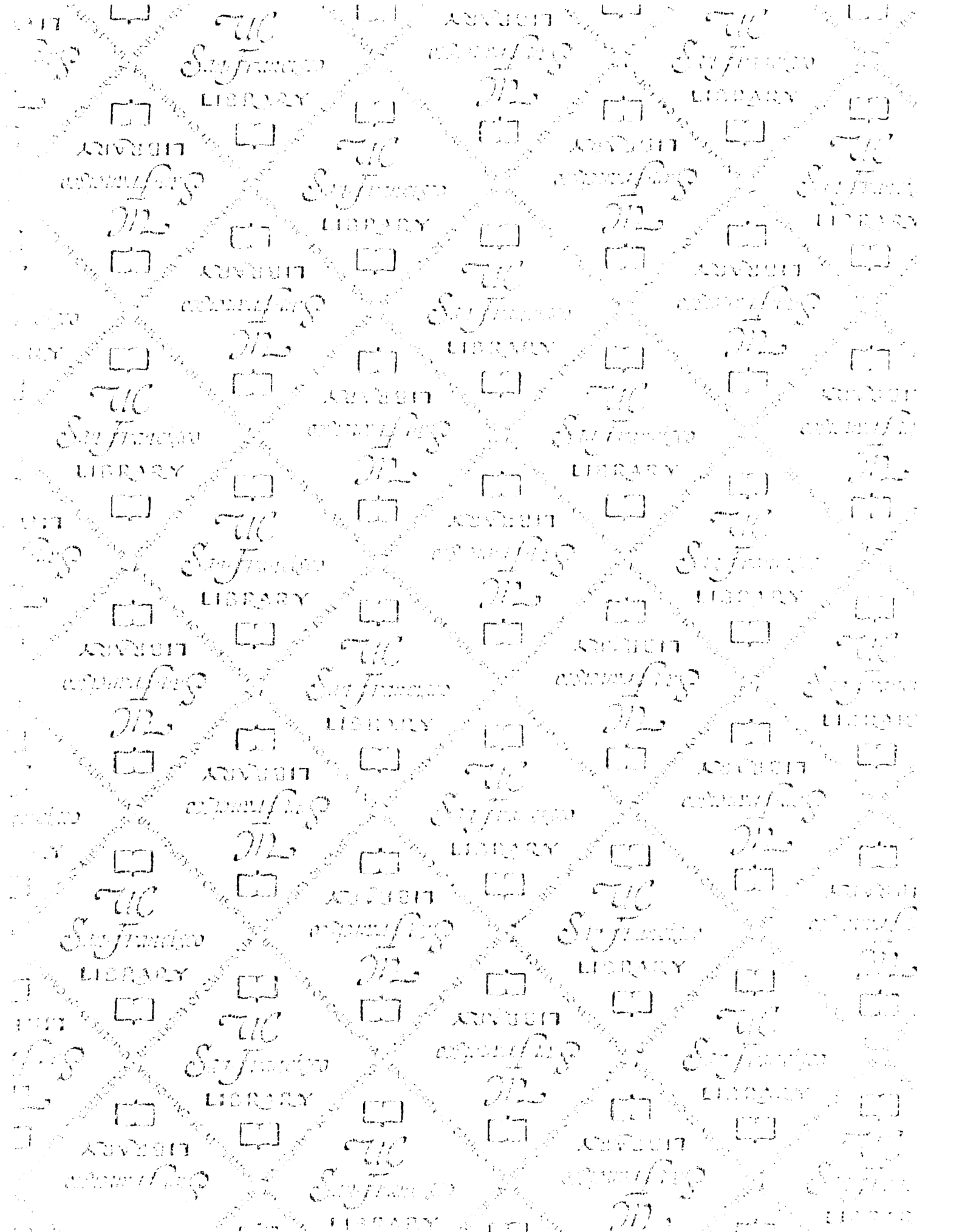
especially grateful to Dr. Jennifer Tirnauer for generously and thoughtfully reviewing multiple drafts of this manuscript and for her insightful suggestions. We thank all members of the Mitchison lab for their help and support. T.J.M. is supported by grants from the NIH. D.T.M. and Z.E.P. are Howard Hughes Medical Institute Predoctoral Fellows.

#### REFERENCES

- Mitchison, T. J. and Salmon, E. D. (2001) *Nat Cell Biol* 3, E17-21.
- Cavaletti, G., Cavalletti, E., Montaguti, P., Oggioni, N., De Negri, O. and Tredici, G. (1997) *Neurotoxicology* 18, 137-145.
- Desai, A. and Mitchison, T. J. (1997) *Annu Rev Cell Dev Biol* 13, 83-117.
- Belmont, L. D., Hyman, A. A., Sawin, K. E. and Mitchison, T. J. (1990) *Cell* 62, 579-589.
- Gliksman, N. R., Parsons, S. F. and Salmon, E. D. (1992) *J Cell Biol* 119, 1271-1276.
- Rusan, N. M., Fagerstrom, C. J., Yvon, A. M. and Wadsworth, P. (2001) *Mol Biol Cell* 12, 971-980.
- Jordan, M. A. and Wilson, L. (1998) *Methods Enzymol* 298, 252-276.
- Compton, D. A. (2000) *Annu. Rev Biochem* 69, 95-114.
- Jallepalli, P. V. and Lengauer, C. (2001) *Nature Rev Cancer* 1, 109-117.
- Gilbert, S. P. and Mackey, A. T. (2000) *Methods* 22, 337-354.
- Iancu, C., Mistry, S. J., Arkin, S., Wallenstein, S. and Atweh, G. F. (2001) *J Cell Sci* 114, 909-916.
- Moore, R. C., Durso, N. A. and Cyr, R. J. (1998) *Cell Motil Cytoskeleton* 41, 168-180.
- Eichenmuller, B., Everley, P., Palange, J., Lepley, D. and Suprenant, K. A. (2002) *J Biol Chem* 277, 1301-1309.
- Martin, L., Fanarraga, M. L., Aloria, K. and Zabala, J. C. (2000) *FEBS Lett* 470, 93-95.
- Maney, T., Wagenbach, M. and Wordeman, L. (2001) *J Biol Chem* 276, 34753-34758.
- Desai, A., Verma, S., Mitchison, T. J. and Walczak, C. E. (1999) *Cell* 96, 69-78.
- Wordeman, L. and Mitchison, T. J. (1995) *J Cell Biol* 128, 95-104.
- Walczak, C. E., Mitchison, T. J. and Desai, A. (1996) *Cell* 84, 37-47.
- Maney, T., Hunter, A. W., Wagenbach, M. and Wordeman, L. (1998) *J Cell Biol* 142, 787-801.
- Andersen, S. S. (2000) *Trends Cell Biol* 10, 261-267.
- McNally, F. J. and Vale, R. D. (1993) *Cell* 75, 419-429.
- McNally, F. J., Okawa, K., Iwamatsu, A. and Vale, R. D. (1996) *J Cell Sci* 109, 561-567.
- Buster, D., McNally, K. and McNally, F. J. (2002) *J Cell Sci* 115, 1083-1092.
- Ahmad, F. J., Yu, W., McNally, F. J. and Baas, P. W. (1999) *J Cell Biol* 145, 305-315.
- Errico, A., Ballabio, A. and Rugarli, E. I. (2002)

- Hum Mol Genet* 11, 153-163.
26. Burk, D. H., Liu, B., Zhong, R., Morrison, W. H. and Ye, Z. H. (2001) *Plant Cell* 13, 807-827.
  27. Webb, M., Jouannic, S., Foreman, J., Linstead, P. and Dolan, L. (2002) *Development* 129, 123-131.
  28. Srayko, M., Buster, D. W., Bazirgan, O. A., McNally, F. J. and Mains, P. E. (2000) *Genes Dev* 14, 1072-1084.
  29. Cassimeris, L. (2002) *Curr Opin Cell Biol* 14, 18-24.
  30. Sobel, A. (1991) *Trends Biochem Sci* 16, 301-305.
  31. Gavet, O., Ozon, S., Manceau, V., Lawler, S., Curmi, P. and Sobel, A. (1998) *J Cell Sci* 111, 3333-3346.
  32. Howell, B., Larsson, N., Gullberg, M. and Cassimeris, L. (1999) *Mol Biol Cell* 10, 105-118.
  33. Di Paolo, G., Pellier, V., Catsicas, M., Antonsson, B., Catsicas, S. and Grenningloh, G. (1996) *J Cell Biol* 133, 1383-1390.
  34. Howell, B., Deacon, H. and Cassimeris, L. (1999) *J Cell Sci* 112, 3713-3722.
  35. Andersen, S. S., Ashford, A. J., Tournebize, R., Gavet, O., Sobel, A., Hyman, A. A. and Karsenti, E. (1997) *Nature* 389, 640-643.
  36. Budde, P. P., Kumagai, A., Dunphy, W. G. and Heald, R. (2001) *J Cell Biol* 153, 149-158.
  37. Mistry, S. J. and Atweh, G. F. (2001) *J Biol Chem* 276, 31209-31215.
  38. Gigant, B., Curmi, P. A., Martin-Barbey, C., Charbaut, E., Lachkar, S., Lebeau, L., Siavoshian, S., Sobel, A. and Knossow, M. (2000) *Cell* 102, 809-816.
  39. Andersen, S. S. (1998) *Cell Motil Cytoskeleton* 41, 202-213.
  40. Chang, W., Gruber, D., Chari, S., Kitazawa, H., Hamazumi, Y., Hisanaga, S. and Bulinski, J. C. (2001) *J Cell Sci* 114, 2879-2887.
  41. Drewes, G., Ebneith, A., Preuss, U., Mandelkow, E. M. and Mandelkow, E. (1997) *Cell* 89, 297-308.
  42. Tournebize, R., Popov, A., Kinoshita, K., Ashford, A. J., Rybina, S., Pozniakovskiy, A., Mayer, T. U., Walczak, C. E., Karsenti, E. and Hyman, A. A. (2000) *Nat Cell Biol* 2, 13-19.
  43. Kinoshita, K., Arnal, I., Desai, A., Drechsel, D. N. and Hyman, A. A. (2001) *Science* 294, 1340-1343.
  44. Tirnauer, J. S. and Bierer, B. E. (2000) *J Cell Biol* 149, 761-766.
  45. Nakamura, M., Zhou, X. Z. and Lu, K. P. (2001) *Curr Biol* 11, 1062-1067.
  46. Inoue, Y. H., do Carmo Avides, M., Shiraki, M., Deak, P., Yamaguchi, M., Nishimoto, Y., Matsukage, A. and Glover, D. M. (2000) *J Cell Biol* 149, 153-166.
  47. Vasquez, R. J., Gard, D. L. and Cassimeris, L. (1994) *J Cell Biol* 127, 985-993.
  48. Popov, A. V., Pozniakovskiy, A., Arnal, I., Antony, C., Ashford, A. J., Kinoshita, K., Tournebize, R., Hyman, A. A. and Karsenti, E. (2001) *Embo J* 20, 397-410.
  49. Cullen, C. F., Deak, P., Glover, D. M. and Ohkura, H. (1999) *J Cell Biol* 146, 1005-1018.
  50. Nakaseko, Y., Goshima, G., Morishita, J. and Yanagida, M. (2001) *Curr Biol* 11, 537-549.
  51. Garcia, M. A., Vardy, L., Koonrugsa, N. and Toda, T. (2001) *Embo J* 20, 3389-3401.
  52. He, X., Rines, D. R., Espelin, C. W. and Sorger, P. K. (2001) *Cell* 106, 195-206.
  53. Kinoshita, K., Hyman, A.A. (2002) *Trends Biochem Sci* 12, 267-273.
  54. Lee, M. J., Gergely, F., Jeffers, K., Peak-Chew, S. Y. and Raff, J. W. (2001) *Nat Cell Biol* 3, 643-649.
  55. Cullen, C. F. and Ohkura, H. (2001) *Nat Cell Biol* 3, 637-642.
  56. Charrasse, S., Mazel, M., Taviaux, S., Berta, P., Chow, T. and Larroque, C. (1995) *Eur J Biochem* 234, 406-413.
  57. Kosco, K. A., Pearson, C. G., Maddox, P. S., Wang, P. J., Adams, I. R., Salmon, E. D., Bloom, K. and Huffaker, T. C. (2001) *Mol Biol Cell* 12, 2870-2880.
  58. Wasteneys, G. O. (2002) *J Cell Sci* 115, 1345-1354.
  59. Degterev, A., Lugovskoy, A., Cardone, M., Mulley, B., Wagner, G., Mitchison, T. and Yuan, J. (2001) *Nat Cell Biol* 3, 173-182.
  60. Foster, B. A., Coffey, H. A., Morin, M. J. and Rastinejad, F. (1999) *Science* 286, 2507-2510.
  61. McMillan, K., Adler, M., Auld, D. S., Baldwin, J. J., Blasko, E., Browne, L. J., Chelsky, D., Davey, D., Dolle, R. E., Eagen, K. A., Erickson, S., Feldman, R. L., Glaser, C. B., Mallari, C., Morrissey, M. M., Ohlmeyer, M. H., Pan, G., Parkinson, J. F., Phillips, G. B., Polokoff, M. A., Sigal, N. H., Vergona, R., Whitlow, M., Young, T. A. and Devlin, J. J. (2000) *Proc Natl Acad Sci USA* 97, 1506-1511.
  62. Peterson, J. R., Lokey, R. S., Mitchison, T. J. and Kirschner, M. W. (2001) *Proc Natl Acad Sci USA* 98, 10624-10629.
  63. Maliga, Z. K., T.; Mitchison, T. J. *Chemistry & Biology*, submitted.
  64. Enos, A. P. and Morris, N. R. (1990) *Cell* 60, 1019-1027.
  65. Kashina, A. S., Baskin, R. J., Cole, D. G., Wedaman, K. P., Saxton, W. M. and Scholey, J. M. (1996) *Nature* 379, 270-272.
  66. Sawin, K. E. and Mitchison, T. J. (1995) *Proc Natl Acad Sci USA* 92, 4289-4293.
  67. Blangy, A., Lane, H. A., d'Herin, P., Harper, M., Kress, M. and Nigg, E. A. (1995) *Cell* 83, 1159-1169.
  68. Gaglio, T., Saredi, A., Bingham, J. B., Hasbani, M. J., Gill, S. R., Schroer, T. A. and Compton, D. A. (1996) *J Cell Biol* 135, 399-414.
  69. Ferhat, L., Cook, C., Chauviere, M., Harper, M., Kress, M., Lyons, G. E. and Baas, P. W. (1998) *J Neurosci* 18, 7822-7835.
  70. Baas, P. W. and Ahmad, F. J. (2001) *Trends Cell Biol* 11, 244-249.
  71. Mayer, T. U., Kapoor, T. M., Haggarty, S. J., King, R. W., Schreiber, S. L. and Mitchison, T. J. (1999) *Science* 286, 971-974.
  72. Bergens, G., et al. (2002) meeting abstracts, American Association for Cancer Research.

73. Johnson, R. K., *et al.* (2002) meeting abstracts, American Association for Cancer Research, 1335.
74. Boleti, H., Karsenti, E. and Vernos, I. (1996) *Cell* **84**, 49-59.
75. Sueishi, M., Takagi, M. and Yoneda, Y. (2000) *J Biol Chem* **275**, 28888-28892.
76. Rogers, G. C., Chui, K. K., Lee, E. W., Wedaman, K. P., Sharp, D. J., Holland, G., Morris, R. L. and Scholey, J. M. (2000) *J Cell Biol* **150**, 499-512.
77. Wittmann, T., Wilm, M., Karsenti, E. and Vernos, I. (2000) *J Cell Biol* **149**, 1405-1418.
78. Walczak, C. E., Vernos, I., Mitchison, T. J., Karsenti, E. and Heald, R. (1998) *Curr Biol* **8**, 903-913.
79. Nislow, C., Lombillo, V. A., Kuriyama, R. and McIntosh, J. R. (1992) *Nature* **359**, 543-547.
80. Nislow, C., Sellitto, C., Kuriyama, R. and McIntosh, J. R. (1990) *J Cell Biol* **111**, 511-522.
81. Wright, B. D., Terasaki, M. and Scholey, J. M. (1993) *J Cell Biol* **123**, 681-689.
82. Raich, W. B., Moran, A. N., Rothman, J. H. and Hardin, J. (1998) *Mol Biol Cell* **9**, 2037-2049.
83. Adams, R. R., Tavares, A. A., Salzberg, A., Bellen, H. J. and Glover, D. M. (1998) *Genes Dev* **12**, 1483-1494.
84. Kuriyama, R., Gustus, C., Terada, Y., Uetake, Y. and Matulienė, J. (2002) *J Cell Biol* **156**, 783-790.
85. Kobayashi, N., Reiser, J., Kriz, W., Kuriyama, R. and Mundel, P. (1998) *J Cell Biol* **143**, 1961-1970.
86. Yu, W., Cook, C., Sauter, C., Kuriyama, R., Kaplan, P. L. and Baas, P. W. (2000) *J Neurosci* **20**, 5782-5791.
87. Yen, T. J., Li, G., Schaar, B. T., Szilak, I. and Cleveland, D. W. (1992) *Nature* **359**, 536-539.
88. Wood, K. W., Sakowicz, R., Goldstein, L. S. and Cleveland, D. W. (1997) *Cell* **91**, 357-366.
89. Liao, H., Li, G. and Yen, T. J. (1994) *Science* **265**, 394-398.
90. Lombillo, V. A., Nislow, C., Yen, T. J., Gelfand, V. I. and McIntosh, J. R. (1995) *J Cell Biol* **128**, 107-115.
91. Yao, X., Abrieu, A., Zheng, Y., Sullivan, K. F. and Cleveland, D. W. (2000) *Nat Cell Biol* **2**, 484-491.
92. Yen, T. J., Compton, D. A., Wise, D., Zinkowski, R. P., Brinkley, B. R., Earnshaw, W. C. and Cleveland, D. W. (1991) *Embo J* **10**, 1245-1254.
93. Schaar, B. T., Chan, G. K., Maddox, P., Salmon, E. D. and Yen, T. J. (1997) *J Cell Biol* **139**, 1373-1382.
94. McEwen, B. F., Chan, G. K., Zubrowski, B., Savoian, M. S., Sauer, M. T. and Yen, T. J. (2001) *Mol Biol Cell* **12**, 2776-2789.
95. Abrieu, A., Kahana, J. A., Wood, K. W. and Cleveland, D. W. (2000) *Cell* **102**, 817-826.
96. Crespo, N. C., Ohkanda, J., Yen, T. J., Hamilton, A. D. and Sebti, S. M. (2001) *J Biol Chem* **276**, 16161-16167.
97. Ashar, H. R., James, L., Gray, K., Carr, D., Black, S., Armstrong, L., Bishop, W. R. and Kirschmeier, P. (2000) *J Biol Chem* **275**, 30451-30457.
98. Meluh, P. B. and Rose, M. D. (1990) *Cell* **60**, 1029-1041.
99. Hatsumi, M. and Endow, S. A. (1992) *J Cell Sci* **103**, 1013-1020.
100. Walczak, C. E., Verma, S. and Mitchison, T. J. (1997) *J Cell Biol* **136**, 859-870.
101. Mountain, V., Simerly, C., Howard, L., Ando, A., Schatten, G. and Compton, D. A. (1999) *J Cell Biol* **147**, 351-366.
102. Sharp, D. J., Yu, K. R., Sisson, J. C., Sullivan, W. and Scholey, J. M. (1999) *Nat. Cell Biol* **1**, 51-54.
103. Goldstein, L. S. (1993) *J Cell Biol* **120**, 1-3.
104. Endow, S. A. and Komma, D. J. (1996) *J Cell Sci* **109**, 2429-2442.
105. Kuriyama, R., Kofron, M., Essner, R., Kato, T., Dragas-Granoic, S., Omoto, C. K. and Khodjakov, A. (1995) *J Cell Biol* **129**, 1049-1059.
106. Holzbaue, E. L. and Vallee, R. B. (1994) *Annu Rev Cell Biol* **10**, 339-372.
107. King, S. M. (2000) *Biochim Biophys Acta* **1496**, 60-75.
108. Holleran, E. A., Karki, S. and Holzbaue, E. L. (1998) *Int Rev Cytol* **182**, 69-109.
109. Echeverri, C. J., Paschal, B. M., Vaughan, K. T. and Vallee, R. B. (1996) *J Cell Biol* **132**, 617-633.
110. Busson, S., Dujardin, D., Moreau, A., Dompierre, J. and De Mey, J. R. (1998) *Curr Biol* **8**, 541-544.
111. Karki, S. and Holzbaue, E. L. (1999) *Curr Opin Cell Biol* **11**, 45-53.
112. Banks, J. D. and Heald, R. (2001) *Curr Biol* **11**, R128-131.
113. Dujardin, D. L. and Vallee, R. B. (2002) *Curr Opin Cell Biol* **14**, 44-49.
114. Beaudouin, J., Gerlich, D., Daigle, N., Eils, R. and Ellenberg, J. (2002) *Cell* **108**, 83-96.
115. Salina, D., Bodoor, K., Eckley, D. M., Schroer, T. A., Rattner, J. B. and Burke, B. (2002) *Cell* **108**, 97-107.
116. Howell, B. J., McEwen, B. F., Canman, J. C., Hoffman, D. B., Farrar, E. M., Rieder, C. L. and Salmon, E. D. (2001) *J Cell Biol* **155**, 1159-1172.
117. Li, Y. Y., Yeh, E., Hays, T. and Bloom, K. (1993) *Proc Natl Acad Sci USA* **90**, 10096-10100.
118. Knoblich, J. A. (2001) *Nat Rev Mol Cell Biol* **2**, 11-20.
119. Afzelius, B. A. (1976) *Science* **193**, 317-319.
120. Shpetner, H. S., Paschal, B. M. and Vallee, R. B. (1988) *J Cell Biol* **107**, 1001-1009.
121. Katzung, B. G. (1998) Appleton & Lange: Stamford, CT
122. Yvon, A. M., Wadsworth, P. and Jordan, M. A. (1999) *Mol Biol Cell* **10**, 947-959.
123. Walle, T., Walle, U. K., Kumar, G. N. and Bhalla, K. N. (1995) *Drug Metab Dispos* **23**, 506-512.



San Francisco

LIBRARY

**For** Not to be taken  
from the room.  
**reference**

7315370



3 1378 00731 5370

